

**UNIVERSITA DEGLI STUDI DI MILANO**  
**FACOLTA DI SCIENZE MATEMATICHE, FISICHE E NATURALI**  
**Dipartimento di Chimica Inorganica, Metallorganica e Analitica**  
**“Lamberto Malatesta”**

**Ph.D. STUDIES IN INDUSTRIAL CHEMISTRY – XXIV COURSE**

**Title:**

**Design and development of heterogeneous catalysts for chemo- and regioselective oxidations using sustainable oxidants (H<sub>2</sub>O<sub>2</sub>, O<sub>2</sub>).**

**Ph.D. Student:**

Elena Gavrilova

**Tutor:** Prof. F. Sannicolò

**Co-Tutor:** Dott. M. Guidotti

**Ph.D. Coordinator:** Prof.ssa D. Roberto

Academic Year 2010-2011

## Table of contents

Introduction .....	5
I. Catalysis .....	7
1. Single Site Heterogeneous Catalysis (SSHC) .....	7
1.1. In-matrix synthesis .....	8
1.2. Post-synthesis modifications .....	8
1.2.1 Electrostatic interaction .....	10
1.2.2 Anchoring and Grafting.....	11
1.2.3 Physical deposition .....	15
1.2.4 Encapsulation .....	16
2. Microporous and Mesoporous Silicas .....	18
2.1. The main synthetic approaches to mesoporous materials .....	19
2.2. M41S materials.....	20
2.2.1. MCM-41 .....	21
2.2.2. MCM-48 .....	22
2.3. Hexagonal mesoporous silica: SBA-15.....	23
II. Use of Sustainable oxidants in epoxidation reactions over Ti-containing Single-Site Heterogeneous Catalysts .....	25
Aim of the thesis .....	27
References.....	29
Chapter 1. Ti-containing heterogeneous catalysts in cyclohexene epoxidation with hydrogen peroxide. ....	38
Results and discussion .....	41
Set-up for the determination of surface concentration of OH groups .....	45
Conclusions.....	47
Chapter 2. Ti-containing heterogeneous catalysts in methyl oleate epoxidation with hydrogen peroxide. ....	48
Results and discussion .....	50
Improving the epoxide yield.....	54
1) Effect of the temperature.....	54
2) Effect of the amount of hydrogen peroxide .....	55
3) Effect of the amount of catalyst .....	56
Reasons of trans-epoxide formation.....	56
Effect of the solvent.....	58
Conclusions.....	59
Chapter 3. The effect of surface silylation on the catalytic performance of Ti-MCM-41 in the epoxidation of limonene. ....	60
Results and discussion .....	61
Conclusions.....	64
Chapter 4. Ti-POSS covalently immobilized onto mesoporous silica. ....	66
A model for active sites in heterogeneous catalytic epoxidation. ....	66
Results and discussion .....	67
Conclusions.....	78
Chapter 5. Use of Au in the epoxidation reactions with molecular O <sub>2</sub> .....	80
Results and discussion .....	81

Epoxidation of trans-stilbene .....	82
Limonene epoxidation .....	84
1. The role of the Au particles' size.....	84
2. Effect of the solvent.....	85
3. Influence of the radical's initiator nature .....	86
4. Influence of pH and preparation method.....	87
Conclusions.....	89
Chapter 6. Production of H <sub>2</sub> O <sub>2</sub> in-situ by means of (Glucose Oxidase) GOx in air .....	91
Structure of Glucose Oxidase .....	93
Results and discussion .....	94
1. DMSO oxidation .....	94
Determination of GOx activity .....	96
2. Epoxidation of trans-stilbene.....	96
Conclusions.....	97
Experimental Part .....	99
Reagents.....	100
Materials used .....	102
Preparation of the catalysts .....	103
Preparation of ordered mesoporous silicas .....	103
Preparation of Ti-Silica Catalysts.....	103
Preparation of TS-1 .....	105
Characterization techniques .....	106
Ti-content determination.....	108
Gas-Chromatography (GC-FID).....	109
Preparation of anhydrous solvents .....	111
Experimental part for Chapter 1 .....	112
TGA analysis .....	113
Experimental part for Chapter 2 .....	114
Experimental part for Chapter 3 .....	122
Experimental part for Chapter 4 .....	123
Experimental part for Chapter 5 .....	126
Measuring the oxygen consumption in limonene oxidation with molecular O <sub>2</sub> and TBHP used as radical initiator.....	130
Experimental part for Chapter 6 .....	131
Encapsulation of glucose oxidase (GOx) .....	131
Measurements of the activity of GOx free and encapsulated GOx by Trinder test.....	133
Measurements of free GOx activity: .....	133
Measurements of encapsulated GOx .....	134
Catalytic test: .....	135
HPLC analysis .....	135
APPENDIX.....	136
Ab-initio DFT calculations results .....	136
General Conclusions.....	99

References Chapter 1 .....	140
References Chapter 2 .....	142
References Chapter 3 .....	145
References Chapter 4 .....	147
References Chapter 5 .....	149
References Chapter 6 .....	151
Acknowledgements .....	153

## Introduction

“Green chemistry” is a general name that represents the 21<sup>st</sup> century’s way to “do chemistry”. It is based on the design of chemical products and processes that reduce or eliminate the use or generation of hazardous substances [1]. In other words, green chemistry consists of using chemicals and chemical processes designed to reduce or eliminate negative environmental impacts. Green chemistry technologies provide a number of benefits, including reduced waste, eliminating costly end-of-the-pipe treatments, safer products, reduced use of energy and resources and improved competitiveness of chemical manufacturers and their customers. The 12 main principles of a green chemistry developed by Paul Anastas and John C. Warner are the following [2]:

### 1) **Prevention**

It is better to prevent waste than to treat or clean up waste after it has been created

### 2) **Atom economy**

Synthetic methods should be designed to maximize the incorporation of all materials used in the process into the final product

### 3) **Less Hazardous Chemical Synthesis**

Wherever practicable, synthetic methods should be designed to use and generate substances that possess little or no toxicity to human health and the environment.

### 4) **Designing Safer Chemicals**

Chemical products should be designed to effect their desired function while minimizing their toxicity

### 5) **Safer Solvents and Auxiliaries**

The use of auxiliary substances (e.g. solvents, separation agents, etc.) should be made unnecessary wherever possible and innocuous when used.

### 6) **Design for Energy Efficiency**

Energy requirements of chemical processes should be recognized for their environmental and economic impacts and should be minimized. If possible, synthetic methods should be conducted at ambient temperature and pressure

### 7) **Use of Renewable Feedstocks**

A raw material of feedstock should be renewable rather than depleting whenever technically and economically practicable

### 8) **Reduce Derivatives**

Unnecessary derivatization (use of blocking groups, protection/deprotection, temporary modification of physical/ chemical processes) should be minimized or avoided if possible, because such steps require additional reagents and can generate waste.

#### **9) Catalysis**

Catalytic reagents (as selective as possible) are superior to stoichiometric reagents

#### **10) Design for Degradation**

Chemical products should be designed so that at the end of their function they break down into innocuous degradation products and do not persist in the environment.

#### **11) Real-time analysis for Pollution Prevention**

Analytical methodologies need to be further developed to allow for real-time, in-process monitoring and control prior to the formation of hazardous substances.

#### **12) Inherently Safer Chemistry for Accident Prevention**

Substances and the form of a substance used in a chemical process should be chosen to minimize the potential for chemical accidents, including releases, explosions, and fires.

The concept of Green Chemistry is a part of the more general approach of Sustainable Chemistry [3]. As evidenced by the principles listed above, one of the most important guideline of Green Chemistry is to avoid the use of hazardous substances.

Obviously, strong oxidants can be listed between the most hazardous reagents. Between them manganese or chromium oxides, metal permanganates or bichromates, nitric acid etc. are often used in industrial oxidations reactions [4-11]. The importance of these processes together with the high impact of strongly oxidising agents leads Green Chemists towards the research of suitable alternative routes for oxidation reactions.

Oxidation catalysis plays a leading role in industry, since the oxidation is the tool for the production of vast quantities of intermediates and monomers for the polymer industry. In particular, alkene epoxidation is a reaction of a great importance of industrial organic synthesis. Epoxides are key raw materials in the production of a wide variety of products [12] and many efforts are devoted to the development of new active and selective epoxidation systems that avoid the formation of by-products and that are environmentally friendly [1, 13].

During last 40 years there has been an increasing interest for the development of heterogeneous catalysts for oxidation reactions in the liquid phase with aqueous H<sub>2</sub>O<sub>2</sub> or organic hydroperoxides such as *tert*-butylhydroperoxide [14, 15]. One of the first important examples of use of a sustainable catalytic system in an industrial processes is titanosilicalite-1, TS-1. In the late 1970s, TS-1 was synthesized by Enichem and it was shown that it can catalytically and selectively oxidize certain organic compounds in the presence of H<sub>2</sub>O<sub>2</sub> (for example, phenol to

hydroquinone [16], propene to propene oxide [17]). Such great features of titanium silicalite-1 are due to a combination of isolated tetrahedral titanium centers in a MFI structure and hydrophobic acid-free environment [18]. Nevertheless, since microporous materials have a limitation in their small pore size, only small and poorly functionalized substrates are able to be converted on such catalysts. The oxidation of bulkier substrates requires the synthesis of materials with larger pores. From here, the idea of using MCM-41 [19] and SBA15 [20–22] as supports or as matrices for titanium atoms. [23].

It has to be underlined that, the need of using less strong oxidants than those typically adopted in industrial oxidations, unavoidably request the use of suitable catalysts.

Therefore, and following 12 principles, the next paragraphs will be devoted to a better explanation of the concepts of “catalysis”, and on “the use of sustainable oxidants”, especially in the particular case of the alkene epoxidation.

## **I. Catalysis**

Catalysis is mainly divided into two branches: homogeneous and heterogeneous. Homogeneous catalysis deals with the use of a catalyst that is in the same phase of the reaction mixture, usually in liquid phase. In heterogeneous catalysis the catalyst is in a different phase: typically, the catalyst is a solid, while the reaction media is in gas/vapour or liquid phase. The main advantage of homogeneous catalysis is that active sites are spatially well distributed and separated one from another, as it also occurs in enzymes in Nature. Thus, there is a constant and optimum interaction between each active site and the substrate molecules [24]. The main drawback of the use of homogeneous catalysts is the difficult recycling and separation of the catalyst from the products. Heterogeneous catalysts, on the contrary, can be quantitatively separated, purified and reused. However, further efforts have to be applied in synthesizing new heterogeneous catalysts to reach the activity and selectivity close to homogeneous ones. One of the most promising strategy is, in this sense, the use of *Single Site Heterogeneous Catalysts* (SSHC).

### **1. Single Site Heterogeneous Catalysis (SSHC)**

During last two decades different attempts have been performed to fill the gap between homogeneous and heterogeneous catalysis, to transfer the homogeneous molecular approach to heterogeneous catalysis that led to the development of Single Site Heterogeneous Catalysis (SSHC) [25, 26]. A single site heterogeneous catalyst is a solid where the catalytically active sites are well-defined, evenly distributed entities (single sites) with a definite chemical surroundings, as in conventional homogeneous systems, but which show all the advantages of

heterogeneous systems, in terms of separation, recover and recyclability. Such single sites are typically located over solid supports with high surface area and present the following general features:

- consist of one or few atoms (as in the case of chemically defined metal clusters);
- are spatially isolated one from another;
- have all identical energy of interaction between the site itself and a reactant;
- are structurally well characterized.

There are two main methods to create single-site centres:

- 1) in-matrix synthesis;
- 2) post-synthesis modifications.

### **1.1. In-matrix synthesis**

In the first case, the atom-isolated catalytically active sites are homogeneously dispersed in the matrix of the support and they are located at or adjacent to ions that have replaced framework ions of the parent structure. The precursor of the active species is already present in the synthesis mixture of the final material, together with the other components, and the single sites are introduced during the synthesis step (e.g., during the hydrothermal synthesis of a zeolite or the co-precipitation step of an amorphous mixed oxide). The chemical environment of the site (in terms of hydrophilic/hydrophobic character, surface acidity, steric constraints, etc.) is strongly dependent on physical-chemical characteristics of the matrix. As a main drawback, some centres can be 'buried' within the bulk of the solid and they can be not accessible and available for catalysis. Moreover, the presence of 'heteroatoms' in the synthesis mixture may affect critically some preparation phases (gelation, crystallization, condensation, etc.) and it is then often necessary to set up a completely new synthesis protocol for every new desired material. Such approach can be very time-consuming, but the possibility of regeneration of these catalysts is generally better than the one of catalysts obtained via post-synthesis techniques.

### **1.2. Post-synthesis modifications**

Metal catalytic active centres can be added to a pre-existing mesoporous support in a second step, by post-synthesis modifications. The metal sites can be deposited, heterogenised, tethered or linked to a previously synthesized silicate (Figure 1) and by these techniques it is possible, in principle, to obtain metal silicate catalysts from any sort of silica solids, also commercially available [27-29].



Metal silicates obtained via post-synthesis modification generally show a very good accessibility of the catalytic metal centres, as they are added onto the surface of a mesoporous silicate. Conversely, one-step in-synthesis techniques lead to solids with an even distribution of metal centres, some of which can be ‘buried’ within the bulk of the solid and therefore they are not accessible and available for catalysis. The different exposure of catalytic sites in isomorphically substituted metal silicates, prepared by in-synthesis techniques, and materials obtained by post-synthesis grafting has been evaluated and quantified, for instance, in the epoxidation of cyclic alkenes over Ti-MCM-41 [30,31]. Under the same conditions, with the same Ti content and fully comparable structural features, grafted Ti-MCM-41 are up to 10 times more active (in terms of initial TOF) than in-matrix Ti-MCM-41.

In terms of regeneration and recoverability, metal silicates obtained by one-step methods can be more easily recycled than those obtained by post-synthesis techniques, since they can efficiently withstand calcination and severe washing treatments without losing their structural stability and chemical integrity. On the contrary, post-synthesis materials are, in principle, more prone to leaching and deactivation since the metal centres are more exposed towards the reaction medium. Moreover, when they contain organic moieties, such as carbon-chain tethers, ligands or organic modifiers, they can be sensitive to calcination and severe oxidation conditions that lead to the disruption of the carbon species. So, according to the catalytic application, either post-synthesis or in-synthesis materials can be the best choice.

Finally, by post-synthesis modification, it is possible to add a further catalytic metal centre to a pre-existing metal centre, obtained by either in-synthesis or post-synthesis techniques. These are therefore catalysts with a bifunctional character where two active centres are present thanks to the spatial segregation offered by the solid support [32,33].

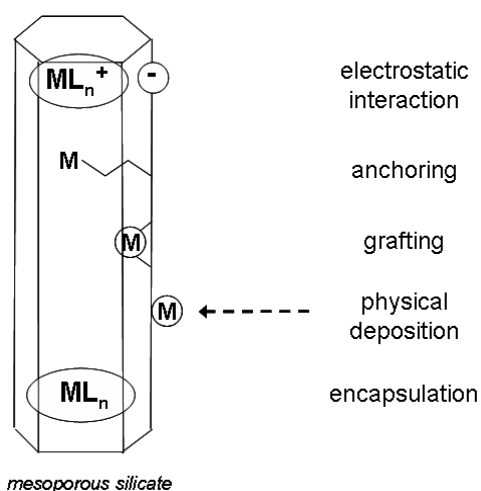


**Figure 1.** Post-synthesis modifications of mesoporous silicates. Several strategies are chosen to introduce catalytic functions onto the support.

*M: catalytically active metal; C: non-active counterion; L: ligand.*

The strategies to obtain metal silicates from mesoporous silica supports can be summarized into five main groups: 1) electrostatic interaction; 2) anchoring; 3) grafting; 4) physical deposition and 5) encapsulation.

### *1.2.1 Electrostatic interaction*

The electrostatic interaction approach derives from the deep know-how in ion exchange techniques developed with zeolites and zeotypes. Typically, metal cationic species (either metal ions or complexes) can exchange labile positively charged counterions (*e.g.* Na<sup>+</sup> or H<sup>+</sup>) on the surface of an acidic support, such as an aluminosilicate, and a ion-exchanged mesoporous silicate is obtained. In these cases, particular attention has to be paid to the physical-chemical properties of both the surface and the solvent the precursor is dissolved in. Factors such as the isoelectric point of the oxidic surface, the nature of the counterions on the surface, the dipolar moment of the solvent or the presence of protic species must be carefully considered. For instance, a Mn(III)-salen complex can be immobilized in the pores of Al-MCM-41 via the *in situ* reaction of the ligand (R,R)-3,5-di-*tert*-butylsalen with a previously exchanged Mn(II)-Al-MCM-41 [34,35]. This system was an effective catalyst for the epoxidation of *cis*-stilbene with PhIO at room temperature with a catalytic performance remarkably different from that obtained with the free homogeneous complex [Mn(<sup>t</sup>Bu<sub>2</sub>salen)Cl] or with the Mn(salen)-Al-MCM-41, in which the complex is deposited on the external surface only of the molecular sieve. Such change in stereoselectivity indicates a confinement effect due to the immobilization of the Mn complex within the mesoporous network of Al-MCM-41 [32]. However, these systems can suffer from metal leaching as a major drawback.

If the mesoporous silica support does not possess exchangeable ionic sites, a ionic moiety, able to create ion pairs, can be covalently deposited onto the support. Then the catalytically active species is bound by ion-pair interaction. Anionic Cr(IV) species or phosphotungstic acid can be immobilized onto imidazolium-functionalized silica (pyrogenic or SBA-15) and the negligible leaching of anions under the reaction conditions indicates a strong interaction between the metal and the imidazole moiety (Figure 2) [36,37]. So, H<sub>2</sub>[PW<sub>12</sub>O<sub>40</sub>]<sup>-</sup> was used as an efficient catalyst for epoxidation of a variety of olefins using aqueous H<sub>2</sub>O<sub>2</sub> [35].

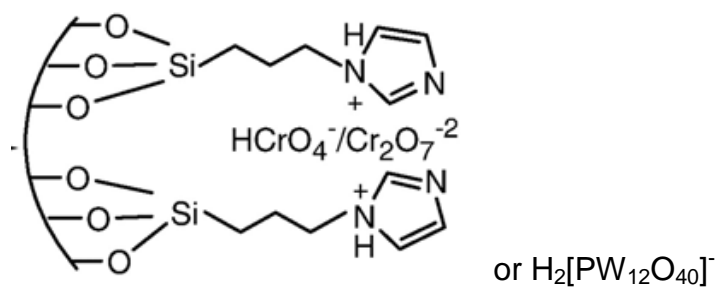


**Figure 2.** Anionic Cr or W species immobilized via ion-pair onto imidazolium-functionalized silica

Ordered mesoporous silicates are the support of choice in the case of very large cationic species, as in the case of a hydroxo-bridged dinuclear cupric complexes,  $[(\text{phen})_2\text{Cu}-\text{OH}-\text{Cu}(\text{phen})_2]^{3+}$  (phen = 1,10-phenanthroline) to mimic catechol oxidases in the oxidation of 3,5-di-*tert*-butylcatechol to the corresponding quinone [38]. The complexes immobilized in MCM-41 or MCM-48 showed a better stability against the irreversible dissociation of dinuclear cupric complexes thanks to their optimal pore size, while Na-Y zeolite has too small a pore size to stabilize them.

### 1.2.2 Anchoring and Grafting

The active centre can be added to the silicate support as a precursor via irreversible deposition, by anchoring or grafting, onto the surface as it is, by the formation of covalent bonds, or after functionalisation with a side chain (a tether) [39,40].

In the anchoring technique (Figure 3a), the active metal maintains the definite chemical surroundings as in the parent homogeneous precursor, since the formation of the covalent bonds takes place only at the opposite end of the tether. Such techniques merges the benefits of homogeneous catalysts (high regio- chemo- and stereoselectivity) to the advantages of heterogeneous systems (easy separation, recover and recyclability).

Conversely, in the grafting technique, the metal site has a different chemical surrounding with respect to the parent precursor, since the coordination shell around the metal centre is partially modified during the covalent deposition and a new reactivity of the active species can be expected (Figure 3b).

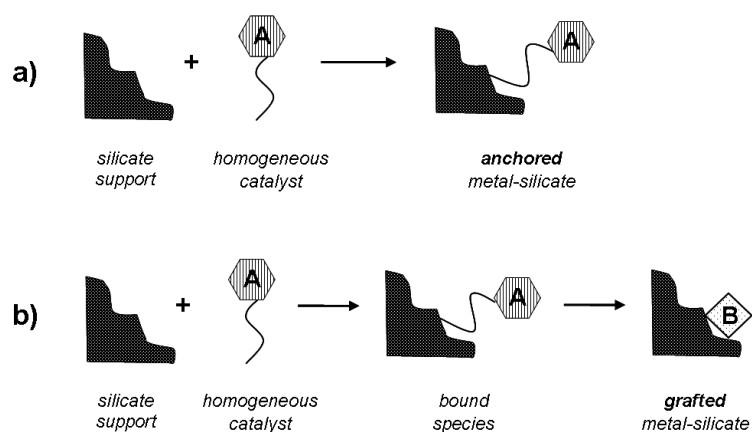


**Figure 3.** Covalent modifications of mesoporous silicates: anchoring and grafting.

Covalent anchoring is a good strategy to immobilize large and bulky moieties onto the surface of mesoporous silicates, provided the mesopores are large enough to accommodate the guest species. As an example, a Ti-containing polysilsequioxane (Ti-POSS), a complex widely used as a soluble model for Ti single sites in a silica matrix, was anchored via covalent bonding to the surface of a mesoporous SBA-15 silica (Figure 4). The final Ti-POSS-SBA-15 material revealed a good dispersion of the Ti sites with catalytic activity in the liquid-phase epoxidation of limonene to limonene oxide [41].

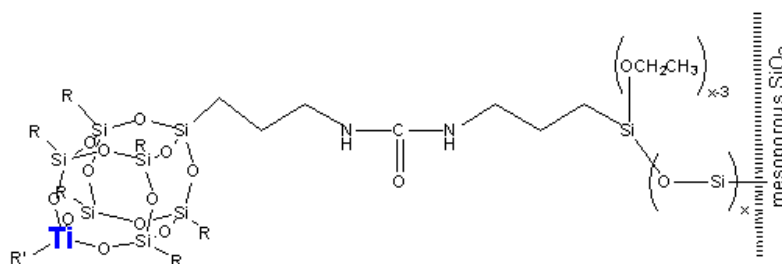


**Figure 4.** Anchoring of a Ti-POSS onto the surface of SBA-15 silica (R = isobutyl; R' = isopropyl group) (adapted from [39])

The techniques of immobilization can be different and rely either on the synthesis of silica-bound ligand followed by complexation with metal ions or by the direct immobilization of preformed metal complex to the silica support [42]. A bulky Ru-porphyrin complex (Ru(TDCPP)(CO)(EtOH) where TDCPP = *meso*-tetrakis(2,6-dichlorophenyl)porphyrin) was anchored onto a propylamine-modified MCM-41 obtained by reaction of (3-aminopropyl)triethoxysilane with the channel surface of the freshly calcined MCM-41 [43]. This system is active for the epoxidation of aromatic and aliphatic alkenes with Cl<sub>2</sub>pyNO. In the (+)-limonene epoxidation (which contains an endocyclic trisubstituted and an exocyclic terminal C=C bond), a preferential formation of the exocyclic epoxide was observed, whereas on the homogeneous system the endocyclic one is favoured, since the hindered endocyclic C=C bond is

more inaccessible to the anchored Ru centre within the MCM-41 structure than the exocyclic alkene. In other cases, the supported Ru catalyst is active in oxidation, whereas the homogenous precursor is not. A *p*-cymene-coordinated Ru-*N*-sulfonyl-1,2-ethylenediamine complex when is tethered onto a Aerosil 200 SiO<sub>2</sub> surface is active in the stilbene epoxidation with a O<sub>2</sub>/isobutyraldehyde system, while Ru(NH<sub>3</sub>)<sub>6</sub>Cl<sub>3</sub> or Ru(bpy)<sub>2</sub>Cl<sub>2</sub> under homogeneous conditions are totally inactive [44, 45].

Anchoring is also particularly suitable in the case of stereoselective oxidations, in order to immobilize homogeneous oxidation catalysts optimised for the use under liquid-phase conditions. These systems are deposited in porous silicates not only without losing their properties (as anchoring preserves the chemical surroundings and the chiral directing species around the active metal), but even enhancing and improving their stereoselectivity due to confinement effects [46, 47, 48]. Mn(salen) complexes, when covalently immobilized inside siliceous nanopores, also exhibit the effect of enhancement of chirality owing to confinement effect in the enantioselective epoxidation of non-functionalized olefins [49, 50, 51]. The confinement effect originating from nanopores not only enhances the chiral recognition of the catalyst, but also restricts the rotation of the intermediate within the nanopores, enhancing the asymmetric induction and giving higher *enantiomeric excess* values than those obtained for the same catalysts anchored on the external surface. In order to introduce the complex exactly and only inside the support mesopores, the silanol groups located on the external surface can be previously 'passivated' (e.g. by selective silylation), so that the chiral catalysts are anchored exclusively via the reaction with the free silanol moieties on the internal surface [33,52].

On the other hand, grafting methods were developed expanding the concept of surface organometallic chemistry in the 1980s [53]. Thanks to the systematic study of the reactivity of organometallic complexes or coordination compounds with the surface of non-porous pyrogenic (Aerosil) silica [54], the surface of the silicate can be considered as a ligand for an organometallic molecular species, where the pendant silanol groups (on Aerosil whose typical surface area is 200 m<sup>2</sup>g<sup>-1</sup>, the silanol surface concentration is ca. 0.7 ≡SiOH nm<sup>-2</sup>) bind covalently the organometallic precursor [55,56]. Later, a significant advance was made when Ti(IV) centres were grafted onto MCM-41 mesoporous silica using titanocene dichloride [Ti(Cp)<sub>2</sub>Cl<sub>2</sub>] (Cp = C<sub>5</sub>H<sub>5</sub>) [30,57]. This sort of Ti(IV)-grafted mesoporous silica could be applied to the epoxidation of a large variety of alkenes and to the oxidation of alkylphenols with high selectivity and good activity [58-64]. In principle, the bulky cyclopentadienyl ligand should limit the coalescence of Ti species on the surface and control the formation of undesired large TiO<sub>2</sub>-like domains, but with high Ti loadings (higher than ca. 5 wt.% in Ti) some important bands due to TiO<sub>2</sub>-like connectivity are observed [58,65]. Nevertheless, the Ti(IV)-SiO<sub>2</sub> catalyst for olefin

epoxidation developed by Shell for the styrene monomer-propylene oxide (SMPO) process can be considered a grafted catalyst as well, since  $\text{TiCl}_4$  is deposited onto an amorphous silica support and the Ti(IV) species active in epoxidation are formed by surface hydrolysis of the inorganic precursor [66-68]. The catalyst is prepared in a multistep gas-phase process by deposition of the Ti precursor ( $\text{TiCl}_4$  or an organotitanium compound), heating the obtained material, followed by steaming and silylation [69, 70]. The Shell Ti(IV)/ $\text{SiO}_2$  catalyst is effective because of the formation of site-isolated Ti species on the surface of the support and because of the increased Lewis acidity of the Ti(IV) due to electron withdrawing effect by the siloxy ligands [71]. More recently, an exponential evolution of the Shell approach can be seen in the synthesis of Ti(IV)-silica catalysts by grafting  $\text{TiCl}_4$  onto ordered mesoporous silicates MCM-41, MCM-48 and SBA-15 [72,73] as well as other alkoxides, such as  $\text{Ti}(\text{OiPr})_4$  [74-79],  $\text{Ti}(\text{OBu})_4$  [80] or  $\text{Ti}(\text{OEt})_4$  [81] onto both ordered and non-ordered mesoporous silicas. In fact, they showed interesting results in the epoxidation of non-functionalized alkenes, dienes and allylic alcohols with *tert*-butylhydroperoxide as oxidant and aqueous hydrogen peroxide, sometimes, under mild conditions [82, 83]. Again, in the particular case of Ti(IV), a huge variety of non-conventional different precursors has been investigated for grafting: e.g. Ti(triethanolaminate)-isopropoxide [84],  $[\text{SiMe}_2(\eta^5\text{-C}_5\text{H}_4)_2]\text{TiCl}_2$  [85],  $[\{\text{Ti}(\text{OiPr})_2(\text{OMent})\}_2]$  and  $[\text{Ti}(\text{OMent})_4]$  (OMent = 1*R*,2*S*,5*R*-(-)-menthoxo) [86],  $[(^t\text{BuO})_2\text{Ti}\{\mu\text{-O}_2\text{Si}[\text{OSi}(\text{O}^t\text{Bu})_3]_2\}]_2$  [87] or  $[\text{Ti}_6(\mu_3\text{-O})_6(\mu\text{-O}_2\text{CC}_6\text{H}_4\text{OPh})_6(\text{OEt})_6]$  [88].

Different transition metals too can be grafted onto mesoporous silica using the metallocene route and active centers composed of isolated Zr(IV), Hf(IV), Mo(VI), Cr(VI) and VO(IV) have been described [89, 90, 91]. So, grafting techniques are often used to obtain isolated catalytic centres in single-site supported heterogeneous catalysts for oxidations. For instance, tin centres on MCM-41 were recently prepared by grafting  $\text{SnMe}_2\text{Cl}_2$  and subsequent calcination. The Sn single sites obtained in such way were compared to the ones obtained via direct synthesis and they proved to be active in the Baeyer–Villiger oxidation of adamantanone, with a TOF value ( $160 \text{ h}^{-1}$ ) very close to the one recorded over Sn-BEA ( $165 \text{ h}^{-1}$ ) prepared by isomorphous substitution [92]. Similarly, a wide series of transition and post-transition metals, such as Fe, Zr, Cr, Mo, Ta, Mo, Cu or Al, can be grafted onto the surface of mesoporous silica [93-103]. A controlled grafting process can be obtained through atomic layer deposition (ALD), which uses organic solvents and anhydrous conditions to control the deposition of tungsten oxide species onto the silica surface and to avoid the formation of  $\text{WO}_x$  oligomers prevalent in aqueous solutions at nearly neutral pH [104]. Tungsten oxide species are highly dispersed on SBA-15 surfaces, even at 30 wt.%  $\text{WO}_x$  content, with surface density of  $1.33 \text{ WO}_x/\text{nm}^2$ . ALD methods led to samples with much better thermal stability than those prepared via impregnation.

Another complementary approach to grafting relies on molecular precursors of Ti, Cr, Fe, Ta or VO, that are deposited by thermolysis [105-108], rather than by liquid-phase nucleophilic attack of the Si-OH groups on the metal centre, as in the examples mentioned above (Figure 5). In these cases, the desired atomic environment aimed at in the final catalyst (e.g.  $\text{Ti}(\text{OSi}\equiv)_4$  or  $\text{-Ti}(\text{OSi}\equiv)_3$ ) is already present in the thermolytic precursor and in the final material it is always covalently bound to the silicate support (as in all grafted catalysts). So, for instance, starting from  $(i\text{PrO})\text{Ti}[\text{OSi}(\text{OtBu})_3]_3$ , the local environment achieved at the end in the single-site catalyst is  $\text{-Ti}(\text{OSi})_3$ . Typical supports are the high-area mesoporous silicas MCM-41 and SBA-15, the latter being, for this purpose, distinctly more thermally stable than the former.

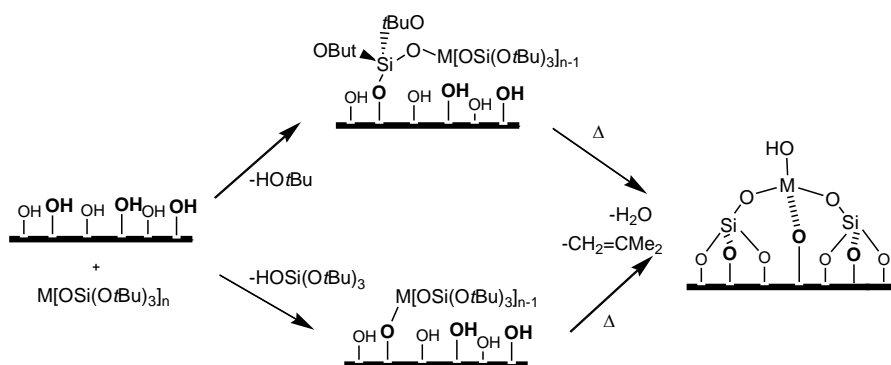


**Figure 5.** Preparation of single-site catalysts on mesoporous silica through thermolytic molecular precursors such as  $\text{M}[\text{OSi}(\text{OtBu})_3]_n$ . Adapted from [87].

Finally, redox-active metal centres can be added by simple impregnation of inorganic metal salts (typically nitrates, chlorides or, less frequently, sulfates) onto the silicate support and by a calcination step to fix it irreversibly on the surface as  $\text{MO}_x$  species [109, 110]. Such impregnation-calcination approach has also been employed to obtain oligomeric  $(\equiv\text{Ti}-\text{O}-\text{Ti}\equiv)_n$  species with controlled nuclearity (dinuclear or tetranuclear) for the highly selective oxidation of alkylphenols to benzoquinones with hydrogen peroxide [58, 111].

### 1.2.3 Physical deposition

Metal active centres can be immobilized onto the surface of a silicate support by physical deposition, based on non-covalent interactions, such as hydrogen bonding, weak van der Waals interactions,  $\pi$ -stacking, etc. A Ti-SiO<sub>2</sub> catalyst with highly isolated Ti centres was prepared by ion-beam implantation directly from Ti metal [112, 113]. The Ti atoms are ionized first and the ionized Ti beam is accelerated under high voltage to be implanted at high speed onto a non-ordered silica. The Ti ions implanted onto the support are highly isolated since the ion density

ion the beam is low and the ions are repelled from each other in the beam. Analogously, a deposition by gentle adsorption (with no further treatments under harsh conditions) allows one to obtain to heterogenize complex species without altering their pristine nature. So, a Ti(IV) silsesquioxane [ $\{(c-C_6H_{11})_7Si_7O_{12}\}Ti(\eta^5-C_5H_5)$ ] can be irreversibly adsorbed on the surface of Al-free MCM-41 to give a self-assembled heterogeneous catalyst that is prone to neither leaching nor deactivation [114]. According to the authors, the poorly hydrophilic nature of the support, in comparison with an aluminosilicate-containing MCM-41, is ideal for the strong adsorption and confinement of the silsesquioxane complex in the mesoporous network. In all the systems deposited by physical deposition, a careful evaluation about the absence of leaching and/or degradation of the active species must be carried out, especially when, in liquid-phase oxidations, any change in the polarity or the solvating properties of the reaction medium can lead to a re-dissolution and re-dispersion of the heterogenized metal species.

#### 1.2.4 Encapsulation

Encapsulation covers a large selection of methods for immobilising catalytically active species within the pores of microporous and mesoporous silicates and it does not require any attractive interaction between the metal precursor (typically, a bulky metal complex) and the support. It allows one to keep unaffected the optimal performances of the original homogeneous catalysts. In some cases, thanks to a positive cooperative effect, it is also possible to have a final system with improved characteristics (in terms of activity and/or selectivity) with respect to the parent precursor. For instance, encapsulated metal complexes are assembled *in situ* via intrazeolite synthesis and complexation and, for this reason, they are referred to as ‘ship-in-the-bottle’ complexes [115, 116]. Once formed, the metal complexes are spatially entrapped in the molecular sieve, since they are too bulky to diffuse out, whereas the reactants and the products can freely move through the pores. Alternatively, the preformed metal complex can be added to the silicate synthesis gel and the solid is induced to grow around the catalytically active metal complex. Encapsulated metal complexes are easily separated from the reaction media and can be reused, with no metal leaching. This kind of materials often show, with respect to the homogeneous parent complex, enhanced: (1) activity, thanks to sorption by the solid matrix and/or concentration effects; (2) selectivity, as detrimental free-radical side reaction, that occur in solution, are mostly suppressed in encapsulated systems, and (3) stability, since catalyst deactivation pathways are hindered by local site isolation of the complexes inside the matrix.

The most remarkable examples of encapsulation were developed on zeolites (typically, faujasite X or Y zeolites with pore diameters of 0.74 nm), in particular for high-added value chiral



oxidations. Chiral Mn(salen) species was encapsulated within a Y-zeolite (FAU) by the ship-in-a-bottle method and used in oxidation of various olefins using PhIO and these are the encapsulated forms of Jacobsen's catalyst [117-119] Analogously, the dicationic  $[\text{VO}(\text{bipy})_2]^{2+}$  complex was encapsulated via intrazeolite complexation method, by reacting  $\text{VO}^{2+}$ -exchanged NaY zeolite with 2,2'-bipyridine and tested in the oxidation of cyclohexane with  $\text{H}_2\text{O}_2$  [120]. Again, a highly efficient chiral dichlororuthenium(IV) porphyrin-silica catalyst was prepared via sol-gel method, synthesizing the mesoporous silica matrix around the complex, and it showed to be active in the asymmetric epoxidation of alkenes [121]. Some attempts of metal complex encapsulation (Cu phthalocyanines and porphyrins) in ordered MCM-41 were reported [122, 123], but the lack of catalytic data on these catalyst suggests their stability to leaching is not high. However, mesoporous silicates with an adequate geometry, suitable for spatial confinement, such as the cage-and-channel structure of SBA-16, can be efficiently used for encapsulation. Co(salen) complexes can be synthesized in the mesoporous cages of SBA-16 via the ship-in-a-bottle method. The pore entrance size of SBA-16 was then precisely tailored by varying the autoclaving time and silylation with phenyltrimethoxysilane to trap Co(salen) complex in the cage of SBA-16 [124, 145].

## 2. Microporous and Mesoporous Silicas

According to IUPAC, porous materials can be divided into three groups: microporous (<2 nm), mesoporous (2-50 nm) and macroporous (>50 nm) materials. Microporous and mesoporous inorganic solids are extensively used as heterogeneous catalysts and adsorption media [126]. The utility of these materials is manifested in their microstructures which allow molecules access to large internal surfaces and cavities that enhance catalytic activity and adsorptive capacity. A major subclass of the microporous materials are molecular sieves. These materials are exemplified by the large family of aluminosilicates (zeolites), that are the most widely used catalysts in industry [127]. They are crystalline microporous materials which have become extremely successful as catalysts for oil refining, petrochemistry, and organic synthesis in the production of fine and speciality chemicals, particularly when dealing with molecules having kinetic diameters higher than 1 nm. Zeolites have the following features that make them being so successful in catalysis: [128]

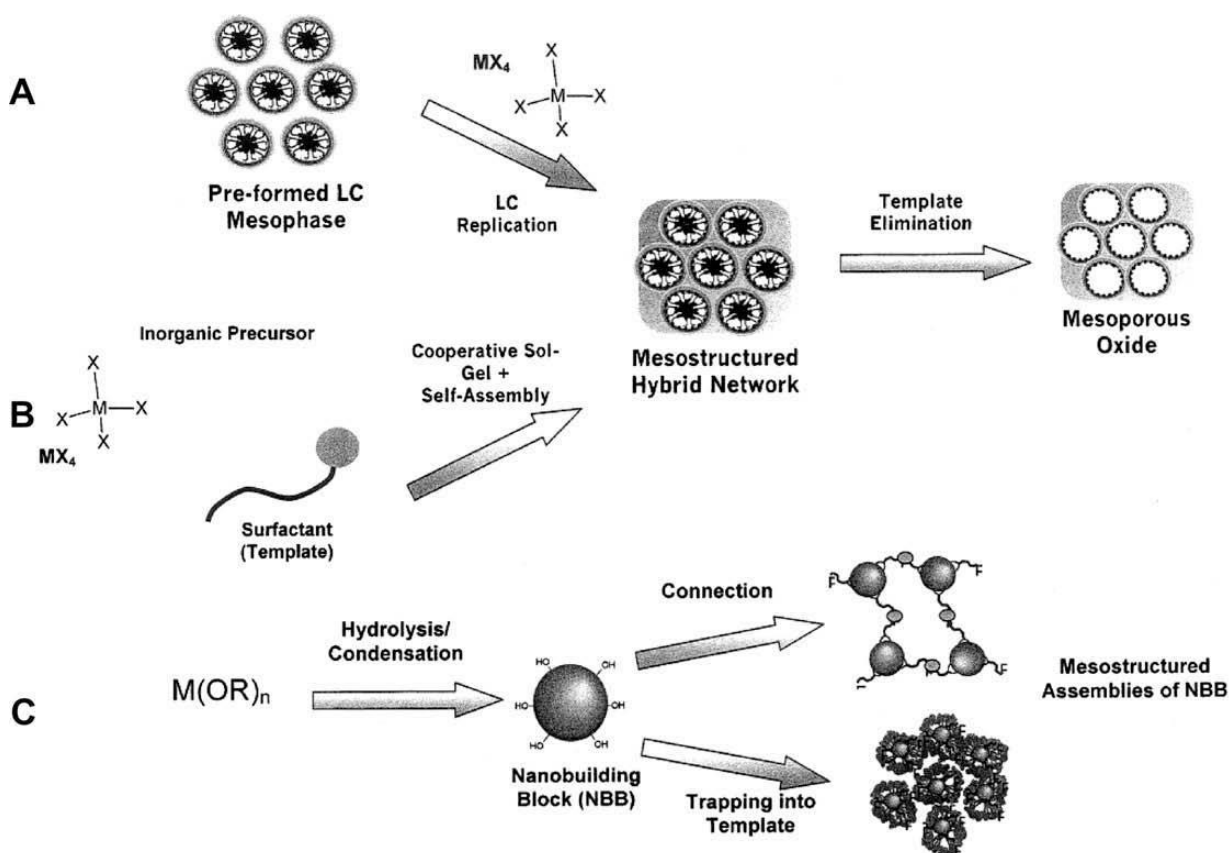
- 1) They have very high surface area and adsorption capacity;
- 2) The adsorption properties of the zeolites can be controlled, and they can be varied from hydrophobic to hydrophilic type materials.
- 3) Active sites, such as acid sites, can be generated in the framework and their strength and concentration can be tailored for a particular application.
- 4) The sizes of their channels and cavities are in the range typical for many molecules of interest (0.5-1.2 nm).
- 5) Their intricate channel structure allows the zeolites to present different types of shape selectivity, i.e., product, reactant, and transition state shape selectivity, which can be used to direct a given catalytic reaction toward the desired product avoiding undesired side reactions.
- 6) All of these properties of zeolites, which are very important in catalysis and make them attractive choices for the types of processes listed above, are ultimately dependent on the thermal and hydrothermal stability of these materials.

Despite these catalytically desirable properties of zeolites, they prove to be inadequate when reactants whose size is above the dimensions of the pores have to be processed. In this case, the rational approach to overcome such a limitation is to maintain the porous structure, which is responsible for the benefits described above, and to increase their diameter to bring them into the mesoporous region. Thanks to innovative synthesis strategies, an evolution towards structured materials with larger pores is obtained. After the first reports, introducing the M41S family of ordered mesoporous silicas at the beginning of the 1990s, the synthesis of advanced mesoporous

materials has undergone exponential growth. The synthesis of mesoporous materials is an ever-increasing and active field of research.

## 2.1. The main synthetic approaches to mesoporous materials

The synthesis of inorganic mesoporous materials is based on the use of organic template molecules that are used in different assembly processes or textural templates, around which the inorganic precursor can condense (Scheme 1) [129-134].



**Scheme 1.** Main synthetic approaches to mesostructure materials. A) Liquid crystal templating, B) self-assembly and cooperative self-assembly, C) nanometric building blocks.

A large diversity in synthesis approaches is known for the formation of different materials, and relatively similar materials (e.g. MCM-41, MCM-48, SBA-15) can be made by different synthesis methods and surfactants, each of them allowing other parameters to be altered and controlled. Next to differences in chemical ratios, the nature of the chemicals and additives that are applied as well as synthesis temperatures and times, also alternative synthesis set-ups and combinations thereof are used to obtain the necessary synthesis conditions (reflux set-ups, autoclaves for hydrothermal treatments and microwaves) [135–141]. Basically, the synthesis of

mesoporous materials and its control can be limited to the altering of the combination of the chosen surfactant type, the specific synthesis mechanism and the interaction of the silica source with the template molecules (if present) [132]. For example, M41S materials are made by S<sup>+</sup>T (cationic surfactants and anionic silicate species) direct interaction between an ionic, positively charged MOS (molecular-based organized system) surfactant and a negatively charged silica source in a basic environment. Three types of mechanisms, liquid crystal templating, self-assembly and cooperative self-assembly have been suggested for the synthesis of M41S materials based on the applied synthesis conditions [128, 132, 136]. SBA materials, on the other hand, have been made by use of POS (polymeric based organized system) surfactants that interact through an indirect reaction of the template with the positively charged silica source ((S<sup>0</sup>H<sup>+</sup>)(X<sup>-</sup>)) in acid medium [142-144].

A general synthesis for the preparation of templated mesoporous materials can be described as the dissolution of the template molecules in the solvent (with attention for pH, temperature, additives, co-solvents) followed by addition of the silica source (TEOS, metasilicate, fumed silica) After a stirring period at a certain temperature to allow hydrolysis and precondensation, the temperature is increased (sometimes combined with hydrothermal treatment or microwave synthesis, the addition of additives or changes in the pH) in order to direct the condensation process. Then, in the following step, the products are recovered, washed and dried. Finally, the template needs to be removed by calcination procedures or extraction methods. The latter is environmentally and economically the preferred procedure since it allows the recovery and recycling of the templates. However, extraction processes are often incomplete [145] and cannot be executed for all surfactants and materials. Moreover, in contrast to calcination procedures at high temperatures, extraction methods do not result in an additional condensation of the silica framework.

## **2.2. M41S materials**

M41S is the generic name for a whole family of various types of MCM (Mobil Composition of Materials) materials in the mesoporous range. The first ordered mesoporous materials known as M41S were reported in 1992 by Mobil [146-152]. The Mobil researches introduced self-assembling surfactants as structure directing agents to direct the formation of SiO<sub>2</sub> mesostructured materials.

All M41S materials have well-defined uniform of pores consisting of amorphous silica. Various heteroelements (Al, Ti, Co, Zr, Cu, Fe, Zn) can also be added to the main matrix. By changing

the synthesis conditions it is possible to alter the topology of the material and therefore create new types of structures belonging to the M41S family. In general, most M41S materials are made in basic environment with quaternary ammonium salts ( $C_nH_{2n+1}(C_mH_{2m+1})_3NX$  with  $n = 6-22$ ,  $m = 1-4$  and  $X = OH/Cl, OH, Cl, Br$  or  $HSO_4$ ) or *gemini* surfactants ( $[C_mH_{2m+1}(CH_3)_2N-C_sH_{2s}-N(CH_3)_2C_nH_{2n+1}]_2Br$  with  $m$  and  $n = 16-18$  and  $s = 2-12$ ). The key parameters for the M41S synthesis are the following: hydrogel composition, the type and length of the surfactant, the alkalinity, the temperature and the synthesis time.

### 2.2.1. MCM-41

MCM-41 possesses an amorphous (alumino, metallo)-silicate framework forming a hexagonal array of pores. MCM-41 has high surface areas of up to  $1200 \text{ m}^2/\text{g}$  and broad pore volumes. The pores are very uniform causing narrow pore size distributions [153]. The pores are unidirectional and arranged in a honeycomb structure over micrometer length scales (Fig. 1).

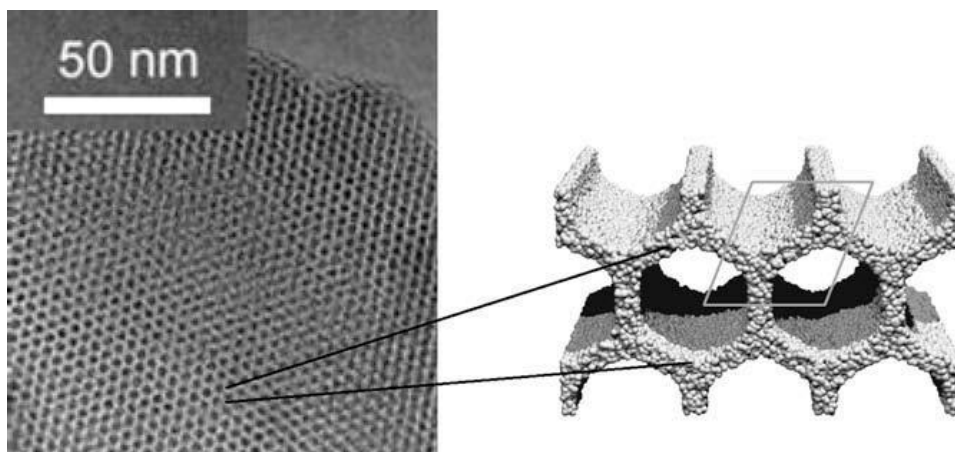


**Figure 1.** TEM image of the honeycomb structure and a schematic representation of the hexagonal shaped one-dimensional pores.

The pore diameters of MCM-41 span between  $d_p=1.5$  and  $20 \text{ nm}$ . The pore walls are quite thin with a thickness between  $1$  and  $1.5 \text{ nm}$ . The presence of this thin pore walls leads to low chemical and hydrothermal stabilities [154]. To improve the stability, various techniques can be applied: addition of various salts, post-modification methods such as ion exchange, treatment in acid, grafting of organosilane functional groups to produce hydrophobic organic chains on the surface [155, 156, 157].

Thanks to the simplicity and ease in the preparation of MCM-41, this material is often used as a model in comparison with other materials or to study fundamental aspects in sorption, catalysis, etc. [158].

### 2.2.2. MCM-48

MCM-48 is a mesoporous material with a three-dimensional array of pores. The BET surface area can reach the value of  $1400 \text{ m}^2\text{g}^{-1}$ , while pore sizes and volumes are similar to MCM-41. The wall thickness of the pores is thin for the MCM-48 as for MCM-41 causing limited chemical and hydrothermal stabilities. The structure of MCM-48 can be described as a gyroid. The gyroid surface divides the cube into two identical but separate compartments, creating two independent but interwinning enantiomeric 3D pore systems (Fig. 2) [159].

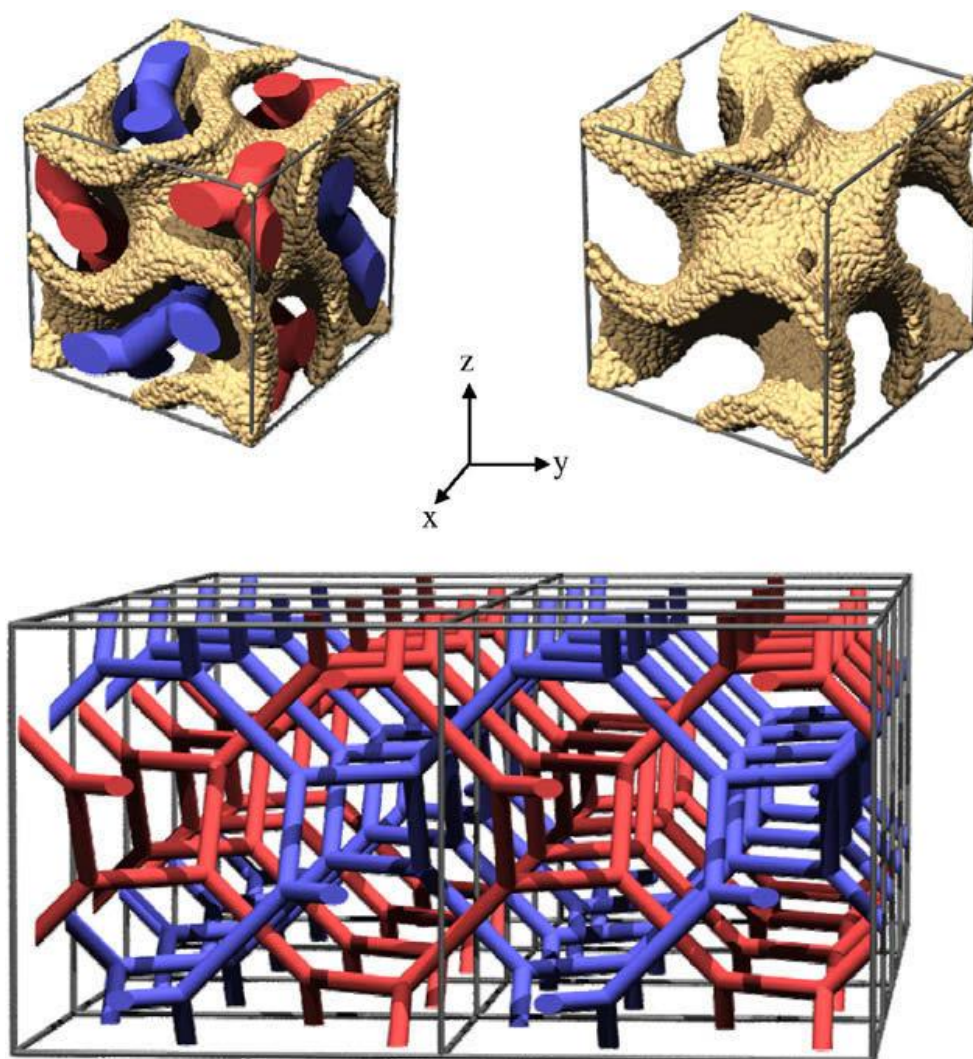


**Figure 2.** Cubic unit cell of MCM-48 with two independent micelle systems (red and blue rods) separated by the pore wall (upper right).

Increased interest in three-dimensional materials can be attributed to the expectation that the 3D pore network could have some important advantages in catalysis compared with one-dimensional ones. There is more agitation in the system due to an increased curvature in the pores. Moreover,

the 3D network reduces the chance of restrictions in diffusion, which is not limited to one dimension [160].

### 2.3. Hexagonal mesoporous silica: SBA-15

In 1998 the family of highly ordered mesoporous materials of SBA type was synthesized using triblock poly(ethylene oxide) – poly(propylene oxide) - poly(ethylene oxide) copolymers (PEO<sub>x</sub>-PPO<sub>y</sub>-PEO<sub>x</sub>) [161]. The family includes materials with cubic cage structures *Im3hm* (SBA-16), cubic *Pm3hm* (SBA-11) (or others), the three-dimensional hexagonal *P63/mmc* cage structure (SBA-12), a honeycomb hexagonal *p6mm* structure (SBA-15), and lamellar (LR) and possibly continuous L3 sponge, mesophases. Under acidic conditions, non-ionic alkyl-ethylene oxide oligomeric surfactants often favour the formation of cubic mesoporous silica phases at room temperature, while poly(alkylene oxide) triblock copolymers tend to favor the hexagonal (*p6mm*) mesoporous silica structure.

SBA-15 is a combined micro- and mesoporous material with hexagonally ordered tuneable uniform mesopores (4–14 nm) [162,163]. The size of the micropores depends on the synthesis conditions and can vary between 0.5 and 3 nm in size [164-170]. It consists of thick microporous silica pore walls (3–6 nm) responsible for the high hydrothermal stability of SBA-15 compared to other mesoporous materials with thin pore walls like MCM-41, MCM-48 [154, 171]. The micropores in the walls of the SBA-15 mesopores originate from the polyethyleneoxide blocks (PEO) in the triblockcopolymers that are directed to the aqueous solution [163, 170, 172, 173, 174], whereas the polypropyleneoxide blocks (PPO) are more hydrophobic and give rise to the internal structure of the mesopore [175, 176, 177]. A schematic representation of the structure-directing assembly of the PEO and PPO blocks in SBA-15 can be seen in Fig. 3.

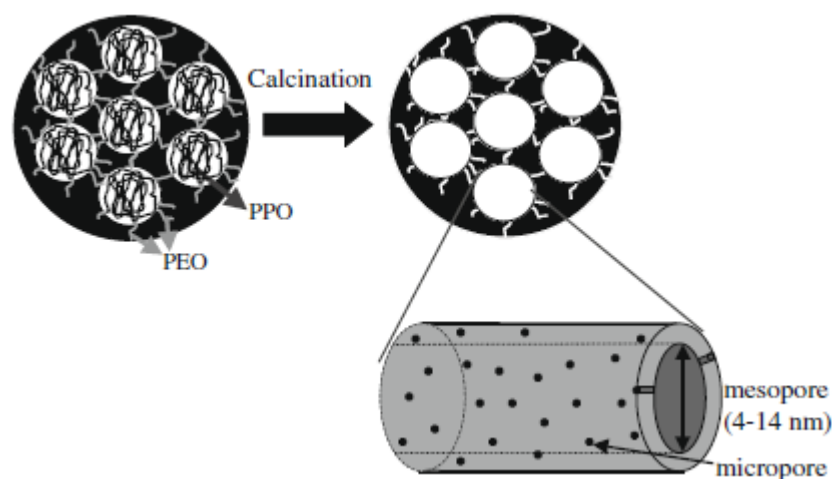


**Figure 3.** SBA-15 before and after calcination.

Because of their large pores, high hydrothermal stability, and easy preparation, SBA-15 materials have been considered very promising materials and have been tested for several applications: as catalysts (Al-SBA-15 [178, 179] or Ti-SBA-15 [180,181]), supports for grafted catalysts [182,183], sorbents for polluting heavy metals [184], advanced optical materials [185] templates for metal nanowires (Pt, Ag) [170, 186], or selective sorbents for proteins [187].



## II. Use of Sustainable oxidants in epoxidation reactions over Ti-containing Single-Site Heterogeneous Catalysts

Typical oxidants used in the intermediate and fine industrial synthesis nowadays are: HNO<sub>3</sub>, Cl<sub>2</sub>, ROOH, H<sub>2</sub>O<sub>2</sub>. For example, in Table 1 many important intermediates for chemical industry are shown [3]. It is important to note, that in last 10 years the efforts have been devoted to use more sustainable oxidants in the production of the shown below intermediates for the polymer industry. If considerable effort had not been spent on the continuous improvement of the technologies used for the productions of these chemicals, the influence of these productions on the environment might have been much greater than it is now.

Table 1. Organic base chemicals produced by means of oxidation.							
Chemical	Capacity [Mta <sup>-1</sup> ]	Oxidant					
		Air	O <sub>2</sub>	HNO <sub>3</sub>	Cl <sub>2</sub>	ROOH	H <sub>2</sub> O <sub>2</sub>
Terephthalic acid	44	X					
Fomaldehyde	19	X					
Ethene oxide	18		X				
1,2-Dichloroethane	18	X	X		X		
Propene oxide	8				X	X	X
Cyclohexanone	6	X	X				
Vinyl acetate	6	X	X				
Acrylonitrile	6	X					
Styrene (ex PO/SM) <sup>[a]</sup>	5	X	X				
Phenol/acetone	5	X					
Phthalic anhydride	5	X					
Acrylic acid	5	X					
MTBE (ex PO/TBA) <sup>[a]</sup>	4		X				
Adipic acid	3			X			
Maleic anhydride	2	X					
Hydrogen cyanide	2	X					

[a] MTBE: methyl-*tert*-butyl ether; PO: propene oxide; SM: styrene (monomer); TBA: *tert*-butyl alcohol.

However, some processes still co-produce large amounts of wastes. For example, nitric acid that is used in the adipic acid production, [188] is cheap, but unavoidably forms various nitrous oxides, among which the N<sub>2</sub>O. N<sub>2</sub>O is believed to contribute to the greenhouse effect and global warming because of its strong IR adsorption, which is about 300 times stronger than that of CO<sub>2</sub> [3]. Moreover, the amount produced is around 300 kg of N<sub>2</sub>O per tonne of adipic acid.

For the catalytic epoxidation of olefins over heterogeneous Ti(IV) catalysts, organic peroxides and hydrogen peroxide are used [12]. Although organic peroxides are generally much more active than hydrogen peroxide, they are more expensive, since the active oxygen content is rather low and they often are not considered as fully sustainable reagents. The epoxidation reaction generates stoichiometric amounts of corresponding alcohols, which, in most cases, are quite easily recycled via a reaction with hydrogen peroxide, but this process requires at least two extra separation and one extra reaction steps. There is a strong need for the development of new epoxidation methods which employ safer oxidants and produce little waste. The employment of hydrogen peroxide is an attractive option both on environmental and economic grounds. It is cheap, readily available and gives water as the only by-product [189]. It can oxidize organic compounds with an atom efficiency of 47% and with the generation of water as the only theoretical co-product. It is relatively cheap, < 0.7 US dollar per kg (100% H<sub>2</sub>O<sub>2</sub>), and about 2.4 million metric tonnes are produced for use, mainly as bleach [190]. The reaction should be achieved with an H<sub>2</sub>O<sub>2</sub> concentration of < 60% because the use, storage, and transportation of higher concentrations of H<sub>2</sub>O<sub>2</sub> are not desirable for safety reasons [191]. The H<sub>2</sub>O<sub>2</sub> oxidation is particularly useful for the synthesis of high-value fine chemicals, pharmaceuticals or agrochemicals, and electronic materials which require high chemical purity. There is a trend to use H<sub>2</sub>O<sub>2</sub> as an oxidant for large volume processes such as caprolactam synthesis (Sumitomo Chemical Co.) [192] and propylene oxidation (BASF and Dow Chemical Co.) [193]. One of the major advantages of the H<sub>2</sub>O<sub>2</sub> oxidation is the high tunability of the reaction parameters. Moreover, H<sub>2</sub>O<sub>2</sub> displays good results with microporous TS-1, whereas with mesoporous Ti silicas [194], it leads to a rapid deactivation of the active sites, due to the detrimental interaction of water with Ti(IV) centres in the silica matrix. For these reasons, the use of H<sub>2</sub>O<sub>2</sub> or, in the best case, molecular O<sub>2</sub> is a challenging and looked after topic for a selective oxidation of fine chemicals.

## Aim of the thesis

In order to have a sustainable and environmentally friendly oxidation process, the use of heterogeneous easily recyclable catalysts and of sustainable oxidants ( $\text{H}_2\text{O}_2$ , TBHP, molecular  $\text{O}_2$  or air) are necessary factors. However, the progress in this direction is obstructed by the difficulties in finding efficient and stable heterogeneous catalysts for selective oxidations in liquid phase [195,196].

**Therefore, the aim of the present PhD thesis is the design and development of efficient and robust heterogeneous catalysts that can be used with TBHP,  $\text{H}_2\text{O}_2$  or, in the best case, molecular  $\text{O}_2$  or air.**

Ti in siliceous matrices [197,198] appears to be the most suitable system to perform oxidation with peroxidic reagents, since it is more robust to leaching and selective with respect to, e.g., Co, Mn or V-based systems [199]. In the past 20 years, a number of ordered mesoporous titanium-silicates was synthesized and tested in liquid-phase selective oxidation reactions. Here, the *post-synthesis modification* (e.g., *grafting or anchoring*) to obtain Ti(IV) heterogeneous silicas was used. The main advantage of the grafting procedure is that Ti(IV) sites are situated on the surface and all the species are virtually active and accessible in the catalyst. Furthermore, a careful tuning of the metal and metal loading is also possible. Different precursors can be used to obtain Ti(IV) heterogeneous silicas, such as  $\text{TiCp}_2\text{Cl}_2$ ,  $\text{TiCl}_4$ ,  $\text{Ti}(\text{O}i\text{Pr})_4$ . The disadvantage of  $\text{Ti}(i\text{OPr})_4$  is that the oligomerization process can easily occur, leading to  $\text{TiO}_2$  domains, which are often detrimental in oxidation processes. At the same time, with the use of  $\text{TiCl}_4$ , the quantities of evolved HCl are potentially damaging to the siliceous MCM-41. Titanocene dichloride ( $\text{TiCp}_2\text{Cl}_2$ ) was therefore chosen as the most promising precursor, because relatively stable cyclopentadienyl ligands protect the titanium centre and, hence, prevent dimerization and oligomerization of the Ti species.

Ti-silica catalysts were prepared by grafting of titanocene dichloride ( $\text{TiCp}_2\text{Cl}_2$ ) onto silicas with different characteristics:  $\text{SiO}_2$  Aerosil (non porous pyrogenic material), SBA-15 (with micro and mesoporous network), MCM-41 (mesoporous one-dimensional) and MCM-48 (mesoporous three-dimensional).

As already introduced previously, the preferential oxidants employed in the oxidation over heterogeneous Ti(IV) catalysts are  $\text{H}_2\text{O}_2$  or organic hydroperoxides, such as *tert*-butylhydroperoxide (TBHP) [200].  $\text{H}_2\text{O}_2$  displays good results with microporous TS-1, whereas with mesoporous Ti silicas, it leads to a rapid deactivation of the active sites. TBHP has the advantage of high selectivity, thanks to a heterolytic oxidation pathway, but it is not generally

considered as a fully sustainable reagent. For these reasons, the use of H<sub>2</sub>O<sub>2</sub> or, in the best case, air or molecular O<sub>2</sub> is a challenging topic for a selective oxidation of fine chemicals. This last aspect was also considered in this work. In fact, the last chapter of the present manuscript is devoted to the description of different strategies for O<sub>2</sub> activation: 1) the enzymatic approach and 2) the use of Au metal nanoparticles.

The PhD thesis is divided into six chapters, according to six main phases and topics of the research work. In all chapters major attention was paid to the design and development of heterogeneous catalyst for the epoxidation of unsaturated substrate molecules in liquid phase. For all the considered catalysts and approaches, the following substrates were used: methyl oleate, cyclohexene, *trans*-stilbene, limonene, dimethyl sulfoxide (DMSO). Cyclohexene and *trans*-stilbene were chosen as model substrates of relatively bulky alkenes, with and without free allylic positions, respectively. Methyl oleate was chosen as a representative substrate for the wide series of unsaturated fatty acid derivatives used in oleochemistry. Limonene was chosen as a model substrate of alkenes found in flavour and fragrances chemistry. Moreover, the reaction of limonene epoxidation is useful to understand chemo- and regioselectivity of the epoxidation process. Finally, dimethyl sulfoxide was chosen as a model substrate of recalcitrant sulfur-containing pollutants typically found in wastewater treatment processes.

## References

- [1] US Environmental Protection Agency. 2010 Green engineering. See <http://www.epa.gov/oppt/greenengineering/>
- [2] Anastas, P. T. & Warner, J. C. **1998** Green chemistry: theory and practice. New York, NY: Oxford University Press.
- [3] F. Cavani, J.H. Teles, *Chem. Sus. Chem.*, 2, **2009**, 508
- [4] J.H. Clark, C N Rhodes, Cambridge: Royal Society of Chemistry, **2000**
- [5] R.A. Sheldon, *Chem. Ind.*, 903, **1992**
- [6] R.A. Sheldon, J Dakka, *Catal. Today*, 19, **1994**, 215,
- [7] G.Centi, M Misono, *Catal. Today*, 41, **1998**, 287
- [8] R.A. Sheldon, R.S. Downing, *Appl. Catal. A*, 189, **1999**, 163
- [9] J.S. Rafelt, J.H. Clark, *Catal. Today*, 57, **2000**, 33
- [10] W.F. Hoelderich, *Catal. Today*, 62, **2000**, 115
- [11] W.R. Sanderson, *Pure Appl. Chem.*, 72, **2000**, 1289
- [12] T. Sreethawong, Y. Yamada, T. Kobayashi, S. Yoshikawa, *J. Mol. Catal. A: Chem.*, 241, **2005**, 23.
- [13] B.K. Min, C. Friend, *Chem. Rev.*, 107, **2007**, 2709
- [14] G-J Brink, I.W.C.E. Arends, R.A. Sheldon, *Science*, 287, **2000**, 1636
- [15] D. Mandelli, C.A.M. van Vliet, R.A. Sheldon, U. Schuchardt, *Appl. Catal. A: General*, 219, **2001**, 209–213
- [16] M. Keshavaraja, V. Ramaswamy, H.S. Soni, A.V. Ramaswamy, P. Ratnasamy, *J. Catal.*, 157, **1995**, 501-511
- [17] M.G. Clerici, G. Belussi, U. Romano, *J. Catal.*, 129, **1991**, 159-167
- [18] B. Notari, *Adv. Catal.*, 41, **1996**, 253
- [19] Piaggio P, McMorn P, Langham C, Bethell D, Bulman Page PC, Hancock FE, Hutchings GJ., *New J. Chem.*, **1998**, 1167.
- [20] Piaggio P, McMorn P, Murphy D, Bethell D, Bulman Page PC, Hancock FE, Sly C, Kerton OJ, Hutchings GJ. , *J. Chem. Soc., Perkins Trans.*, 2, **2000**, 2008.
- [21] Li J, Qi T, Wang L, Liu C, Zhang Y., *Mater. Lett.*, 61, **2007**, 3197.
- [22] Aany Sofia LT, Krishnan A, Sankar M, Kala Raj NK, Manikandan P, Rajamohanan PR, Ajithkumar TG., *J. Phys. Chem. C*, 113, **2009**, 21114.
- [23] F. Chiker, J.Ph. Nogier, F. Launay, J.L. Bonardet, *Appl Catal A:Gen*, 243, **2006**, 309
- [24] V. Dal Santo, F. Liguori, C. Pirovano, M. Guidotti, *Molecules*, 15, **2010**, 3829
- [25] Thomas, J.M.; Raja, R.; Lewis, D.W., *Angew. Chem. Int. Ed.*, 44, **2005**, 6456-6482.

- [26] Thomas, J.M.; Raja, R., *Top. Catal.*, 40, **2006**, 3-17.
- [27] Corma A., *Catal. Rev.*, 46, **2004**, 369.
- [28] Thomas JM, Hernandez JC, Raja R, Bell RG., *Phys. Chem. Chem. Phys.*, 11, **2009**, 2799.
- [29] Dal Santo V, Liguori F, Pirovano C, Guidotti M., *Molecules*, 15, **2010**, 3829
- [30] Oldroyd RD, Thomas JM, Maschmeyer T, MacFaul PA, Snelgrove DW, Ingold KU, Wayner DDM., *Angew. Chem. Int. Ed.*, 35, **1996**, 2787.
- [31] Berlini C, Guidotti M, Moretti G, Psaro R, Ravasio N., *Catal. Today.*, 60, **2000**, 219.
- [32] Guisnet M, Guidotti M. One-pot Reactions on Bifunctional Catalysts, In: Derouane EG, editor. *Catalysts for Fine Chemical Synthesis*. Wiley: Weinheim, Germany; **2006.**, 157.
- [33] Bisio C, Gatti G, Marchese L, Guidotti M, Psaro R. Design and Applications of Multifunctional Catalysts Based on Inorganic Oxides. In: Rios G, Kannellopoulos N, Centi G, editors. *Nanoporous Materials for Energy and the Environment*. Pan Stanford Publishing Pte Ltd; 2011: in the press.
- [34] Piaggio P, McMorn P, Langham C, Bethell D, Bulman Page PC, Hancock FE, Hutchings GJ., *New J. Chem.*, **1998**, 1167.
- [35] Piaggio P, McMorn P, Murphy D, Bethell D, Bulman Page PC, Hancock FE, Sly C, Kerton OJ, Hutchings GJ. , *J. Chem. Soc., Perkins Trans.*, 2, **2000**, 2008.
- [36] Li J, Qi T, Wang L, Liu C, Zhang Y., *Mater. Lett.*, 61, **2007**, 3197.
- [37] Aany Sofia LT, Krishnan A, Sankar M, Kala Raj NK, Manikandan P, Rajamohanan PR, Ajithkumar TG., *J. Phys. Chem. C*, 113, **2009**, 21114.
- [38] Lee CH, Lin HC, Cheng SH, Lin TS, Mou CY., *J. Phys. Chem. C*, 113, **2009**, 16058.
- [39] Campbell IM. The Constitution of the Catalytic Surfaces, In *Catalysis at Surfaces*; Chapman & Hall, London. **1988**, 64.
- [40] Louis C, Che M. Anchoring and Grafting of Coordination Metal Complexes onto Oxide Supports. In *Preparation of Solid Catalysts*. Ertl G, Knözinger H, Weitkamp J. (editors). Wiley-VCH, Weinheim (Germany). **1999**, 341.
- [41] Carniato F, Bisio C, Boccaleri E, Guidotti M, Gavrilova E, Marchese, L., *Chem. Eur. J.*, 14, **2008**, 8098.
- [42] Rana BS, Jain SL, Singh B, Bhaumik A, Sain B, Sinha AK., *Dalton Trans.*, 39, **2010**, 7760.
- [43] Liu CJ, Yu WY, Li SG, Che CM., *J. Org. Chem.*, 63, **1998**, 7364.
- [44] Haak KJ, Hashiguchi S, Fujii A, Ikariya T, Noyori R., *Angew. Chem. Int. Ed.*, 36, **1997**, 285.
- [45] Tada M, Coquet R, Yoshida J, Kinoshita M, Iwasawa Y., *Angew. Chem. Int. Ed.*, 46, **2007**, 7220.

- [46] Thomas JM, Maschmeyer T, Johnson BFG, Shephard DS., *J. Mol. Catal. A: Chem.*, 141, **1999**, 139.
- [47] Goettmann F, Sanchez C., *J. Mater. Chem.*, 17, **2007**, 24.
- [48] Fraile JM, Garcia JI, Mayoral JA., *Chem. Rev.*, 109, **2009**, 360.
- [49] Bigi F, Franca B, Moroni L, Maggi R, Sartori G., *Chem. Comm.*, **2002**, 716.
- [50] Xiang S, Zhang YL, Xin Q, Li C., *Chem Commun.*, **2002**, 2696.
- [51] Zhang H, Zhang Y, Li C., *J. Catal.*, 238, **2006**, 369.
- [52] Thomas JM, Johnson BFG, Raja R, Sankar G, Midgley PA., *Acc. Chem. Res.*, 36, **2003**, 20.
- [53] Basset JM, Choplin A., *J. Mol. Catal.*, 21, **1983**, 95.
- [54] Basset JM, Ugo R., Modern Surface Organometallic Chemistry. In: Basset JM, Psaro R, Roberto D, Ugo R, editors. Wiley-VCH: Weinheim, Germany; **2009**, 1.
- [55] Ugo R, Psaro R, Zanderighi GM, Basset JM, Theolier A, Smith AK. Fundamental Research in Homogeneous Catalysis. Tsutsui M, editor; Plenum Press: New York, NY, USA; **1979**; vol. 3: 579.
- [56] Besson B, Moraweck B, Smith AK, Basset JM, Psaro R, Fusi A, Ugo R., *J. Chem. Soc., Chem. Commun.*, **1980**, 569.
- [57] Maschmeyer T, Rey F, Sankar G, Thomas JM., *Nature.*, 378, **1995**, 159.
- [58] Corma A, Diaz U, Fornes V, Jorda JL, Domine M, Rey F., *Chem. Commun.*, **1999**, 779.
- [59] Guidotti M, Ravasio N, Psaro R, Ferraris G, Moretti G., *J. Catal.*, 214, **2003**, 242.
- [60] Ravasio N, Zaccheria F, Guidotti M, Psaro R., *Top. Catal.*, 27, **2004**, 157.
- [61] Guidotti M, Ravasio N, Psaro R, Gianotti E, Marchese L, Coluccia S., *J. Mol. Catal. A Chem.*, 250, **2006**, 218.
- [62] Kholdeeva OA, Ivanchikova ID, Guidotti M, Ravasio N., *Green Chem.*, 9, **2007**, 731.
- [63] Kholdeeva OA, Ivanchikova ID, Guidotti M, Pirovano C, Ravasio N, Barmatova MV, Chesalov YA., *Adv. Synth. Catal.*, 351, **2009**, 1877.
- [64] Guidotti M, Pirovano C, Ravasio N, Lázaro B, Fraile JM, Mayoral JA, Coq B, Galarneau A., *Green Chem.*, 11, **2009**, 1421.
- [65] Guidotti M, Pirovano C, Ravasio N, Lázaro B, Fraile JM, Mayoral JA, Coq B, Galarneau A., *Green Chem.*, 11, **2009**, 1421.
- [66] Sheldon RA., *J. Mol. Catal.*, 7, **1980**, 107.
- [67] Wulff HP, Wattimena F, inventors; Shell Oil Co., assignee. Olefin epoxidation. US Patent 4,021,454. **1977**, May 3.

- [68] Joustra AH, de Bruijn W, Drent E, Reman WG, inventors; Shell Int Research, assignee. A process for the preparation of an oxirane compound. EU Patent 0 345 856. **1989**, December 13.
- [69] Sheldon RA, Kochi JK. Metal-catalyzed oxidations of organic compounds. New York: Academic Press; **1981**., 275.
- [70] Buijink JKF, VanVlaanderen JJM, Crocker M, Niele FGM., *Catal. Today*, 93-95, **2004**, 199
- [71] Sheldon RA, Dakka J., *Catal. Today*, 19, **1994**, 215.
- [72] Chiker F, Launay F, Nogier JP, Bonardet JL., *Green Chem.*, 5, **2003**, 318.
- [73] Li KT, Lin CC, Lin PH. Propylene Epoxidation with Ethylbenzene Hydroperoxide over Ti-Containing Catalysts Prepared by Chemical Vapor Deposition. In: Mechanisms in Homogeneous and Heterogeneous Epoxidation Catalysis, Oyama ST, editor. Elsevier, Amsterdam. **2008**, p 373-386.
- [74] Srinivasan S, Datye AK, Smith MH, Peden CHF., *J. Catal.*, 145, **1994**, 565.
- [75] Cativiela C, Fraile JM, Garcia JI, Mayoral JA., *J. Mol. Catal. A*, 112, **1996**, 259.
- [76] Luan Z, Maes EM, van der Heide PAW, Zhao D, Czernuszewicz RS, Kevan L., *Chem. Mater.*, 11, **1999**, 3680.
- [77] Bouh AO, Rice GL, Scott SL., *J. Am. Chem. Soc.*, 121, **1999**, 7201.
- [78] Fraile JM, Garcia JI, Mayoral JA, Vispe E., *J. Catal.*, 189, **2000**, 40.
- [79] Maksimchuk NV, Melgunov MS, Mrowiec-Białoń J, Jarzębski AB, Kholdeeva OA., *J. Catal.*, 235, **2005**, 175.
- [80] Ahn WS, Lee DH, Kim JH, Seo G, Ryoo R., *Appl. Catal. A: Gen.*, 181, **1999**, 39.
- [81] Yuan Q, Hagen A, Roessner F., *Appl. Catal. A: Gen.*, 303, **2006**, 81.
- [82] Fraile JM, Garcia JI, Mayoral JA, Vispe E., *J. Catal.*, 204, **2001**, 146.
- [83] Fraile JM, Garcia JI, Mayoral JA, Vispe E., *Appl. Catal. A*, 245, **2003**, 363.
- [84] Barrio L, Campos-Martin JM, de Frutos-Escrig MP, Fierro JLG., *Micropor. Mesopor. Mater.*, 113, **2008**, 542.
- [85] Ferreira P, Goncalves IS, Kühn FE, Pillinger M, Rocha J, Santos AM, Thursfield A., *Eur. J. Inorg. Chem.*, **2000**, 551.
- [86] Perez Y, Quintanilla DP, Fajardo M, Sierra I, del Hierro I., *J. Mol. Catal. A: Chem.*, 271, **2007**, 227.
- [87] Brutchey RL, Mork BV, Sirbuly DJ, Yang P, Don Tilley T., *J. Mol. Catal. A: Chem.*, 238, **2005**, 1.
- [88] Tuel A, Hubert-Pfalzgraf LG., *J. Catal.*, 217, **2003**, 343.
- [89] Kim NK, Kim GJ, Ahn WS., *React. Kinet. Catal. Lett.*, 71(2), **2000**, 273.



- [90] Thomas JM, Raja R. , *Stud. Surf. Sci. Catal.*, 148, **2004**, 163.
- [91] Sakthivel A, Zhao J, Kühn FE., *Catal. Lett.*, 102, **2005**, 115.
- [92] Boronat M, Concepcion P, Corma A, Navarro MT, Renz M, Valencia S., *Phys. Chem. Chem. Phys.*, 11, **2009**, 2876.
- [93] Vidal V, Theolier A, Thivolle-Cazat J, Basset JM., *Science*, 276, **1997**, 99.
- [94] Fraile JM, Garcia JI, Mayoral JA, Pires E, Salvatella L, Ten M., *J. Phys. Chem. B.*, 103, **1999**, 1664.
- [95] Meunier D, Piechaczyk A, Mallmann A, De A, Basset JM., *Angew. Chem. Int. Ed.*, 38, **1999**, 3540.
- [96] Nozkaki C, Lugmair CG, Bell AT, Tilley TD., *J. Am. Chem. Soc.*, 124, **2002**, 13194.
- [97] Ahn H, Nicholas CP, Marks TJ., *Organometallics*, 21, **2002**, 1788.
- [98] Ahn H, Marks TJ., *J. Am. Chem. Soc.*, 124, **2002**, 7103.
- [99] Bell AT., *Science*, 299, **2003**, 1688.
- [100] Coperet C, Chabanas M, Saint-Arroman MP, Basset JM., *Angew. Chem. Int. Ed.*, 42, **2003**, 156.
- [101] Yang Q, Coperet C, Li C, Basset JM., *New J. Chem.*, 27, **2003**, 319.
- [102] Nenu CN, Weckhuysen BM., *Chem. Commun.*, **2005**, 1865.
- [103] Herrera JE, Kwak JH, Hu JZ, Wang Y, Peden CHF, Macht J, Iglesia E., *J. Catal.*, 239, **2006**, 200.
- [104] Jarupatrakorn J, Tilley JD., *J. Am. Chem. Soc.*, 124, **2002**, 8380.
- [105] Furdala KL, Tilley TD., *J. Catal.*, 216, **2003**, 265.
- [106] Bell AT., *Science*, 299, **2003**, 1688.
- [107] Drake IJ, Furdala KL, Bell AT, Tilley TD., *J. Catal.*, 230, **2005**, 14.
- [108] Ruddy DA, Ohler NL, Bell AT, Tilley TD., *J. Catal.*, 238, **2006**, 277.
- [109] Ryoo R, Jun S, Man Kim J, Jeong Kim M., *Chem. Commun.*, **1997**, 2225.
- [110] Gu YY, Zhao XY, Zhang GR, Ding HM, Shan YK., *Appl. Catal. A: Gen.*, 328, **2007**, 150.
- [111] Kakihana M, Tada M, Shiro M, Petrykin V, Osada M, Nakamura Y., *Inorg. Chem.*, 40, **2001**, 891.
- [112] Yang Q, Li C, Yuan S, Li J, Ying P, Xin Q, Shi W., *J. Catal.*, 183, **1999**, 128.
- [113] Anpo M, Dohshi S, Kitano M, Hu Y, Takeuchi M, Matsuoka M., *Annu. Rev. Mater. Res.*, 35, **2005**, 1.
- [114] Krijnen S, Abbenhuis HCL, Hanssen RWJM, Van Hooff JHC, Van Santen RA., *Angew. Chem. Int. Ed.*, 37, **1998**, 356.
- [115] Heinrichs C, Hölderich WF., *Catal. Lett.*, 58, **1999**, 75.

- [116] De Vos D, Hermans I, Sels B, Jacobs P. Hybrid Oxidation Catalysts from Immobilized Complexes on Inorganic Microporous Supports. In: Catalysts for Fine Chemical Synthesis. Derouane E.G., editor. Wiley-VCH: Weinheim (Germany). **2006**, 207-240.
- [117] Bowers C, Dutta PK., *J. Catal.*, 122, **1990**, 271.
- [118] Sabater MJ, Corma A, Domenech A, Fornes V, Garcia H., *Chem. Commun.*, **1997**, 1285
- [119] Ogunwumi SB, Bein T., *Chem. Commun.*, **1997**, 901.
- [120] Knops-Gerrits PP, Trujillo CA, Zhan BZ, Li XY, Rouxhet P, Jacobs PA., *Top. Catal.*, 3, **1996**, 437.
- [121] Zhang R, Yu WY, Wong KY, Che CM., *J. Org. Chem.*, 66, **2001**, 8145.
- [122] Algarra F, Esteves MA, Fornes V, García H, Primo J., *New J. Chem.*, 22, **1998**, 333.
- [123] Tanamura Y, Uchida T, Teramae N, Kikuchi M, Kusaba K, Onodera Y., *Nano Lett.*, 1, **2001**, 387.
- [124] Yang HQ, Li J, Yang J, Liu ZM, Yang QH, Li C., *Chem. Commun.*, **2007**, 1086.
- [125] Yang H, Zhang L, Su W, Yang Q, Li C., *J. Catal.*, 248, **2007**, 204.
- [126] J.S. Beck, J.C. Vartuli, W.J. Roth, M.E. Leonowicz, C.T. Kresge, K.D. Schmitt, C.T.-W. Chu, D.H. Olson, E.W. Sheppard, S.B. McCullen, J.B. Higgins, J.L. Schlenkert, *J. Am. Chem. Soc.*, 114, **1992**, 10834
- [127] W.M. Meier, D.H. Olson, *Atlas of Zeolite Structure Types, 3rd. ed. revised; Butterworth-Heineman & Co.: Guildford, 1992.*
- [128] A. Corma, *Chem.Rev.*, 97, **1997**, 2373
- [129] G.D. Stucky, D. Zhao, P. Yang, W. Lukens, N. Melosh, B.F. Chmelka, in: L. Bonneviot, F. Béland, C. Danumah, S. Giasson, S. Kaliaguine (Eds.), *Mesoporous Molecular Sieves, Studies in Surface Science and Catalysis*, vol. 117, Elsevier, Amsterdam, **1998**, p. 1.
- [130] A.E.C. Palmqvist, *Curr. Opin. Colloid Interface Sci.*, 8, **2003**, 145.
- [131] J. Patarin, B. Lebeau, R. Zana, *Curr. Opin. Colloid Interface Sci.*, 7, **2002**, 107.
- [132] G.J.A.A. Soler-Illia, C. Sanchez, B. Lebeau, J. Patarin, *Chem. Rev.*, 102, **2002**, 4093.
- [133] P. Cool, T. Linssen, K. Cassiers, E.F. Vansant, *Recent Res. Devel. Mater. Sci.*, 3, **2002**, 871.
- [134] T. Linssen, K. Cassiers, P. Cool, E.F. Vansant, *Adv. Colloid Interface Sci.*, 103, **2003**, 121.
- [135] Y.K. Hwang, J.S. Chang, Y.U. Kwon, S.E. Park, in: S.E. Park (Ed.), *Nanotechnology in Mesoporous Materials, Studies in Surface Science and Catalysis*, vol. 146, Elsevier, Amsterdam, **2003**, p. 101.
- [136] P. Selvam, S.K. Bhatia, C.G. Sonwane, *Ind. Eng. Chem. Res.*, 40, **2001**, 3237.

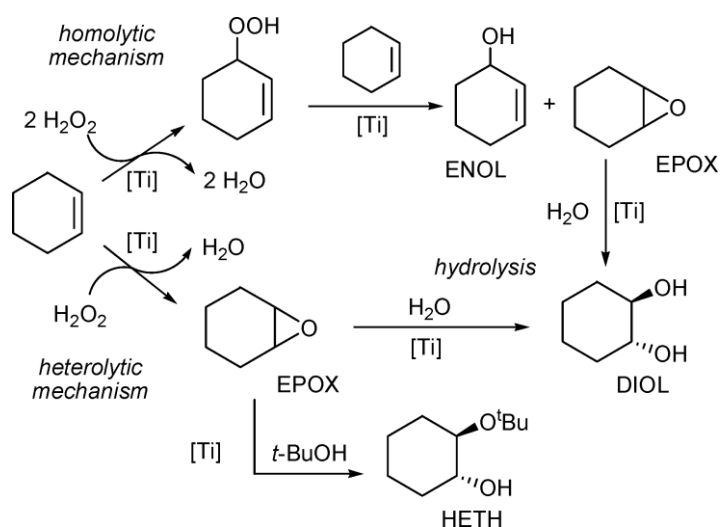
- [137] Y.K. Hwang, J.-S. Chang, Y.-U. Kwon, S.-E. Park, *Micropor. Mesopor. Mater.*, **68**, **2004**, 21.
- [138] B.L. Newalkar, S. Komarneni, H. Katsuki, *Chem. Commun.*, **2000**, 2389
- [139] E.B. Celer, M. Jaroniec, *J. Am. Chem. Soc.*, **128** (44), **2006**, 14408
- [140] B.L. Newalkar, S. Komarneni, *Chem. Commun.*, **2002**, 1774
- [141] K. Szczodrowki, B. Prélôt, S. Antenois, J. Zajac, M. Lindheimer, D. Jones, A. Julbe, A. Van Der Lee, *Micropor. Mesopor. Mater.*, **110**, **2008**, 111
- [142] D. Zhao, Q. Huo, J. Feng, B.F. Chmelka, G.D. Stucky, *J. Am. Chem. Soc.*, **120**, **1998**, 6024.
- [143] Y. Bennadja, P. Beaunier, D. Margolese, A. Davidson, *Micropor. Mesopor. Mater.*, **44–45**, **2001**, 147.
- [144] S. Ruthstein, V. Frydman, S. Kababya, M. Landau, D. Goldfarb, *J. Phys. Chem. B*, **107**, **2003**, 1739.
- [145] D. Huang, G.S. Lou, Y.J. Wang, *Micropor. Mesopor. Mater.*, **84**, **2005**, 27.
- [146] C.T. Kresge, M.E. Leonowics, W.J. Roth, J.C. Vartuli, *US Patent 5 098 684*, **1992**
- [147] J.S. Beck, C.T. Chu, I.D. Johnson, C.T. Kresge, M.E. Leonowics, W.J. Roth, J.C. Vartuli, *US Patent 5 108 725*, **1992**.
- [148] J.S. Beck, D.C. Calabro, S.B. McCullen, B.P. Pelrine, K.D. Schmitt, J.C. Vartuli, *US Patent 5 145 816*, **1992**
- [149] J.S. Beck, C.T. Kresge, M.E. Leonowicz, W.J. Roth, J.C. Vartuli, *US Patent 5 264 203*, **1993**
- [150] J.S. Beck, K.D. Smith, J.C. Vartuli, *US Patent 5 334 368*, **1994**
- [151] C.T. Kresge, M.E. Leonowicz, W.J. Roth, J.C. Vartuli, J.C. Beck, *Nature*, **359**, **1992**, 710.
- [152] J.S. Beck, J.C. Vartuli, W.J. Roth, M.E. Leonowicz, C.T. Kresge, K.D. Schmitt, C.T.W. Chu, D.H. Olson, E.W. Sheppard, S.B. McCullen, J.B. Higgins, J.L. Schlenker, *J. Am. Chem. Soc.*, **114**, **1992**, 10834.
- [153] J. Silvestre-Albero, A. Sepúlveda-Escribano, F. Rodríguez-Reinoso, *Micropor. Mesopor. Mater.*, **113**, **2008**, 362
- [154] K. Cassiers, T. Linsen, M. Mathieu, M. Benjelloun, K. Schrijnemakers, P. Van Der Voort, P. Cool, E.F. Vansant, *Chem. Mater.* **14**, **2002**, 2317
- [155] J.M. Kim, S. Jun, R. Ryoo, *J. Phys. Chem. B*, **103**, **1999**, 6200
- [156] R. Ryoo, S. Jun, *J. Phys. Chem.*, **101**, **1997**, 317
- [157] J.M. Kim, J.H. Kwak, S. Jun, R. Ryoo, *J. Phys. Chem. B*, **99**, **1995**, 16742

- [158] J. Silvestre-Albero, J.C. Serrano-Ruiz, A. Sepúlveda-Escribano, F. Rodríguez-Reinoso, *Appl. Catal. A: Gen.*, 135 (1), **2008**, 16
- [159] V. Meynen, P. Cool, E.F. Vansant, *Microp. Mesop. Mater.*, 125, **2009**, 170
- [160] G. Oye, J. Sjöblom, M. Stöcker, *Adv. Colloid Interface*, 89, **2001**, 439
- [161] D. Zhao, Q. Huo, J. Feng, B.F. Chmelka, G.D. Stucky, *J. Am. Chem. Soc.*, 120, **1998**, 6024
- [162] Y. Bennadja, P. Beaunier, D. Margolese, A. Davidson, *Micropor. Mesopor. Mater.*, 147, **2001**, 44
- [163] M. Kruk, M. Jaroniec, C.H. Ko, R. Ryoo, *Chem. Mater.*, 12, **2000**, 1961
- [164] A. Nossov, E. Haddad, F. Guenneau, A. Galarneau, F. Di Renzo, F. Fajula, A. Gedeon, *J. Phys. Chem. B*, 107, **2003**, 12456
- [165] K. Miyazawa, S. Inagaki, *Chem. Commun.*, **2000**, 2121
- [166] A. Galarneau, H. Cambon, F. Di Renzo, R. Ryoo, M. Choi, F. Fajula, *New. J. Chem.*, 27 **2003**, 73
- [167] A. Galarneau, H. Cambon, F. Di Renzo, F. Fajula, *Langmuir*, 17, **2000**, 8328
- [168] A.M. Silvestre-Albero, E.O. Jardim, E. Bruijn, V. Meynen, P. Cool, A. Sepúlveda-Escribano, J. Silvestre-Albero, F. Rodríguez-Reinoso, *Langmuir*, 25, **2009**, 939
- [169] Y. Ueno, A. Tate, O. Niwa, H.-S. Zhou, T. Yamada, I. Honma, *Chem. Commun.*, **2004**, 746
- [170] R. Ryoo, C.H. Ko, M. Kruk, V. Antochshuk, M.J. Jaroniec, *J. Phys. Chem. B*, 104, **2000**, 11465
- [171] D. Zhao, Q. Huo, J. Feng, B.F. Chmelka, G.D. Stucky, *J. Am. Chem. Soc.*, 120, **1998**, 6024
- [172] S. Ruthstein, V. Frydman, S. Kababya, M. Landau, D. Goldfarb, *J. Phys. Chem. B*, 107 **2003**, 1739
- [173] Y. Zheng, Y.-Y. Won, F.S. Bates, G.T. Davis, L.E. Scriven, Y. Talmon, *J. Phys. Chem. B*, 103, **1999**, 10331
- [174] P. Kipkemboi, A. Fodgen, V. Alfredsson, K. Flodström, *Langmuir*, 17, **2001**, 5398
- [175] P. Alexandridis, T.A. Hatton, *Colloid Surf. A*, 96, **1995**, 1
- [176] S. Ruthstein, V. Frydman, S. Kababya, M. Landau, D. Goldfarb, *J. Phys. Chem. B*, 107, **2003**, 1739
- [177] M. Impéror-Clerc, P. Davidson, A. Davidson, *J. Am. Chem. Soc.*, 122, **2000**, 11925
- [178] Z.H. Luan, M. Hartmann, D.Y. Zhao, W.Z. Zhou, L. Kevan, *Chem. Mater.*, 11, **1999**, 1621

- [179] Y.H. Yue, A. Gedeon, J.L. Bonardet, N. Melosh, J.B. DEspinose, J. Fraissard, *Chem. Commun.*, **1999**, 1967
- [180] Z.H. Luan, E.M. Maes, P.A.W. VanderHeide, D.Y. Zhao, R.S. Czernuszewicz, L. Kevan, *Chem. Mater.*, **11**, **1999**, 3680
- [181] M.S. Morey, S. O'Brien, S. Schwarz, G.D. Stucky, *Chem. Mater.*, **12**, **2000**, 898
- [182] S.J. Bae, S.W. Kim, T. Hyeon, B.M. Kim, *Chem. Commun.*, **2000**, 31
- [183] D. Margolese, J.A. Melero, S.C. Christiansen, B.F. Chmelka, G.D. Stucky, *Chem. Mater.*, **12**, **2000**, 2448
- [184] A.M. Liu, K. Hidajat, S. Kawi, D.Y. Zhao, *Chem. Commun.*, **2000**, 1145
- [185] P.D. Yang, G. Wirnsberger, H.C. Huang, S.R. Cordero, M.D. McGehee, B. Scott, T. Deng, G.M. Whitesides, B.F. Chmelka, S.K. Buratto, G.D. Stucky, *Science*, **287**, **2000**, 465
- [186] M.H. Huang, A. Choudrey, P.D. Yang, *Chem. Commun.*, **2000**, 1063
- [187] A. Galarneau, H. Cambon, F. Di Renzo, F. Fajula, *Langmuir*, **17**, **2001**, 8328
- [188] W. Buchner, R. Schliebs, G. Winter, K.H. Buchel, *Industrielle Anorganische Chemie*, VCH, Weinheim, Germany, 2nd edn., **1986**
- [189] C.W. Jones, *Applications of Hydrogen Peroxide and Derivatives*, Royal Society of Chemistry, Cambridge, **1999**
- [190] *Kirk-Othmer Encyclopedia of Chemical Technology*, ed. J.I. Kroschwitz and M. Howe-Grant, John Wiley & Sons, Inc., New York, 4<sup>th</sup> edn., **1995**, Vol. 13, p. 961
- [191] R. Noyori, M. Aoki, K. Sato, *Chem. Comm.*, **2003**, 1977
- [192] Sumitomo Chemical News Release, 2000, Oct. 11; <http://www.sumitomo-chem.co.jp/english/elnewsrelease/pdf/20001011e.pdf>.
- [193] Dow Products and Business News, 2002, Aug. 1; [http://www.dow.com/dow\\_news/prodnews/2002/20020801a.htm](http://www.dow.com/dow_news/prodnews/2002/20020801a.htm).
- [194] F. Carniato, C. Bisio, E. Boccaleri, M. Guidotti, E. Gavrilova, L. Marchese, *Chem. Eur. J.*, **14**, **2008**, 27
- [195] Y. Deng, C. Lettmann, W.F. Maier, *Appl. Catal. A: General*, **214**, **2001**, 31
- [196] M. Ziolk, *Cat. Today*, **90**, **2004**, 145
- [197] O.A. Kholdeeva, N.N. Trukhan, *Russ. Chem. Rev.*, **75**, **2006**, 411
- [198] J. Li, C. Zhou, H. Xie, Z.M. Ge, L. Yuan, X. Li, *J. Nat. Gas. Chem.*, **15**, **2006**, 164
- [199] R. A. Sheldon, M. Wallau, I.W.C.E. Arends, U. Schuchardt, *Acc. Chem. Res.*, **31**, **1998**, 485
- [200] L.Y. Chen, G.K. Chuahand, S. Jaenicke, *Catal. Lett.*, **50**, **1998**, 107.

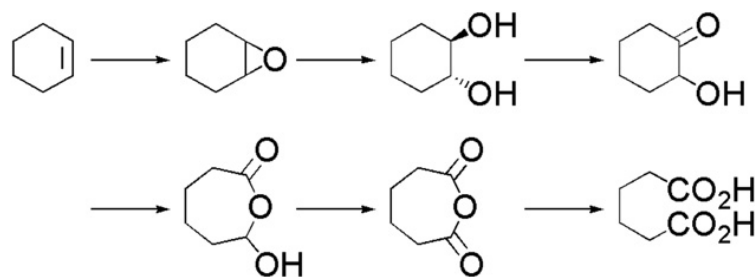
## Chapter 1. Ti-containing heterogeneous catalysts in cyclohexene epoxidation with hydrogen peroxide.

The epoxidation of cyclohexene is a reaction of a great interest. It is used as a test reaction which allows to evaluate the activity of the catalyst and to differentiate which pathway is taking place during the reaction: homolytic or heterolytic one (Scheme 1.1) [1]. Moreover, cyclohexene oxide is a useful monomer in polymerization and coating industries [2].



**Scheme 1.1.** Homolytic and heterolytic pathways

Cyclohexene epoxide is used in the synthesis of pesticides, pharmaceuticals, perfumery, and in the production of adipic acid [3, 4]. Adipic acid is an important chemical, which production is necessary for the manufacture of nylon-6,6 that is used in carpet fibers, upholstery, tire reinforcements, auto parts, apparel, and other products. Worldwide industrial adipic acid production is up to 2.5 billion kilograms per year [3] and it is currently produced by the oxidation of a cyclohexanol/cyclohexanone mixture or cyclohexane with nitric acid [5]. During this synthesis, nitrous oxide (N<sub>2</sub>O), which has a strong impact on global warming and ozone depletion [6] is generated (0.3 tonne emitted per tonne of adipic acid produced). Therefore, the development of environmentally friendly practical procedure is highly desirable. A potential alternative route for adipic acid production is the epoxidation of cyclohexene by hydrogen peroxide with the following opening and transformation to a diol, then a Bayer-Villiger oxidation and multiple hydrolysis steps resulting in adipic acid (Scheme 1.2) [3, 7].



**Scheme 1.2.** The reaction pathway for the direct oxidation of cyclohexene with aqueous  $\text{H}_2\text{O}_2$  to adipic acid.

For this purpose, various homogeneous and heterogeneous systems were studied. Different homogeneous systems showed to be active. However, a complete separation of the homogeneous catalyst from the final mixture can pose some problems.

In the field of heterogeneous catalysis, all the titanium-containing heterogeneous catalysts showed poor activity in the cyclohexene epoxidation with aqueous  $\text{H}_2\text{O}_2$  [8,9,10,11]. Mesoporous Ti-silicates are easily deactivated in the presence of aqueous  $\text{H}_2\text{O}_2$  due to the presence and the in situ co-production of water. Most transition metal catalysts are very sensitive to water which cause hydrolysis of Ti-O-Si bonds and, hence, leaching of the active metallic sites [4, 12-16]. Gianotti et. al. have studied the adsorption of  $\text{H}_2\text{O}_2$  and TBHP on Ti-MCM-41 (Fig. 1.1) [17]. They have observed that after the Ti-MCM-41 contact with anhydrous TBHP, the sample turns yellow, signifying the formation of Ti(IV)-peroxo complex. The adsorption of TBHP and produced a shift of the band at 210 nm (Fig 1.1 A, curve a), typical of Ti (IV) tetrahedral centers, to higher wavelength (Fig. 1.1 A, curve b). After reactivation in  $\text{O}_2$  at  $550^\circ\text{C}$  the features related to the presence of Ti(IV)-peroxo species were removed (Fig. 1.1 A, curve c) and the adsorption edge is almost completely restored. In the case of  $\text{H}_2\text{O}_2$  adsorption, the UV-Vis spectra changes irreversibly. The band at 210 nm is broadened and shifted to 250 nm upon  $\text{H}_2\text{O}_2$  contact (Fig. 1.1 B, curve b). This shift is larger than one observed upon TBHP interaction attributed to the formation of 6-coordinated Ti(IV) species. After the reactivation of the catalyst in  $\text{O}_2$  at  $550^\circ\text{C}$  (Fig. 1.1 B, curve c) the original absorption maximum at 210 nm is not restored and a relevant fraction of species absorbing in the range 300-350 nm is still present.

A

B

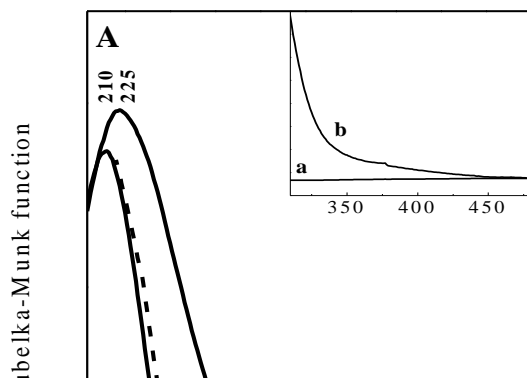
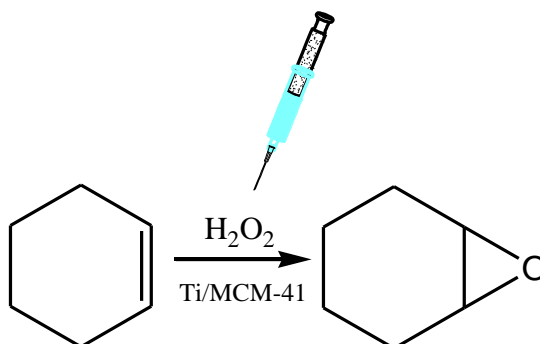


**Figure 1.1.** DR-UV-Vis spectra of calcined Ti-MCM-41 (spectra A, B curve a), after TBHP (spectra A)  $\text{H}_2\text{O}_2$  (spectra B) adsorption at room temperature (b), after reactivation in  $\text{O}_2$  at  $550^\circ\text{C}$  (c).

Better results were achieved by applying the slow dropwise addition of  $\text{H}_2\text{O}_2$  technique (Scheme 3) [18, 19], thus increasing the yield of cyclohexene epoxide formation with respect to the addition of the oxidant in one aliquot. Several authors focused their attention on the slow dropwise addition technique of hydrogen peroxide were published [18,20,21,22]. The positive role of the slow dropwise addition of aqueous hydrogen peroxide (Scheme 1.3) was highlighted not only in terms of reduced  $\text{H}_2\text{O}_2$  decomposition into oxygen and water, but also of lower degree of titanium leaching and enhanced catalyst stability [23].



**Scheme 1.3.** Slow dropwise addition of  $\text{H}_2\text{O}_2$

However, some key factors deserve a deeper understanding: 1) the role of the silica support in the epoxidation reaction of cyclohexene by the slow addition of  $\text{H}_2\text{O}_2$  (aq. 30%) and, 2) how the



morphology and topology of the support (convexity and concavity) may affect the stability to hydrolysis and to leaching in repeated recycles.

## Results and discussion

For these reasons, the first part of the work was aimed at testing the stability, re-usability and heterogeneous character of the systems.

Three kinds of titanocene-grafted silica solids with different textural properties were chosen as catalysts: Ti/SiO<sub>2</sub> Aerosil, with a non-ordered network of mesopores, Ti/MCM-41, with an ordered one-dimensional array of mesopores with hexagonal symmetry, and Ti/MCM-48, with an ordered three-dimensional network of mesopores with cubic symmetry. To check the stability and re-usability, the catalyst was recovered after 3 h of reaction (that corresponds to the end of the slow-addition time). The catalyst was then filtered off, dried and calcined for 3 h at 550°C (this high-temperature calcination step is essential to have a complete and thorough removal of the adsorbed heavy organic by-products). The recovered catalyst was again used for the epoxidation reaction under the same conditions (Table 1.1) for two catalytic runs more.

**Table 1.1** Epoxidation of cyclohexene by slow addition of H<sub>2</sub>O<sub>2</sub>

Catalyst	Ti content <sup>a</sup> (wt.%)	Catalytic run	Epoxide yield (%)	TON <sup>b</sup> at 3h
Ti/SBA-15	0.78	1	26	16
		2	37	22
		3	35	21
Ti/SiO <sub>2</sub> Aerosil	0.61	1	33	30
		2	33	30
		3	36	29
Ti/MCM-41	0.80	1	33	21
		2	11	7
		3	11	8
Ti/MCM-48	0.79	1	25	15
		2	29	17
		3	31	17

Reaction conditions: cyclohexene = 2,5 mmol, mesitylene = 1mmol, H<sub>2</sub>O<sub>2</sub> (30% w/w aqueous solution)= 1 mmol, solvent acetonitrile, reaction temperature = 85°C, reaction duration = 3h; <sup>a</sup>determined by ICP; <sup>b</sup>Turn-Over Number (moles of produced epoxide per mole of titanium).

The activity of the studied catalysts follows the order: Ti/SiO<sub>2</sub> Aerosil > Ti/SBA-15 > Ti/MCM-48 > Ti/MCM-41. In all tests, the only detected product was cyclohexene epoxide (chemoselectivity > 98%). In particular, the formation of enol and enone, due to oxidation at the allylic position, was not detected. This means that the reaction follows a heterolytic mechanism

(Scheme 1.1). It was observed that Ti/SBA-15 and Ti/SiO<sub>2</sub> Aerosil possess both good activity and stability even after three catalytic runs. Ti/MCM-48 shows a slight lower activity, even if its stability is maintained after three cycles. On the contrary, Ti/MCM-41 is the least stable catalyst. All the data fit well with the DRS-UV-VIS analysis (performed in collaboration with the “Institut de Chimie Moléculaire et des Matériaux de Montpellier” - CNRS, in Montpellier).

The band at 210-230 nm, a characteristic of Ti(IV) isolated sites existence in tetrahedral environment [24,25,26], is present in all the catalysts spectra (Fig. 1.2-1.5). In all UV spectra after catalysis, a shift towards lower wavelength is observed, that suggests a better organization of Ti occurring during the catalysis. This might be an explanation for the increase in epoxide yield after recycling for all catalysts (Table 1.1), except MCM-41. Only in the case of Ti/MCM-41, UV spectra recorded after the recycling procedure (Fig. 1.2) present a wide shoulder between 300 and 400 nm, which is often related to the formation of TiO<sub>2</sub> nanodomains. This could explain the loss in activity observed for this catalyst after the first and the second recycle (epoxide yield decreasing from 33 to 11%).

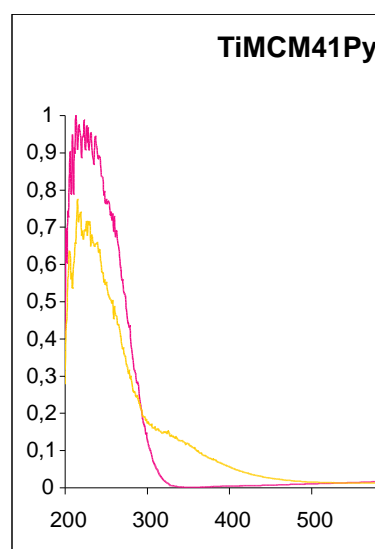


**Figure 1.2.** DR-UV-Vis spectra of calcined Ti/MCM-41 before (red line) and after three runs of catalysis (yellow line) in the presence of aqueous H<sub>2</sub>O<sub>2</sub>.

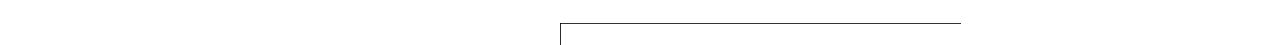


**Figure 1.3.** DR-UV-Vis spectra of calcined Ti/SBA-15 before (blue line) and after three runs of catalysis (purple line) in the presence of aqueous H<sub>2</sub>O<sub>2</sub>

**Figure 1.4.** DR-UV-Vis spectra of calcined Ti/MCM-48 before (pink line) and after three runs of catalysis (yellow line) in the presence of aqueous H<sub>2</sub>O<sub>2</sub>

**Figure 1.5.** DR-UV-Vis spectra of calcined Ti/SiO<sub>2</sub>-Aerosil before (blue line) and after three runs of catalysis (purple line) in the presence of aqueous H<sub>2</sub>O<sub>2</sub>

Another factor that is not fully clarified yet is the effect of the morphology and topology of the silica support (in particular, its convexity or concavity) and its role in the stability to repeated catalytic cycles. In principle, parameters such as the hydrophobic/hydrophilic character or the curvature radius of the mesopores could be taken into account. It was observed that the influence of the convexity of the support surface showed a positive effect on the catalytic stability. In fact, the stability is good on Ti/SiO<sub>2</sub> Aerosil and Ti/MCM-48, both having a convex silica surface, whereas it is very poor on Ti/MCM-41, with a concave internal surface. The case of Ti/SBA-15 is apparently difficult to interpret, but the bimodal micro- and mesoporous network (with mesopores ca. 10 nm) can account for the notable stability of this catalyst. Moreover, after the analysis of N<sub>2</sub> adsorption/desorption isotherms, it was found that the inner porosity of SBA-15 has changed from cylindrical with rugosity to a more constricted one keeping the hexagonal arrangement after catalysis (Fig. 1.6).

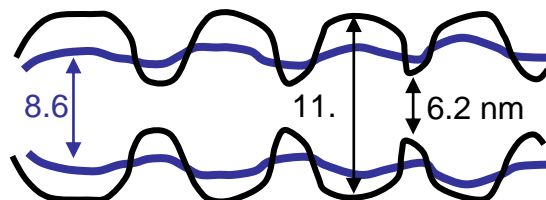


**Figure 1.6.** Restructuration of SBA-15 during catalysis.

Furthermore, the different surface silanol density population can account for the improved robustness of this catalyst. To calculate the silanol density population, thermogravimetric analyses (TGA) were performed and they are described in the following paragraph.

### Set-up for the determination of surface concentration of OH groups

By TGA analysis it is possible to determine:

- 1) the temperature of the pretreatment of the material (= the temperature at which the condensation of silanols occurs);
- 2) the quantity of free SiOH groups (can be obtained from  $\Delta W$ );
- 3) the temperature at which free SiOH groups are still present;
- 4) hydrophobicity / hydrophilicity.

To evaluate the SiOH concentration at the surface of the materials a series of TGA measurements was performed (Fig. 1.7, 1.8).  $\Delta W$  (weight loss) was calculated in the range of 120 – 900°C. On the analysis of Ti/SBA-15 the presence of two steps is observed. At the temperatures 50-120°C the desorption of physisorbed water occurs. Then, the weight loss between 120°C and 600°C corresponds to the gradual condensation of hydrogen-bonded and free silanols. Between 600°C and 900°C the collapse and vitrification of the mesoporous structure occurs [27,28].

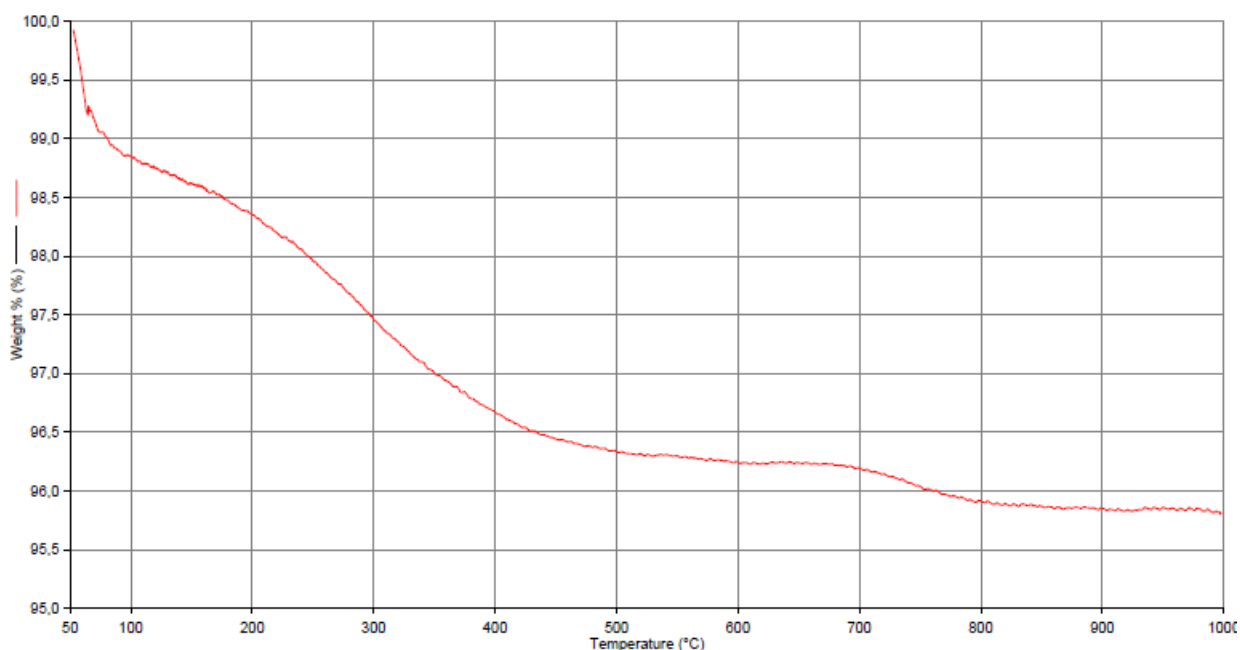


**Figure 1.7.** TGA analysis of Ti/SBA-15. Analysis temperature range: 50-1000°C, heating rate 5°C min<sup>-1</sup>

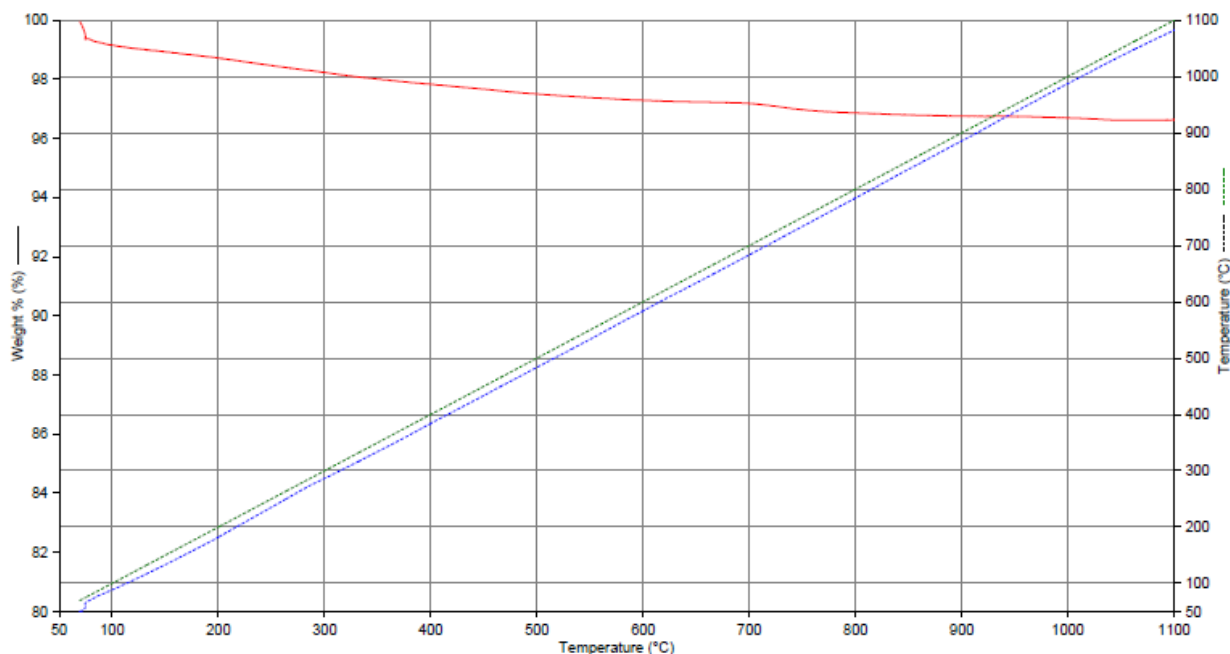


**Figure 1.8.** TGA analysis of SBA-15. Analysis temperature: 50-1000°C, rate 5°C min<sup>-1</sup>. Programme and sample temperature, blue and green line, respectively.

The silanol density SiOH/Ti mol/mol (Table 1.2) was calculated according to the following relations:

$$\text{SiOH}^a = [\Delta W (\text{g}/100\text{g}_{\text{material}}) \cdot 1000 \cdot 2] / [\text{Mr}(\text{H}_2\text{O}) \cdot 100 \text{g}_{\text{material}}]$$

$$\text{OH}/\text{nm}^2 = [\text{SiOH mmol}/\text{g} \cdot 10^{-3} \cdot N_A] / [\text{nm}^2/\text{g} \cdot 10^{18}]$$

$$\text{SiOH}/\text{Ti mol}/\text{mol} = [\text{SiOH mmol}/\text{g} \cdot 100\text{g}_{\text{material}} \cdot \text{Mr}(\text{Ti})] / [\text{Ti content} (\%) \cdot 1000]$$

**Table 1.2**  $\Delta W$  (%): weight loss (%) in the temperature range 120-900°C; OH/nm<sup>2</sup>: considering that 1 molecule of H<sub>2</sub>O is generated by the condensation of 2 OH groups; <sup>a</sup> computed directly from TGA

Catalysts	Surface area (m <sup>2</sup> g <sup>-1</sup> )	Ti content (%)	$\Delta w$ (%)	SiOH <sup>a</sup> mmol/g	SiOH/Ti mol/mol	OH/nm <sup>2</sup>
Ti/SBA-15	514	0.78	2.897	3.2	19.65	3.77
Ti/MCM-41	930	~0.8	1.352	1.5	8.98	0.97
Ti/MCM-48	982	~0.8	1.097	1.2	7.19	0.74

As supposed, the silanol density of Ti/SBA-15 is higher than in other materials. That explains the higher stability of Ti/SBA-15 to catalytic recycles.

## Conclusions

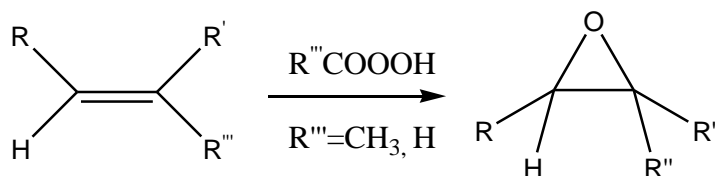
The stability, reusability and the influence of the topology and morphology of the support (convexity, concavity) on the repeated recycles were studied in this chapter. The activity of the studied catalysts follows the order: Ti/SiO<sub>2</sub> Aerosil > Ti/SBA-15 > Ti/MCM-48 > Ti/MCM-41. The formation of TiO<sub>2</sub> nanodomains, detected on Ti/MCM-41 during the recycles, can lead to a partial loss in activity, whereas the interesting performance of Ti/SBA-15 and Ti/MCM-48 can be attributed to good and stable site isolation. The convexity of the support surface showed a positive effect on the catalytic stability. The stability and the robustness of the catalyst is good for Ti/SiO<sub>2</sub> Aerosil and Ti/MCM-48, which both have a (quasi) convex silica surface, whereas it is very poor for Ti/MCM-41, with a concave internal surface. The case of Ti/SBA-15 is somehow difficult to interpret, but the bimodal micro and mesoporous network can account for the notable stability of this catalyst. The work is still in progress in this field.

Some *ab-initio* DFT calculations reporting some studies about the role of the topology of the silica support, performed few weeks ago by Dr. Tzonka Mineva, are inserted as supplementary material in Appendix I.

## Chapter 2. Ti-containing heterogeneous catalysts in methyl oleate epoxidation with hydrogen peroxide.

Epoxides of fatty acid methyl esters (FAMEs) are a class of oleochemicals playing a pivotal role as intermediates in the production of a wide series of important industrial products and materials. Derivatives of FAMEs epoxides and, especially, of methyl epoxystearate (the epoxide obtained from methyl oleate epoxidation), find indeed applications in several domains, *e.g.* in the manufacture of lubricants [1-5], plasticizers in polymers [6,7], wood impregnants [8], stabilizers in chlorine-containing resins [9], cosmetics [10], pharmaceuticals [11,12] and, in the near future, bio-fuel additives [13].

Nowadays, at industrial scale, epoxides of FAMEs are generally obtained in homogeneous phase via the Prilezhaev reaction (Scheme 2.1). In this epoxidation process, discovered in 1908, the unsaturated fatty compound reacts with peracetic or performic acids obtained through the acid-catalyzed oxidation of the corresponding acid with hydrogen peroxide [14,15]. To avoid the handling of hazardous species, the peracid is generally formed *in situ* for large-scale epoxidations.



**Scheme 2.1.** Prilezhaev epoxidation reaction

However, carboxylic acids and mineral acids (such as sulfuric acid) are essential for peracid formation and the presence of these strongly acid reactants leads to some major drawbacks such as: 1) an uncontrolled opening of the oxirane ring, that leads to low selectivity in epoxide, and 2) a cumbersome separation of the excess organic acids from the final reaction mixture. Thus, during last decades, several studies have been performed searching for an active catalytic system for the epoxidation of vegetable oils and their derivatives, in particular FAMEs, using hydrogen peroxide instead of peroxyacids [16-19]. In this aim, some recent papers reported interesting results using homogeneous, heterogeneous and chemoenzymatic systems. For instance, tungsten-containing heteropolyacid catalysts (“*Tetrakis*” tetrahexylammonium tetrakis(diperoxotungsto)phosphate (3-)) were used in the presence of hydrogen peroxide and excellent epoxide yields up to 94% under solvent-free conditions were reached [19]. Similarly, the use of methyltrioxorhenium with an amine adduct led to outstanding selectivity (99%) and



conversion (99%) in the epoxidation of soybean oil [20]. However, in these two cases, a complete separation of the homogeneous catalyst from the final mixture can pose some problems.

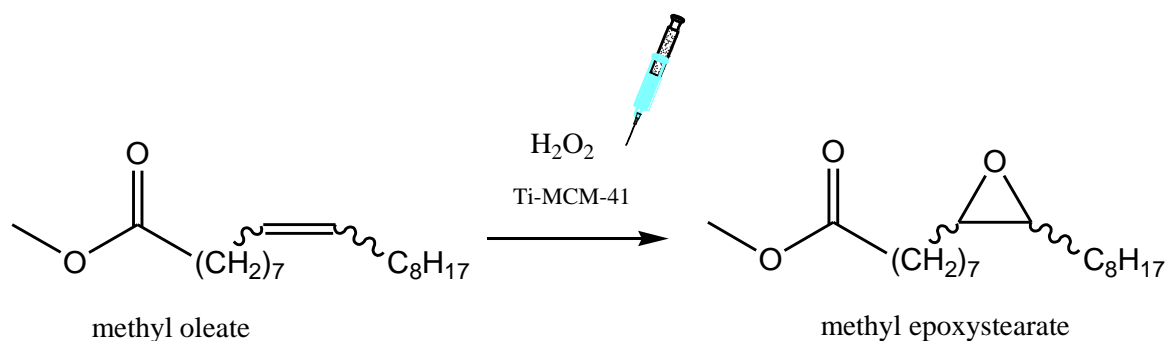
In the field of heterogeneous catalysis, different works over heterogeneous systems based on pure alumina in the presence of hydrogen peroxide were also described and led to high yields in methyl epoxystearate with very good selectivity (>97%), even though a large amount of oxidant with respect to the substrate (7.5 mol oxidant/ mol substrate) is necessary [17,18]. Similarly, a very high selectivity of 97% to methyl epoxystearate was obtained over a large-pore zeolite Ti-BEA and H<sub>2</sub>O<sub>2</sub> in the epoxidation of methyl oleate [16] with an interesting oxidant to substrate molar ratio (0.25 mol/ mol). However, with this system, a maximum yield in methyl epoxystearate of only 45% was reached. Then, the epoxidation of soybean oil over the amorphous heterogeneous Ti/SiO<sub>2</sub> in the presence of *tert*-butanol with H<sub>2</sub>O<sub>2</sub> in organic solution led to an epoxide yield of 87% [21]. In this case, however, the separation of the high-boiling alcoholic solvent from the reaction mixture can lead to some difficulties.

Chemoenzymatic epoxidation gained much interest too, as the process typically occurs under mild conditions and with very good chemoselectivities. For instance, Novozym 435, a *Candida antarctica* lipase B immobilized on polyacrylate, is one of the most efficient and stable catalyst for the epoxidation of oleochemicals. Yields in the range 72-91% for vegetable free fatty acids were obtained with high selectivity (>98%) [22]. Similarly, the use of Amano A. lipase (from *Aspergillus niger*) in hydrophobic and hydrophilic ionic liquids gave the epoxidized compound with yields in the range 67-89% after one hour [23]. Since chemoenzymatic systems are highly chemospecific, they can unfortunately be less versatile for a wide series of oleochemical substrates.

Previously, some of us have reported that titanium-grafted silicates are efficient catalysts for the epoxidation of FAMES with *tert*-butylhydroperoxide (TBHP) [24,25]. Mesoporous materials with 3–10 nm ordered pores are suitable systems for such transformation as Ti sites are easily accessible by the bulky reactants and a peculiar cooperative interaction between the hydrophilic one-dimensional pores of Ti-MCM-41 enhances the formation of epoxy FAME derivatives with noteworthy performance. Nevertheless, even though TBHP has the advantage of high selectivity, it is not the most sought-after oxidant from the point of view of atom economy and environmental sustainability. Hydrogen peroxide represents a more promising alternative [26-28]. As a main drawback, the use of hydrogen peroxide usually leads to a rapid deactivation of mesoporous Ti-silica catalysts due to a clustering of surface Ti species [29]. By applying a slow dropwise addition of hydrogen peroxide in the reaction mixture, it has been possible to

minimize the detrimental irreversible transformation of isolated Ti centers into titanium oxide-like species, in cyclohexene epoxidation [30-31].

In the present work, we have applied the experimental protocol of the controlled slow addition of aqueous hydrogen peroxide (described in the Chapter 2) to the epoxidation of methyl oleate (Scheme 2.2).



**Scheme 2.2.** Epoxidation of methyl oleate with slow dropwise addition of H<sub>2</sub>O<sub>2</sub>.

Thanks to this procedure we expect to reduce the decomposition of the oxidant, increase the catalyst stability and reach high yields in epoxide.

## Results and discussion

Titanium-grafted silica materials were used as heterogeneous catalysts in the liquid-phase epoxidation of methyl oleate with hydrogen peroxide under batch conditions.

Titanium active centers were obtained by grafting titanocene dichloride (Ti(Cp)<sub>2</sub>Cl<sub>2</sub>), as previously proposed by Maschmeyer et al. [32] (described in Experimental part) and then optimized by some of us for a wide series of silica supports [33]. Three silica materials with different structural and textural features (Table 2.1) were used as supports to evaluate the influence of the silica support on the catalytic performance.

The main advantage of such grafting methodology is that Ti(IV) sites are situated on the surface, are well dispersed and are all virtually active and accessible to the reactants. In particular, Ti(Cp)<sub>2</sub>Cl<sub>2</sub> was grafted over: 1) one-dimensional hexagonal ordered mesoporous material (MCM-41); 2) three-dimensional cubic ordered mesoporous material (MCM-48); and 3) non-porous pyrogenic nanosized silica particles (Aerosil).

The titanium content is comparable in all the samples and it gave rise to an even dispersion of titanium sites on the silica. Actually, the surface concentration of Ti sites was always lower than 0.3 Ti/nm<sup>2</sup> and this reduces the aggregation of catalytic centres during the

epoxidation in the presence of hydrogen peroxide, as previously shown in the cyclohexene epoxidation on similar materials [30].

**Table 2.1.** Specific surface area ( $S_{\text{BET}}$ ), mean pore diameter ( $D_p$ ), titanium loading of Ti-containing silica catalysts after calcination

Catalyst	$S_{\text{BET}}/\text{m}^2\text{g}^{-1}$	$D_p/\text{nm}$	Ti content (wt.%)
Ti/MCM-41	930	3.6	0.80
Ti/MCM-48	982	3.8	0.79
Ti/Aerosil	262	n.d.	0.64

n.d. not determined

The DRS-UV-Vis spectroscopic analysis is a tool to evaluate the coordination state of Ti(IV) (species in tetrahedral coordination at 220-260 nm and species in octahedral coordination at 260-290 nm) as well as the degree of isolation of Ti(IV) in the silica matrix. Indeed, absorption bands above 290 nm indicate the aggregation of some Ti through the formation of Ti-O-Ti bonds. The DRS-UV-Vis spectra of the three samples were performed in collaboration with the “Institut de Chimie Moléculaire et des Matériaux de Montpellier” - CNRS, in Montpellier) The DRS-UV-Vis spectra showed mainly isolated Ti(IV) sites in Ti/MCM-41 and Ti/MCM-48 with a higher proportion of tetrahedral Ti for MCM-41. For Ti/Aerosil a broader distribution of Ti sites was evidenced by a larger band revealing not only the presence of Ti(IV) isolated sites in octahedral coordination, but also some additional aggregation of Ti centres (Figure 2.1).

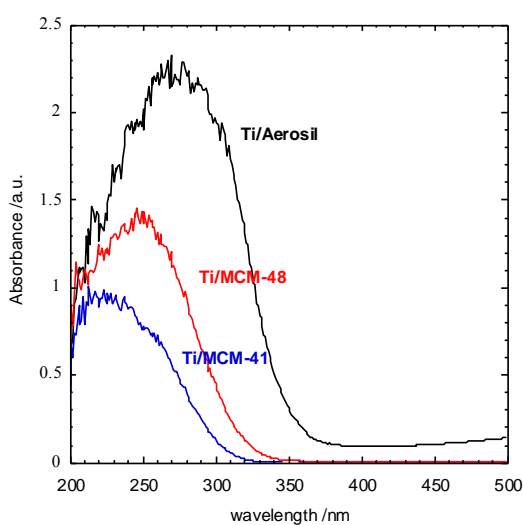


**Figure 2.1** DR-UV-Vis spectra of Ti/MCM-41, Ti/MCM-48 and Ti/Aerosil after calcination.

The results obtained in the methyl oleate epoxidation with hydrogen peroxide are summarized in Table 2.2.

**Table 2.2.** Liquid-phase epoxidation of methyl oleate with aqueous hydrogen peroxide over Ti-silica catalysts after 24 h reaction

Entry	Catalyst	C (%)	S EPOX (%)	S ENON (%)	S KETO (%)	Y EPOX (%)	<i>cis/trans</i> EPOX ratio	Ox Eff (%)
1	Ti/MCM-41	52	83	11	6	43	80:20	39
2	Ti/MCM-48	52	78	12	10	41	72:28	39
3	Ti/Aerosil	47	83	13	10	39	78:22	38
4	MCM-41	33	50	25	22	17	38:62	25
5	No catalyst	24	40	38	22	10	26:74	18

Reaction conditions: 1,5 mmol methyl oleate, 2 mmol aq. H<sub>2</sub>O<sub>2</sub> (50%), 50 mg catalyst, H<sub>2</sub>O<sub>2</sub>:substrate molar ratio=1,3:1, CH<sub>3</sub>CN, 24h, 85°C, dropwise oxidant addition 0.01 ml min<sup>-1</sup>. C: substrate conversion; S: selectivity; Y: yield; Ox Eff: oxidant efficiency.

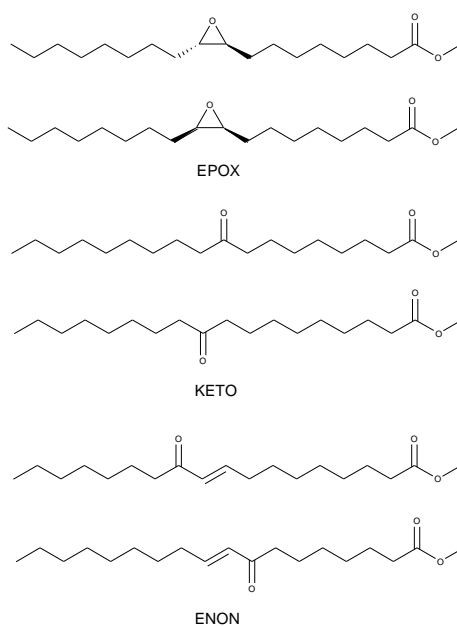
Earlier, some of us reported that Ti(IV) sites grafted onto the walls of a well-ordered one-dimensional mesoporous MCM-41 showed outstanding performances in the selective epoxidation of fatty acid methyl esters with TBHP than Ti(IV) centres grafted on non-ordered mesoporous or nonporous silicas [24,25]. This particular behaviour was attributed to a synergistic interaction between the elongated shape of quasi-linear FAMES (especially the methyl elaidate [25]) and to a favoured approach of partially oxidised FAMES (especially methyl ricinoleate [34] and methyl vernolate [24]) to the inner hydrophilic pore surface of MCM-41.

During this work, on the contrary, all materials (Ti/MCM-41, Ti/MCM-48 and Ti/Aerosil; Table 2, entries 1 to 3) showed a very similar behaviour in terms of conversion, selectivity and yield, with values of ca. 50%, 80% and 40%, respectively. Such results are in the same order of magnitude with those obtained over Ti-BEA [16]. They are also the first ones obtained, to our best knowledge, in methyl oleate epoxidation with aqueous hydrogen peroxide over Ti-grafted silica materials. Interestingly, the presence of some Ti-O-Ti domains in Ti/Aerosil (as evidenced by DRS-UV-Vis absorption bands above 300 nm) did not affect negatively the epoxidation performance and such behaviour can be attributed to the favorable conditions due to the slow oxidant addition protocol [35].

In addition, in these examples, it is evident that the morphology and the texture of the silica support do not play a key role in terms of catalytic activity (Table 2.2, entries 1-3). In fact, when hydrogen peroxide is used as oxidant instead of the sterically more demanding TBHP, the steric interactions between the FAME substrate and the porous catalyst are not decisive and the morphology of the catalyst is not a critical factor.

Such result is consistent with other recent observations on different Ti-based catalytic systems, where, in the narrow interlayer space of a Ti-containing layered clay, the epoxidation reaction takes place with H<sub>2</sub>O<sub>2</sub> as oxidant, but it does not with TBHP [36].

In terms of selectivity, methyl epoxystearate (EPOX), the epoxidised derivative, is the major product (ca. 80%). The most relevant side products are methyl oxooctadecanoate (KETO; a mixture of methyl 8-oxooctadec-9-enoate and methyl 11-oxooctadec-9-enoate) and methyl oxooctadecenoate (ENON; a mixture of methyl 9-oxooctadecanoate and methyl 10-oxooctadecanoate) (Scheme 2.3). ENON is obtained by allylic oxidation of methyl oleate, whereas KETO is formed via oxirane ring rearrangement from the epoxide. In both cases, no particular regioselectivity was detected and the two regioisomers for each product were obtained in practically equimolar amounts. The selectivity values to ENON and KETO are ca. 10% over the three catalysts. Blank reactions with pure silica MCM-41 (without Ti; Table 2.2, entry 4) and with no catalyst (Table 2.2, entry 5) led to 17% and 10% yield in methyl epoxystearate, respectively.



**Scheme 2.3.** Products of the reaction: methyl epoxystearate (EPOX), methyl oxooctadecanoate (KETO) and methyl oxooctadecenoate (ENON)

This behaviour shows that uncatalysed oxidation pathways have a non-negligible influence under these conditions and the presence of purely siliceous MCM-41 is not fully innocent. Actually, in the absence of Ti most of the methyl epoxystearate observed is due to a free-radical oxidation process (vide infra).

In terms of stereoselectivity, the epoxidation of methyl oleate can lead to the formation of *cis* and *trans* epoxides depending on the reaction pathway. In fact, when TBHP is used as oxidant, the epoxidation of *cis* methyl oleate proceeds via a heterolytic mechanism with retention of the C=C double bond configuration [25,37]. On the contrary, if a free-radical pathway prevails over the heterolytic one, the formation of the *trans* form, the thermodynamically more stable isomer, is predominant. For this reason, in the absence of Ti (Table 2.2; entries 4-5) the formation of methyl *trans*-epoxystearate dominates.

In terms of oxidant efficiency (the ratio between the moles of oxidised products produced and the moles of H<sub>2</sub>O<sub>2</sub> consumed), the achieved results (slightly less than 40%; Table 2.2) are interesting and comparable with the values obtained on homogeneous and heterogeneous systems [16,17,38]. Also for this parameter, the slow dropwise addition of the oxidant helps in reducing the disproportionation of H<sub>2</sub>O<sub>2</sub> into O<sub>2</sub> and H<sub>2</sub>O [21,31].

## **Improving the epoxide yield**

To improve the final epoxide yield different strategies have been contemplated and Ti/MCM-41 was used for this optimization.

### **1) Effect of the temperature**

The first strategy was to see the effect of temperature, to decrease the reaction temperature from 85°C to 40°C. In fact, in the work by E. Poli, using tungsten-containing heteropolyacid homogeneous catalysts “tetrakis” with H<sub>2</sub>O<sub>2</sub> as oxidant, a yield in EPOX reached 94% when the reaction temperature was 40°C [19]. While at the reaction temperatures higher than 40°C the formation of dimers was occurred. In our case, (Table 2.3), at 40°C the activity of the catalyst significantly decreases (from 52% to 24%), and the selectivity to epoxystearate remains at the same order.

**Table 2.3.** Influence of the reaction temperature on the catalytic performance after 24 h reaction.

Tests performed over Ti/MCM-41

Entry	Reaction T (°C)	C (%)	S EPOX (%)	S ENON (%)	S KETO (%)	S others (%)	Y EPOX (%)	<i>cis/trans</i> EPOX ratio	Ox Eff (%)
-------	-----------------	-------	------------	------------	------------	--------------	------------	-----------------------------	------------

1	85	52	83	11	6	5	43	80:20	39
2	40	24	70	19	10	0	17	82:18	18

Reaction conditions: 1.5 mmol methyl oleate, 2 mmol aq. H<sub>2</sub>O<sub>2</sub> (50%), H<sub>2</sub>O<sub>2</sub>:substrate molar ratio = 1.3:1, CH<sub>3</sub>CN, 24 h, dropwise oxidant addition 0,01 ml min<sup>-1</sup>. C: substrate conversion; S: selectivity; Y: yield; Ox Eff: oxidant efficiency.

**2) Effect of the amount of hydrogen peroxide**

Another strategy was the increase of the oxidant/substrate molar ratio from 1.3 to 4.0, the yield to epoxide rised up, but, at the same time, an increase in the formation of *trans*-epoxide was observed as well (Table 2.4; entries 2 and 4, Table 2.5). Such increase can be explained by a higher fraction of free-radical pathway of the reaction taking place when an excess of hydrogen peroxide is present.

**Table 2.4.** Influence of the amount of hydrogen peroxide on the catalytic performance after 24 h reaction. Tests performed over Ti/MCM-41

Entry	Catalyst (mg)	H <sub>2</sub> O <sub>2</sub> (mmol)	C (%)	S EPOX (%)	S ENON (%)	S KETO (%)	S others (%)	Y EPOX (%)	<i>cis/trans</i> EPOX ratio	Ox Eff (%)
-------	---------------	--------------------------------------	-------	------------	------------	------------	--------------	------------	-----------------------------	------------

1	50	2	52	83	11	6	5	43	80:20	39
2	50	6	83	82	12	6	0	68	61:39	20
3	200	2	73	96	1	2	1	70	92:8	55
4	200	6	82	92	5	3	0	75	74:26	20

Reaction conditions: 1.5 mmol methyl oleate, CH<sub>3</sub>CN, 24 h, 85°C, dropwise oxidant addition 0.01 ml min<sup>-1</sup>. C: substrate conversion; S: selectivity; Y: yield; Ox Eff: oxidant efficiency.

**Table 2.5.** Influence of the amount of hydrogen peroxide on the catalytic performance after 24 h reaction. Tests performed over Ti/Aerosil

Entry	Catalyst (mg)	H <sub>2</sub> O <sub>2</sub> (mmol)	C (%)	S EPOX (%)	S ENON (%)	S KETO (%)	Y EPOX (%)	<i>cis/trans</i> EPOX ratio	Ox Eff (%)
-------	---------------	--------------------------------------	-------	------------	------------	------------	------------	-----------------------------	------------

1	50	2	47	83	13	10	39	78:22	38
2	50	6	65	69	18	12	45	62:38	48

Reaction conditions: 1.5 mmol methyl oleate, CH<sub>3</sub>CN, 24 h, 85°C, dropwise oxidant addition 0.01 ml min<sup>-1</sup>. C: substrate conversion; S: selectivity; Y: yield; Ox Eff: oxidant efficiency.

### 3) Effect of the amount of catalyst

Conversely, by increasing the amount of catalyst, the conversion of the reaction rises from 52% to 96% and a high selectivity in epoxide (ca. 90%) is maintained (Table 6, entries 1-5). By augmenting the amount of Ti (substrate:Ti molar ratio from 180 to 22), it was possible to increase the yield from 43% up to 91%. In this case, no remarkable influence on stereoselectivity was noted, the formation of *cis* epoxide being always prevalent (around 80%). Nevertheless, the combination of a higher quantity of Ti/MCM-41 (200 mg) and a large excess of H<sub>2</sub>O<sub>2</sub> (6 mmol) did not lead to a sensible improvement, since the EPOX yield attained 75% with the formation of a lower fraction of *cis* epoxide (Table 2.4, entry 4).

**Table 2.6.** Influence of the amount of catalyst on the catalytic performance after 24 h reaction. Tests performed over Ti/MCM-41

Entry	Catalyst (mg)	C (%)	S EPOX (%)	S ENON (%)	S KETO (%)	S others (%)	Y EPOX (%)	<i>cis/trans</i> EPOX ratio	Ox Eff (%)
1	50	52	83	11	6	5	43	80:20	39
2	100	47	83	9	8	0	39	78:22	35
3	200	73	96	1	2	1	70	92:8	55
4	300	78	86	5	2	7	67	72:28	54
5	400	96	95	3	3	0	91	85:15	73

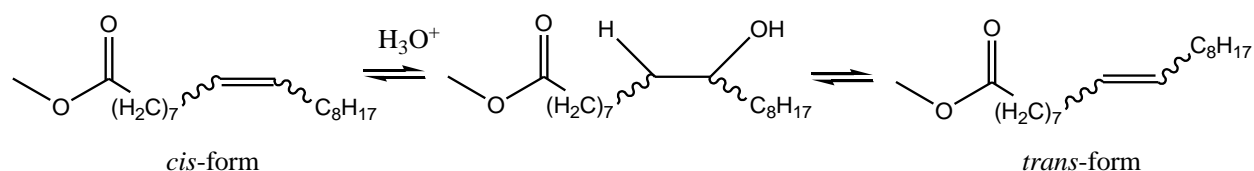
Reaction conditions: 1.5 mmol methyl oleate, 2 mmol aq. H<sub>2</sub>O<sub>2</sub> (50%), H<sub>2</sub>O<sub>2</sub>:substrate molar ratio = 1.3:1, CH<sub>3</sub>CN, 24 h, 85°C, dropwise oxidant addition 0,01 ml min<sup>-1</sup>. C: substrate conversion; S: selectivity; Y: yield; Ox Eff: oxidant efficiency.

Such results in methyl epoxystearate yields (up to 91%) are the highest data obtained in literature so far over titanium-silica molecular sieves catalysts with aqueous hydrogen peroxide. In addition, the effectiveness of oxidant use is promising also in terms of oxidant to catalyst and oxidant to substrate ratios. Under optimized conditions (Table 2.6; entry 5), the oxidant to catalyst ratio (mol H<sub>2</sub>O<sub>2</sub>/mass<sub>cat</sub>) and oxidant to substrate ratio (mol/mol) are as low as 0.005 and 1.3, respectively. Actually, the value of oxidant to catalyst ratio is better than the results typically reported in literature, spanning from 0.008 in the epoxidation of methyl oleate over Ti-BEA [16], up to 0.1, in soybean oil epoxidation over Ti/SiO<sub>2</sub> [21].

### Reasons of trans-epoxide formation

Finally, it is important to understand the reasons leading to *trans* epoxide formation under the tested conditions. Since there is H<sub>2</sub>O<sub>2</sub> (50%) in the reaction medium, the first hypothesis was the influence of the water on the interconversion of C=C double bond in methyl oleate (Scheme 2.4).

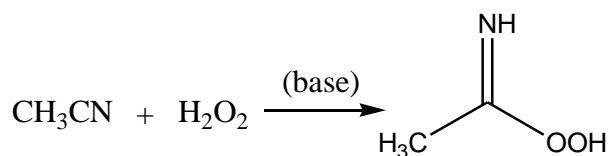




**Scheme 2.4.** Possible role of water in acidic conditions in the interconversion of *cis*-form into *trans*-form of 9-octadecenoic acid methyl ester.

For this purpose, a specific test was done: first, the methyl oleate was in the contact with water (slow dropwise addition of the solution  $H_2O/AcOEt$  or  $H_2O/CH_3CN$ ), solvent and catalyst, with no presence at all of oxidant. After 24 h the solution was filtered, a fresh pretreated catalyst was added and the oxidant (TBHP) was introduced in the reaction. It is commonly accepted that the use of TBHP as oxidant on titanium-based silicate catalysts proceeds via non-radical mechanism with retention of the configuration of the  $C=C$  double bond [37]. Thus, if the water plays a role in the interconversion of  $C=C$  double bond of methyl oleate, we would have detected the *trans*-form of the epoxide after the reaction with TBHP. The performed tests showed that in both the solvents, there is no formation of methyl *trans*-epoxystearate after the reaction, and this means that water is not implied in the isomerisation of the  $C=C$  double bond nor in the formation of methyl *trans*-epoxystearate.

According to a second hypothesis, the simultaneous presence of hydrogen peroxide and acetonitrile is the cause of *trans*-isomer formation. In fact, since, in the reaction medium, acetonitrile and hydrogen peroxide are simultaneously present, it can be assumed that the formation of *trans* epoxide is due to a Payne-type free-radical reaction, where peroxyimidic acid is formed *in situ*, typically under alkaline conditions (Scheme 2.5) [39]. Actually, specific tests have confirmed that the formation of peroxyimidic acid occurs and Payne oxidation takes place.



**Scheme 2.5.** Scheme of Payne reaction, formation of peroxyimidic acid.

However, some of us have recently reported that there is no influence of Payne reaction in the epoxidation of cyclohexene over Ti(IV)-silica catalysts in acetonitrile with dropwise addition of hydrogen peroxide under fully comparable conditions [30]. To understand the apparent

contradiction, according to which Payne-type oxidation occurs only in the epoxidation of methyl oleate, it must be recalled that commercial methyl oleate samples (even reagent grade) always possess some mild alkalinity, due to residual amounts of basic transesterification catalysts during the production steps [40] and such alkalinity promotes the formation of peroxyimidic acid in the reaction mixture. In fact, if methyl oleate undergoes a repeated rinsing and washing with 0.1 M aqueous HNO<sub>3</sub>, *trans* epoxide formation is reduced (from 7% to 3% in *trans*-epoxide yield and *cis/trans* epoxide ratio from 26:74 to 50:50).

### Effect of the solvent

Epoxidation tests carried out in polar solvents other than acetonitrile showed poorer performance (Table 2.7). Similar conversion, but lower selectivities, were obtained in ethyl acetate (Table 2.7, entry 1), while in dichloromethane (Table 2.7, entry 2) comparable epoxide selectivity, but lower conversions, were found. The optimal behaviour observed with acetonitrile is consistent with previous reports in the epoxidation of other substrates. In fact, acetonitrile, thanks to its slightly basic nature, allows to minimize the formation of acid-catalysed secondary products [30, 41].

Moreover, fluorinated alcohols have recently attracted a great attention as solvents for oxidation with hydrogen peroxide and, in general, for their affinity with oxygen-donor reactants [40a]. According to physicochemical and theoretical studies, fluorinated solvents enhance the oxidation processes since they act as a template activating the oxygen transfer through the multiple hydrogen bonding [40b]. Moreover, the presence of fluorinated solvent makes the H<sub>2</sub>O<sub>2</sub> a more active oxidant that can oxidize olefins even in the absence of catalyst. However, in our case the use of a protic solvent is not advisable. For this reason, a fluorinated solvent, such as (trifluoromethyl)benzene (TFMB) ( $\alpha,\alpha,\alpha$ -trifluorotoluene) was the solvent of choice. Unfortunately, however, this solvent did not lead to the expected improvement, either in conversion or in selectivity, but, on the contrary, the catalyst became completely inactive (Table 2.7, entry 4).

**Table 2.7.** Influence of the solvent on the catalytic performance after 24 h reaction. Tests performed over Ti/MCM-48

Entry	Solvent	Conv 24h (%)	Select EPOX 24h (%)	Select ENON 24h (%)	Select KETO 24h (%)	Select others 24h (%)	Y EPOX (%)	Cis/trans EPOX ratio	Ox. Eff. (%)
1	AcOEt	68	68	7	10	21	46	85:15	54
2 <sup>a</sup>	CH <sub>2</sub> Cl <sub>2</sub>	11	100	0	0	0	11	100:0	8

3	CH <sub>3</sub> CN	52	78	12	10	0	41	72:28	39
4	TFMB	-	n.d.	-	-	-	-	-	-

Reaction conditions: 1.5 mmol methyl oleate, 2 mmol aq. H<sub>2</sub>O<sub>2</sub> (50%), H<sub>2</sub>O<sub>2</sub>:substrate molar ratio = 1.3:1, 24 h, 85°C, dropwise oxidant addition 0.01 ml min<sup>-1</sup>. C: substrate conversion; S: selectivity; Y: yield; Ox Eff: oxidant efficiency; <sup>a</sup>Ti/SiO<sub>2</sub>-Aerosil, T reaction 40°C.

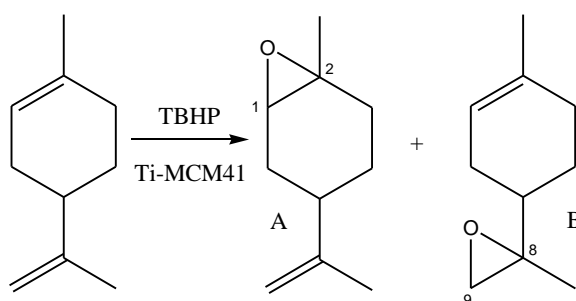
The Ti-silica catalysts were easily recovered by filtration, washed, calcined and reused in a second catalytic run. In particular, after the first recycle, Ti/MCM-41 showed a loss of ca. 3% in both conversion and selectivity. As observed on different lighter alkenes (cyclohexene or unsaturated terpenes [30,42]), it is worth noting that a complete removal of the organic side products adsorbed on the catalyst surface is necessary to restore the original activity of the fresh catalyst. Because of this reason, prior to recycling, the solids were carefully washed with methanol and then calcined under dry air at 500°C.

## Conclusions

Heterogeneous porous and non-porous grafted titanium-silica catalysts proved to be sustainable and efficient catalysts in the epoxidation of methyl oleate with aqueous hydrogen peroxide. The different textural and morphological features of the mesoporous catalysts did not affect noticeably their catalytic performance. Thanks to the applied protocol of the dropwise oxidant addition, the hydrogen peroxide decomposition and local water concentration into the proximity of Ti(IV) sites were minimized. By optimizing the experimental conditions, yields as high as 91% in the desired methyl epoxystearate were achieved. Such results are the highest data obtained in literature so far over titanium-silica molecular sieves catalysts with aqueous hydrogen peroxide.

### Chapter 3. The effect of surface silylation on the catalytic performance of Ti-MCM-41 in the epoxidation of limonene.

Epoxidic compounds are important intermediates in organic synthesis due to the high reactivity of the oxirane ring in their structure, from which a wide variety of functional groups can be obtained. Limonene oxides (Scheme 3.1) prepared by epoxidation of limonene are important building blocks for the synthesis of products from renewable sources [1] and find applications in many areas: *e.g.* as insect repellents [2] or as herbicide components [3]. Limonene 1,2-oxide is a promising monomer for the synthesis of new biodegradable polymers (polylimonene carbonate) [4] and biopolyesters [5], obtained from renewable feedstock. Limonene is the main component of citrus oil and can be easily obtained from citrus peel, a waste material of the fruit juice industry. At industrial scale, limonene oxide is usually obtained via the stoichiometric peracid process, thus the development of potential sustainable alternatives to this route has attracted great attention [6]. Titanium-based catalyst obtained from the ordered mesoporous silica MCM-41 can be applied to the liquid-phase epoxidation of limonene with high activity and selectivity [7,8]. Moreover, thanks to the modification by silylation, the surface hydrophilic character of the catalyst can be decreased to fit the hydrophobic character of alkenes [9-14].



**Scheme 3.1.** Epoxidation reaction of limonene to limonene 1,2-oxide (A) and limonene 8,9-oxide (B).

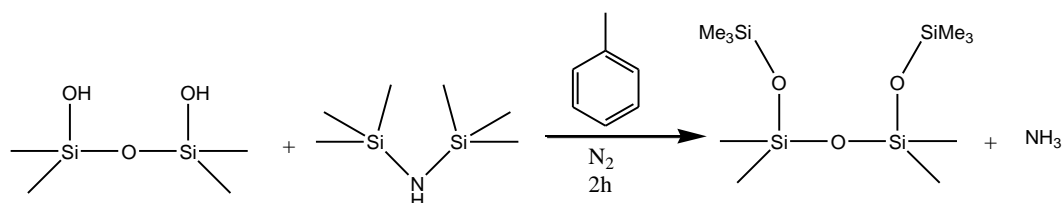
However, all of these studies were performed in the epoxidation of simple model alkenes, aiming at improving the hydrophobic character of the catalyst which can interact with alkene, rather than maximising the interaction with *tert*-butylhydroperoxide (TBHP), used as oxidant.

The aim of the present chapter is to apply the post-synthesis silylation of Ti-silicate catalysts to obtain high yields in a bulky and high added-value molecule, such as limonene oxide, an intermediate getting growing attention in industrial chemistry. The investigation is performed studying the effect of little variations of the surface silylation coverage on activity and selectivity

in the epoxidation of limonene with TBHP. Under these specific conditions and by finely tuning the hydrophilic/hydrophobic properties of the catalyst, promising yields in limonene mono-oxide can be achieved.

## Results and discussion

The redox-active Ti-MCM-41 catalyst (1.8 wt.% Ti; 950 m<sup>2</sup> g<sup>-1</sup> surface area; 2.5 nm mean pore diameter; 1.10 cm<sup>3</sup> g<sup>-1</sup> total pore volume) was obtained by grafting Ti(Cp)<sub>2</sub>Cl<sub>2</sub> onto a purely siliceous ordered mesoporous MCM-41 support [7,15]. The hydrophobic character of the catalyst was varied by post-synthesis silylation with hexamethyldisilazane (HMDS) (Scheme 3.2) [16,17].



**Scheme 3.2.** Post-synthesis silylation with hexamethyldisilazane (HMDS)

First, a series of five modified catalysts with different levels of silylation were obtained by changing gradually the HMDS to Ti-MCM-41 ratio (mol/mol), as shown in Table 3.1 and Figure 3.1.

**Table 3.1.** Features and catalytic performance of Ti-MCM-41 and the series of partially silylated Ti-MCM-41 catalysts in the epoxidation of limonene.

Catalyst	HMDS/ Ti-MCM-41 ratio <sup>a</sup>	CC <sup>b</sup> (%)	SC <sup>c</sup> (%)	A <sub>Ti</sub> <sup>d</sup> (h <sup>-1</sup> )	C <sup>e</sup> 24 h (%)	S <sub>1,2-EPOX</sub> <sup>f</sup> 24 h (%)	S <sub>tot</sub> <sup>g</sup> 24 h (%)
Ti-MCM-41	0	0	0	34	78	76	89
Ti-MCM-41 / Sil1	0.010	1.9	16	52	83	77	91
Ti-MCM-41 / Sil2	0.017	2.2	19	50	80	79	94
Ti-MCM-41 / Sil3	0.048	4.3	36	60	89	78	90
Ti-MCM-41 / Sil4	0.120	6.5	55	54	86	85	98
Ti-MCM-41 / Sil5	0.250	9.1	77	51	92	73	89

Reaction conditions: batch reactor; 5 mL ethyl acetate; 363 K; 25 mg catalyst; 0.5 mmol limonene; TBHP/limonene = 1.10 mol/mol. (a) HMDS/ Ti-MCM-41 molar ratio (mol HMDS / mol SiO<sub>2</sub>); (b) carbon content; (c) catalyst surface coverage; (d) specific activity of the catalyst computed after 1 h ([mol<sub>converted lim</sub>]/[mol<sub>Ti</sub>•h]); (e) conversion of

limonene after 24 h; (f) selectivity to 1,2-oxide after 24 h (sum of *cis* and *trans* isomers); (g) selectivity to mono-oxide after 24 h (sum of 1,2- and 8,9-epoxide).

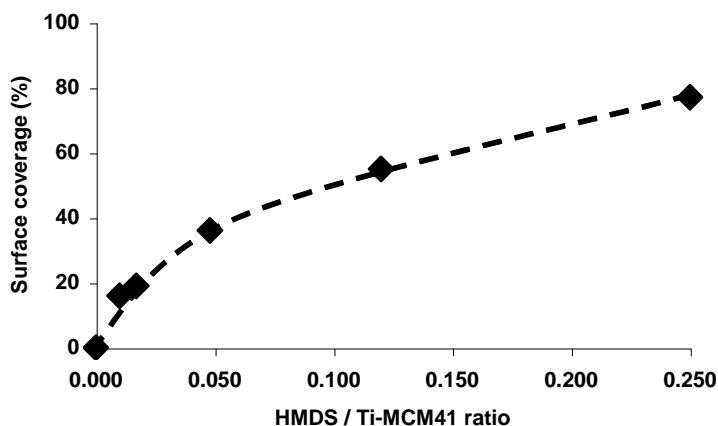


**Figure 3.1.** Profile of the percentage of surface coverage vs. HMDS/Ti-MCM-41 molar ratio.

After performing the silylation with different HMDS to Ti-MCM-41 ratios, spanning from 0.010 to 0.250, it was observed that the silylation of the last surface silanols left is more difficult than that of the first ones and the  $-\text{Si}(\text{CH}_3)_3$  groups already present on the catalyst surface hinder and slow down the extended silylation of the residual silanols [16]. A further increase of the HMDS/Ti-MCM-41 ratio did not lead to a remarkable improvement in coverage and, even for very high HMDS/Ti-MCM-41 ratios, a sensible amount of non-silylated silanols was anyway present [12,18]. The silylated samples are referred to as Ti-MCM-41/Sil X ( $X = 1 \div 5$ ). In all cases, the silylation procedure did not lead to a loss in structural order, the specific surface area and the pore diameter being always around  $900 \text{ m}^2 \text{ g}^{-1}$  and 2 nm, respectively. The carbon content, determined by elemental analysis, was used to estimate the degree of surface coverage by trimethylsilyl groups (see Tab. 3.1), assuming that the surface occupied by each  $-\text{Si}(\text{CH}_3)_3$  group is  $0.476 \text{ nm}^2$  [16,19].

The series of silylated catalysts was tested in the liquid-phase epoxidation of limonene with a modest excess of TBHP (10 mol%). The effect of the surface coverage by silylation on the catalytic performance is summarised in Table 3.1.

The initial activity, expressed as specific activity ( $A_{\text{Ti}}$ ) calculated with respect to the total number of Ti sites, was the most sensible parameter to partial silylation. By tuning the surface coverage, it was possible to increase and maximise considerably the  $A_{\text{Ti}}$  values. The highest value of  $60 \text{ h}^{-1}$  was achieved over Ti-MCM-41/Sil3 (with a surface coverage of 36%) and this

result has to be compared to  $34 \text{ h}^{-1}$  for the non-silylated sample Ti-MCM-41. After 24 h, the conversion of limonene was higher than 85% for all the highly silylated samples (Sil3 through Sil5).

With regard to selectivity, limonene mono-oxides (the sum of 1,2 and 8,9 epoxides) were always the major products. Limonene di-oxide, carveol and carvone were, on the contrary, minor side products (less than 10% overall). Over all the catalysts, the endocyclic limonene 1,2-oxide was the main product (more than 75% of the converted terpene) and a remarkable selectivity of 85% was obtained over Ti-MCM-41/Sil4. The exocyclic 8,9-oxide is the second most abundant product with selectivities in the range 13 to 16%. Thus, over all the catalysts, the total selectivity to limonene mono-oxide (sum of regioisomers) was at least 89%.

*Cis* and *trans* limonene 1,2-oxide can be obtained, but no significant stereoselectivity was observed before or after silylation. In fact, *cis* / *trans* molar ratios between 45:55 and 55:45 were recorded in all tests.

In terms of production of limonene oxide, Figures 3.2 and 3.3 show clearly that the highest yields were achieved over Ti-MCM-41/Sil4.

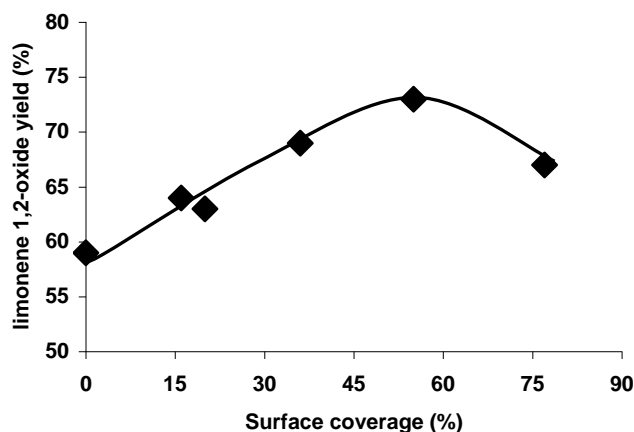


**Figure 3.2.** Yields in limonene 1,2-oxide obtained over Ti-MCM-41 with different silyl surface coverage.

Under these conditions, yields as high as 84% and 73% were obtained for limonene oxide (sum of regioisomers) and 1,2-oxide, respectively.

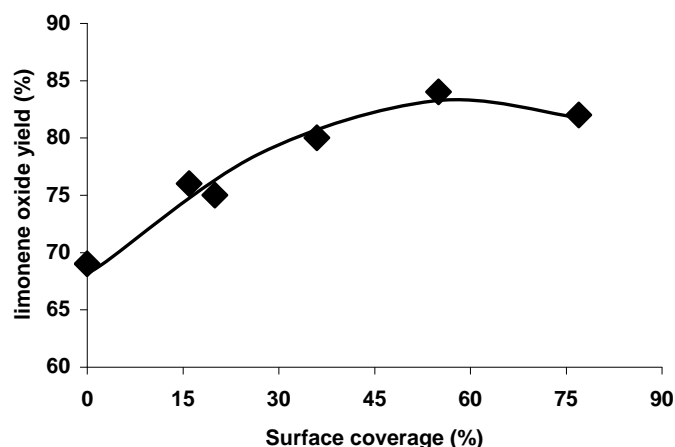


**Figure 3.3.** Yields in limonene mono-oxide (sum of 1,2- and 8,9-epoxide) obtained over Ti-MCM-41 with different silyl surface coverage.

Both graphs show a similar trend: a wide bell-shaped curve with a maximum around 55% of surface coverage. Over this catalyst, yields in limonene oxide as high as 84% were obtained. Such value is the highest among the most effective titanium-silica systems reported so far (over either silylated and non-silylated catalysts, with either organic hydroperoxides or hydrogen peroxide, as oxidant) [6-8, 20-23]. This behaviour suggests that an intermediate surface coverage by silylation can be an ideal compromise in the presence of a hydrophobic substrate, such as limonene, and a rather hydrophilic oxidant, such as TBHP. Actually, highly silylated catalysts, with a remarkable hydrophobic character, can interact more readily with limonene than with TBHP. Conversely, non-silylated samples, with a hydrophilic character, can interact readily with the oxidant rather than with limonene. Therefore, a catalyst with a surface coverage in the range of 50-60% is an appropriate choice for this particular reaction and for this peculiar combination of substrate, oxidant and solvent. In this scenario, the simultaneous presence of silylated and non-silylated silanol moieties on the catalyst's surface can promote the adsorption of both the alkene and the oxidant and the desorption of the epoxide.

## Conclusions

The present study shows that the post-synthesis modification by partial silylation can be an effective tool to obtain good yields in limonene oxide formation. The interaction between substrates and catalyst as well as the catalytic performances are often affected by a delicate counterbalance of several factors, such as the polar character of the substrate, of the oxidant or



the competitive adsorption of the reaction medium. So, a fine tuning of the hydrophilic/hydrophobic character of the catalyst is necessary to have optimal results. By varying gradually the surface coverage of non-silylated sample it was possible to increase the initial activity of the catalyst (expressed as specific activity of Ti sites) from  $34 \text{ h}^{-1}$  to  $60 \text{ h}^{-1}$ . In this case, a partial silylation (55% of the catalyst surface) proved to be the best choice to maximize the production of moderately polar limonene oxide with the yield of 84%.

## **Chapter 4. Ti-POSS covalently immobilized onto mesoporous silica.**

### **A model for active sites in heterogeneous catalytic epoxidation.**

The characterization of the solid catalysts in this chapter was performed in collaboration with Nano-SISTEMI Centre, University of Eastern Piedmont “A. Avogadro”, Alessandria, Italy.

In the last years, large efforts have been devoted to the investigation of silica-based materials containing dispersed titanium centres to be used as heterogeneous catalysts in selective oxidation reactions. In particular, since the successful development of TS-1 (already employed nowadays in industrial oxidation plants [1,2]), several microporous (TS-2, Ti-BEA, Ti-MOR, Ti-MCM-22 [3-6]), mesoporous (Ti-MCM-41, Ti-SBA-15 [7-9]) or layered (Ti-NHM-1 and Ti-NHM-2 [10,11]) Ti-silica materials have been proposed as effective catalysts at lab-scale level. Epoxidation is an ideal reaction to evaluate the catalytic activity of these systems. Typically, four factors have an important influence on the performance of the titanium sites in epoxidation reactions: i) the dispersion of the metal site on the inorganic support (isolated single site); ii) the accessibility to the site by the different substrates involved in the reaction; iii) the hydrophobic or hydrophilic character of the support; and iv) the nature of the chemical environment around the catalytic site (*e.g.* presence of ancillary silanol groups, acid centres on the inorganic support, confinement effects in porous systems, etc.). However, it is often very difficult to control and tune all these factors during the preparation of conventional heterogeneous catalysts. Therefore, the use of Ti(IV) species with a specific *a priori* control of the geometry and of the chemical surroundings of the catalytic site could represent an important tool to understand the mechanism of catalytic heterogeneous epoxidation and it is the main topic of the present chapter.

Ti-containing polyhedral oligomeric silsesquioxanes (Ti-POSS) are good candidates for this purpose. In fact, Ti-POSS are excellent models of isolated and well-dispersed Ti sites in SiO<sub>2</sub> matrix. They proved to be highly active in homogeneous catalysis for the epoxidation of alkenes [12-17] and, thanks to their homogeneous nature, they can be the object of detailed spectroscopic characterization and mechanistic studies [18].

Special attention was recently devoted to the heterogenization of Ti-POSS moieties onto insoluble and easily recoverable supports through ionic or weak non-covalent interactions. Interesting examples encompass the incorporation, following different synthetic approaches, of Ti-POSS into mesoporous MCM-41 silica, into sol-gel matrices, into polysiloxanes or the

preparation of organic–inorganic hybrid materials based on polystyrene polymers containing Ti–POSS moieties [16,19-23].

Recently, the immobilization of a functionalized Ti-POSS via covalent bonding on mesoporous silicas was optimized in our laboratory [24]. The heterogeneous catalyst obtained by anchoring the Ti-POSS on a silica supports was tested in the epoxidation of limonene, showing that the solid is active as an epoxidation catalyst and that it is truly heterogeneous in nature.

Starting from these results, a deeper investigation of the nature of the active metal site present in the Ti-POSS structure after anchoring on the two mesoporous silica surface (an ordered mesoporous SBA-15 and a non-ordered commercial SiO<sub>2</sub>) is performed in this chapter, in terms of coordination state, neighbouring atoms and chemical surroundings of the Ti centre. In addition, the understanding of the distribution of Ti-POSS molecules on the two different silicas is another important objective of this part of PhD thesis. Finally, particular attention is paid to the evaluation of the catalytic performance of the final anchored catalysts, in comparison to classical grafted Ti-containing silica (Ti/SBA-15 and Ti/SiO<sub>2</sub>), in the epoxidation of a series of unsaturated terpenes with various functionalities and morphology. Limonene, carveol and  $\alpha$ -pinene were chosen as test substrates to assess the effect of proximity of Ti(IV) sites to surface silanol groups in the support on the reactivity and the performance in the catalytic epoxidation.

## Results and discussion

Thanks to the presence of three ethoxy groups, Ti-POSS was anchored by covalent bond onto the surface silanols of SBA-15 and SiO<sub>2</sub> Davison (Scheme 4.1) [24]. The content of Ti in the anchored solids, as measured by elemental analysis, was 0.26 and 0.33 wt.% for Ti-POSS/SiO<sub>2</sub> and Ti-POSS/SBA-15, respectively. Several attempts to increase the Ti loading on the solids, by increasing the concentration of Ti-POSS in the anchoring solution were made, but in all cases a maximum Ti content around 0.3 wt% was attained. Such maximum value is due to a physical limitation to extended anchoring rather than to a failure of the anchoring methodology (*vide infra*). For this reason, two reference Ti-containing silica materials were prepared by grafting Ti(Cp)<sub>2</sub>Cl<sub>2</sub> with a comparable Ti loading, namely 0.29 wt% for Ti/SiO<sub>2</sub> and 0.24 wt% for Ti/SBA-15.



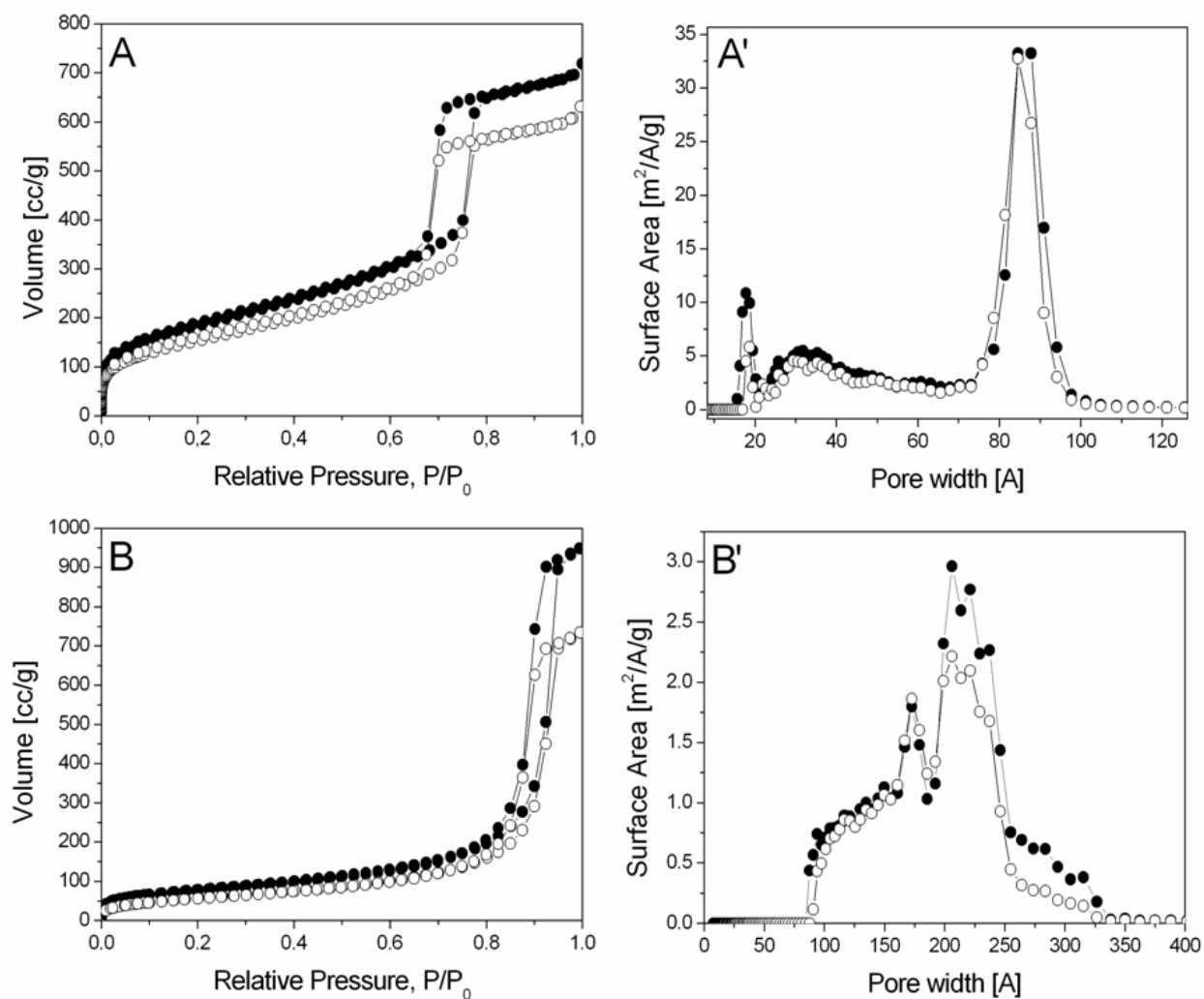


**Figure 4.1.** N<sub>2</sub> adsorption/desorption isotherms at 77 K of A) SBA-15 (-●-) and Ti-POSS/SBA-15 (-○-) and B) SiO<sub>2</sub> (-●-) and Ti-POSS/SiO<sub>2</sub> (-○-). Pores size distribution obtained by NLDFT are reported in A') SBA-15 (-●-) and Ti-POSS/SBA-15 (-○-) and B') SiO<sub>2</sub> (-●-) and Ti-POSS/SiO<sub>2</sub> (-○-).

**Table 4.1.** Textural properties (measured by N<sub>2</sub> adsorption–desorption isotherms) of the porous materials.

Material	$S_{BET}$ (m <sup>2</sup> g <sup>-1</sup> )	PD <sup>a</sup> (nm)	PV <sup>b</sup> (cm <sup>3</sup> g <sup>-1</sup> )
SBA-15	650	8.8	1.04
Ti-POSS/SBA-15	547	8.8-8.5	0.91
SiO <sub>2</sub>	277	10.0-32.5	1.4
Ti-POSS/SiO <sub>2</sub>	210	10.0-32.5	1.1

a: mean pore diameter; b: specific pore volume

SBA-15 showed a high specific surface area (650 m<sup>2</sup> g<sup>-1</sup>), a pore volume of 1.04 cm<sup>3</sup> g<sup>-1</sup> and a mesopores average diameter of 8.8 nm (Table 1 and Fig. 1A). The anchoring of Ti-POSS on

SBA-15 surface did not significantly modify the textural properties of the solid. Ti-POSS/SBA-15 showed a slightly decrease of the specific surface area and pore volume, passing from  $650 \text{ m}^2 \text{ g}^{-1}$  to  $547 \text{ m}^2 \text{ g}^{-1}$  and from  $1.04$  to  $0.91 \text{ cm}^3 \text{ g}^{-1}$ , respectively. No restriction of the pores diameter was observed in the final anchored material (Fig. 4.1A'). This suggests that that Ti-POSS moieties are not present inside the mesopores network, but are in large amount anchored on the external surface of SBA-15 particles.

A different behaviour was observed for Ti-POSS/SiO<sub>2</sub> material (Figures 4.1B and B'). SiO<sub>2</sub> Davison is characterized by the presence of structural irregular large mesopores with diameter values in the range 10.0-32.5 nm, volume close to  $1.4 \text{ cm}^3 \text{ g}^{-1}$  and specific surface area of  $277 \text{ m}^2 \text{ g}^{-1}$  (Table 4.1). The anchoring of Ti-POSS on SiO<sub>2</sub> significantly influenced the surface area, that decreased from 277 to  $210 \text{ m}^2 \text{ g}^{-1}$  (24 % diminution) and affected the pattern of pores size distribution (Fig. 4.1B and B'). Indeed, a significant decrease of larger pores with diameters in the range 25.0-32.5 nm and a diminution of average pore volume (from  $1.4 \text{ cm}^3 \text{ g}^{-1}$  for SiO<sub>2</sub> to  $1.1 \text{ cm}^3 \text{ g}^{-1}$  for the anchored material) was observed, suggesting a partial confinement of Ti-POSS within the silica mesopores.

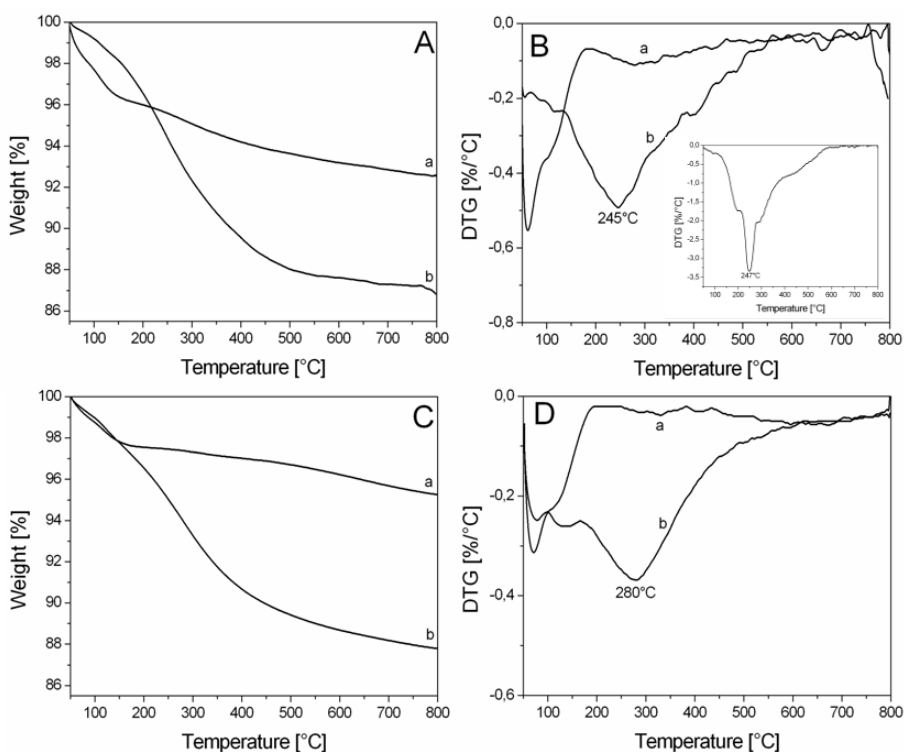


**Figure 4.2.** TGA (left) and DTG (right) of SBA-15 (curve a) and Ti-POSS/SBA-15 (curve b) (A and B) and of SiO<sub>2</sub> (curve a) and Ti-POSS/SiO<sub>2</sub> (curve b) (C and D) under oxygen flow. DTG of pure Ti-POSS is reported in the inset of Figure B.

By studying the thermogravimetric profile of the two anchored materials, pure SBA-15 showed a significant weight loss of 4 wt% around 100°C which was assigned to the evaporation of physisorbed water (Fig. 4.2A and B, curve a). A progressive weight loss at higher temperatures in the range 200-800°C was attributed to the condensation of vicinal silanols on the surface of SBA-15 silica. Ti-POSS/SBA-15 showed a different thermal profile (Fig. 4.2A and B, curve b). In addition to a weight loss around 100°C of ca. 2 wt% (lower than that observed for pure silica), a significant weight loss at 245°C was observed according to the TGA and DTG profiles of Ti-POSS/SBA-15 (Fig. 4.2A and B, curves b). The lower weight loss at 100°C suggests a higher hydrophobic character of the anchored solid, while the weight loss at 245°C is assigned to the thermal decomposition of the Ti-POSS moiety anchored onto the silica surface (see inset in the Fig. 4.2B).

A different thermal behaviour was observed for Ti-POSS/SiO<sub>2</sub> (Fig. 4.2C and D, curves b). In addition to a weight loss of ca. 2 wt% around 100°C, Ti-POSS/SiO<sub>2</sub> showed a maximum of thermal decomposition for the Ti-POSS moiety at 280°C, that is 35°C higher than the value for Ti-POSS/SBA-15 and for the pure Ti-POSS precursor. Such difference suggests that SiO<sub>2</sub> Davison is able to stabilize Ti-POSS moieties slightly more than SBA-15. The confinement of the Ti-POSS molecules inside the pores of SiO<sub>2</sub> Davison could justify the thermal degradation delay of Ti-POSS molecules bound to the silica surface. By contrast, this effect was not observed for Ti-POSS/SBA-15 because Ti-POSS molecules are mainly localized on the particles external surface and their TGA profile is comparable to pure Ti-POSS.

DR-UV-Vis spectroscopy was used to investigate the coordination of Ti centres in Ti-POSS/SBA-15 and Ti-POSS/SiO<sub>2</sub>. Ti-SBA-15 and Ti-SiO<sub>2</sub> obtained by grafting were instead studied as reference materials.

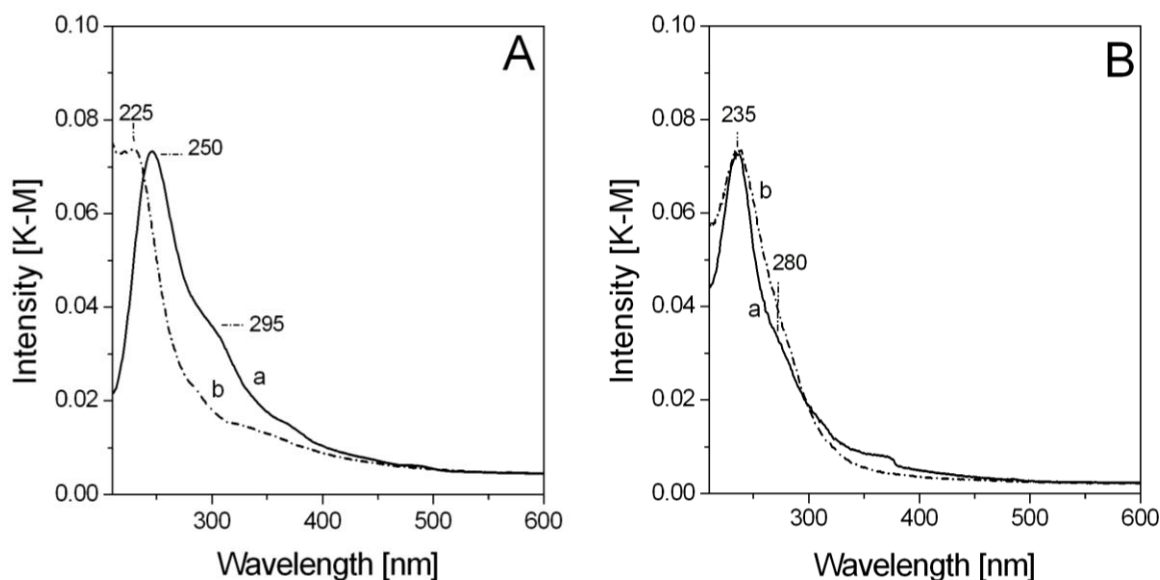


**Figure 4.3.** DR UV-Visible spectra of Ti-POSS/SBA-15 (a) and Ti-SBA-15 (b) (frame A) and Ti-POSS/SiO<sub>2</sub> (a) and Ti-SiO<sub>2</sub> (b) (frame B), after dilution of the sample in BaSO<sub>4</sub> matrix (10 wt%) and treatment at 100°C in vacuo for 1h. UV-Visible spectrum of Ti-POSS sample in BaSO<sub>4</sub> matrix after treatment at 100°C in vacuum for 1h is reported as inset of figure A.

Ti-POSS/SBA-15 showed a main absorption at 250 nm assigned to the charge-transfer transition between oxygen atoms and Ti(IV) centre in distorted five-fold coordination [10,18,30] (Fig. 4.3A, curve a). Moreover, an evident shoulder centred around 295 nm was also found (Fig. 4.3A, curve a) and it was assigned to octahedral hexacoordinated Ti atoms, as also observed in the literature [30], thus suggesting that Ti-POSS molecules anchored on the SBA-15 silica surface exist mainly as a dinuclear  $\equiv\text{Ti}(-\text{OR}-)_2\text{Ti}\equiv$  dimer form. UV-Visible spectrum of pure Ti-POSS diluted in BaSO<sub>4</sub> matrix, after dehydration at 100°C for 1h, was also collected and compared with that of Ti-POSS/SBA-15 (see inset in the Fig. 4.3A). The UV-Visible spectrum of Ti-POSS sample showed the same bands at *ca.* 250 nm and 295 nm observed for Ti-POSS/SBA-15 solid, thus indicating that Ti-POSS molecules also before the chemical anchoring on silicas surface exist mainly as a dinuclear  $\equiv\text{Ti}(-\text{OR}-)_2\text{Ti}\equiv$  dimer form.

Ti-POSS/SiO<sub>2</sub> (Fig. 4.3B, curve a) showed the same bands observed for Ti-POSS/SBA-15 sample, but shifted at lower wavelengths (i.e. at 235 and 280 nm) and with different intensity ratio with respect to those observed for Ti-POSS/SBA-15. This could be due to a different geometry of Ti-POSS dimers when anchored on SiO<sub>2</sub> Davison with respect to ordered mesoporous SBA-15.



DR-UV-Visible spectra of the solids Ti-SBA-15 and Ti-SiO<sub>2</sub>, prepared by grafting similar amount of Ti on the surface of silica, were also collected under the same conditions of the previous solids and compared to spectra of Ti-POSS/SBA-15 and Ti-POSS/SiO<sub>2</sub> (Figure 4.3A and B, curves b). Ti-SBA-15 spectrum showed only one defined band at 225 nm typical of Ti(IV) with isolated tetrahedral geometry (Fig. 4.3A, curve b), whereas the DR-UV-Vis spectrum of Ti-SiO<sub>2</sub> material showed a broader absorption centred at ca. 235 nm with a shoulder at high wavelengths, which can be assigned to the presence Ti(IV) in expanded coordination (Fig. 4.3B, curve b). The different coordination of Ti centres, when grafted on silicas with different morphology, should be related to some diversity in textural properties (i.e. specific surface area) of the two supports [31,32]. The formation of oligomeric Ti species, responsible for the presence of the band centred at ca. 280 nm for Ti/SiO<sub>2</sub>, should be associated to a lower specific surface area of SiO<sub>2</sub> Davison with respect to SBA-15 support.

UV-Visible spectroscopic results were also supported by XAFS studies recorded on pure Ti-POSS and Ti-POSS/SBA-15 which clarified the nature of the local environment of the metal centre. XAS spectra of neat Ti(*i*PrO)<sub>4</sub>, and anatase TiO<sub>2</sub> were also collected (in collaboration with Dr. Laura Sordelli) as references for tetrahedral Ti(IV) and octahedral Ti(IV), respectively.

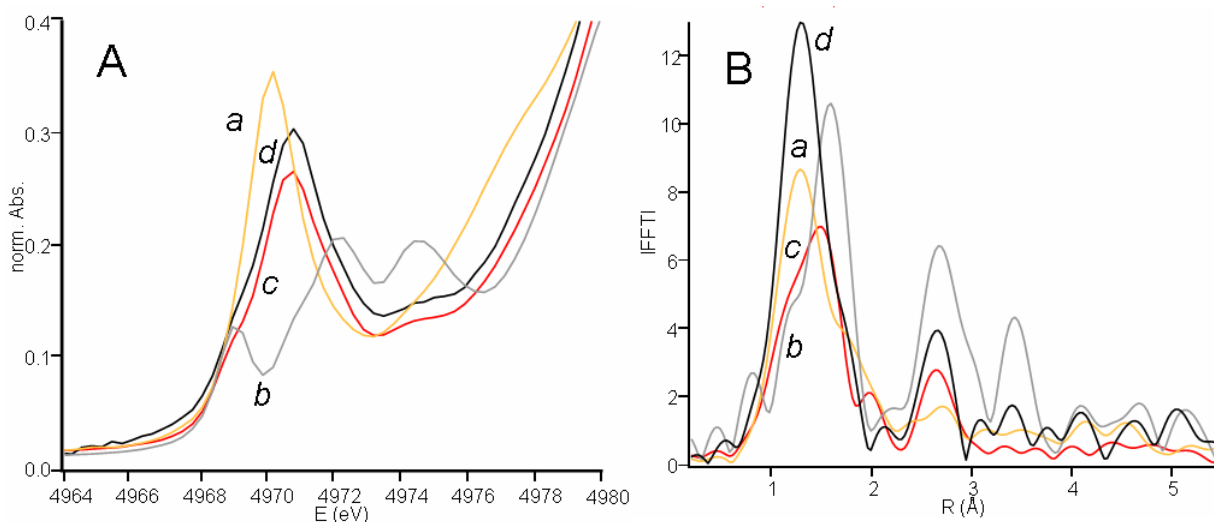
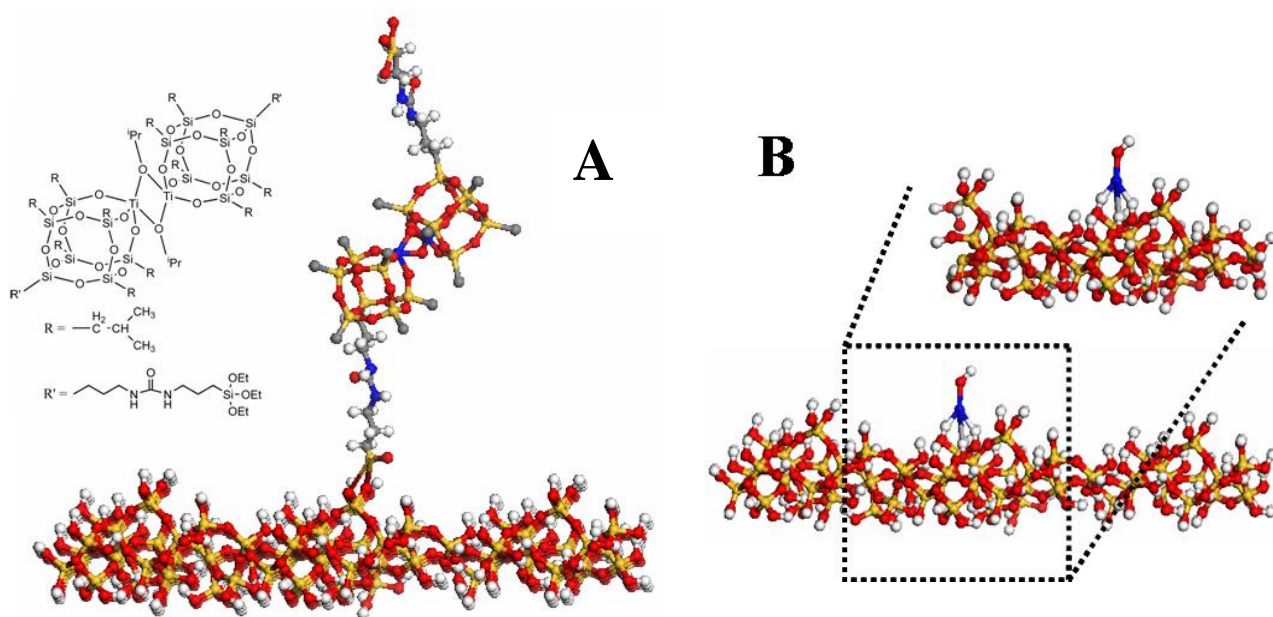


**Figure 4.4.** XANES (A) and EXAFS (B) spectra collected in vacuo of Ti(*i*PrO)<sub>4</sub> (curve a, in yellow), TiO<sub>2</sub> (curve b, in gray), pure Ti-POSS (curve c, in red) and Ti-POSS/SBA-15 (curve d, in black).

EXAFS and XANES spectra (Fig. 4.4A and B, respectively) showed that pure unsupported Ti-POSS and Ti-POSS/SBA-15 species consist of a dinuclear moiety formed by two Ti-POSS units bridged by two oxygen atoms. The resulting Ti(IV) atom is in pentacoordinated geometry, with 5

oxygen atoms in first shell, one Ti neighbour at 3.05 Å belonging to the adjacent monomer unit in the dimer, and 3 Si atoms belonging to the POSS cage in second shell at 3.22 Å. The best fit procedure of EXAFS data of both Ti-POSS and Ti-POSS/SBA-15 showed five overall oxygen atoms in first shell bound to Ti, one Ti-Ti shell at the dimer distance and three silicon atoms belonging to the POSS cage, thus confirming the existence of Ti-POSS dimers.

A representative view of the dimer structure of Ti-POSS anchored on the silicas surface is reported in Scheme 4.2.



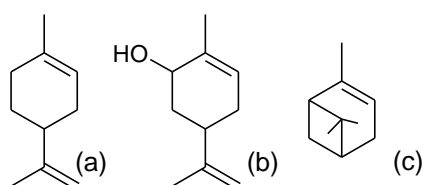
**Scheme 4.2.** Graphical view of A) Ti-POSS in dimeric form anchored on silica surfaces and of (B) Ti-grafted materials.

The existence of Ti-POSS species in form of dinuclear dimeric structures with large molecular sizes could justify the different localization of POSS moieties on the surface of SBA-15 and SiO<sub>2</sub> supports. In the case of SBA-15, which showed pore diameters lower than SiO<sub>2</sub> Davison, the confinement of Ti-POSS inside the pores was drastically hindered. The Ti-POSS species are therefore located mainly on the external surface area (it accounts for about 20% of the total specific surface area) of the mesoporous SBA-15 silica and this accounts for the low maximum titanium content achievable (max ca. 0.3 wt% Ti). On the contrary, in the case of Ti-POSS/SiO<sub>2</sub>, the non-ordered mesopores of SiO<sub>2</sub> Davison are broad enough to accommodate bulky dimeric Ti-POSS species and they are evenly distributed on the external and internal surface of the silica support. However, the poor maximum titanium loading for Ti-POSS/SiO<sub>2</sub> too is likely due to the

lower value of specific surface area of SiO<sub>2</sub> Davison with respect to SBA-15 (290 m<sup>2</sup> g<sup>-1</sup> vs. 650 m<sup>2</sup> g<sup>-1</sup>, respectively).

From the combination of the characterization techniques, in neither of the anchored Ti-POSS-catalysts, Ti(IV) sites were found close to or in direct interaction with the surface silanols of the support. It means Ti-POSS/SBA-15 and Ti-POSS/SiO<sub>2</sub> can be used as heterogeneous model systems in which Ti(IV) centres are deposited onto a silica matrix, but are not in close proximity of silanol groups. The opposite is true for grafted Ti/SBA-15 and Ti/SiO<sub>2</sub>, where Ti(IV) sites are grafted and covalently bound to the silica surface and fully surrounded by silanol groups.

Ti-POSS/SBA-15 and Ti-POSS/SiO<sub>2</sub> were tested as catalysts in the epoxidation with tert-butylhydroperoxide (TBHP) of a series of unsaturated terpenes with various functionalities and morphology (Scheme 4.3). Limonene, carveol and  $\alpha$ -pinene were chosen as test substrates to assess how and how much the proximity of Ti(IV) sites to surface silanol groups in the support can affect the reactivity and the performance in the catalytic epoxidation.



**Scheme 4.3.** Limonene (a), carveol (b) and  $\alpha$ -pinene (c).

First, the heterogeneous character of all the catalysts (both anchored and grafted) over the three substrates was proven by removing the solid catalyst by high-speed centrifugation and testing the residual liquid mixture for further reaction [33]. Since no significant loss of active species and no further activity was detected, the four catalysts were considered truly heterogeneous.

Taking into account the epoxidation of limonene (Table 4.2), the four catalysts were all active. The conversion, the selectivity values and the turn-over number (TON after 24 h) of both Ti-POSS/SBA-15 and Ti-POSS/SiO<sub>2</sub> were comparable. Actually, since Ti-POSS moieties, in both catalysts, are not confined inside narrow mesopores, but they are located at the external surface of SBA-15 or in the wide and open mesopores of SiO<sub>2</sub> Dav, they are not sensitive to the morphology of the support (and to confinement effects) and they show a similar behaviour in terms of activity and selectivity.

**Table 4.2.** Catalytic performance of the catalysts in limonene epoxidation.

Catalyst	Ti content <sup>a</sup> (wt.%)	C <sup>b</sup> 24h (%)	TON <sup>c</sup> 24 h	S <sub>epox</sub> <sup>d</sup> 24 h (%)	S <sub>epox</sub> <sup>e</sup> isoconv. (%)
Ti-POSS-TSIPI/SBA-15	0.23	25	95	88	88
Ti-POSS-TSIPI/SiO <sub>2</sub>	0.33	39	108	85	87
Ti/SBA-15	0.24	48	192	78	82
Ti/SiO <sub>2</sub>	0.29	60	198	82	84
No catalyst	-	4	-	n.d. <sup>f</sup>	n.d
SiO <sub>2</sub>	-	5	-	n.d.	n.d

Glass batch reactor; 10 mL AcOEt; 85°C; 24 h; 50 mg cat.; 1.2 mmol TBHP; 1.0 mmol limonene.

a: obtained by ICP-AES; b: limonene conversion after 24 h; c: after 24 h (mol converted substrate/ mol Ti); d: selectivity to endocyclic limonene monoepoxide after 24 h; e: selectivity to endocyclic limonene monoepoxide at 25% conversion; f: not determined.

However, anchored catalysts showed a lower activity (half of the TON) with respect to the reference grafted materials, i.e. Ti/SBA-15 and Ti/SiO<sub>2</sub>. Such difference is ascribed to the good Ti(IV) site isolation achieved by grafting modest amounts of titanocene dichloride over silica (for Ti/SBA-15 and Ti/SiO<sub>2</sub>), whereas a relevant fraction of Ti(IV) sites in Ti-POSS/SBA-15 and Ti-POSS/SiO<sub>2</sub> are in dimeric form and therefore they are less accessible to the substrate [34].

In terms of selectivity (comparing the values at 25% isoconversion conditions), the anchored materials displayed slightly better results than the grafted catalysts with comparable metal loading. In all cases, the main product was the endocyclic limonene epoxide (from ca. 80% to 88% selectivity). The other main product was the exocyclic epoxide only (10-12%), over anchored Ti-POSS-derived catalysts, whereas acid-derived by-products (9-14%) were found when reference titanocene-grafted catalysts were used. This behaviour suggests that a similar reactivity takes place at the Ti(IV) sites in both cases, but a more marked acid character is present in the reference grafted catalysts than in the anchored ones, due to the Lewis-acid nature of Ti(IV)-silica species obtained by grafting [29,35,36].

With regard to the epoxidation of carveol (Table 4.3), anchored catalysts showed conversion and TON values almost identical to grafted catalysts. This behaviour suggests that thanks to the effect of the OH-group in allylic position on the carveol molecule, the allylic binding of the hydroxyl to the Ti(IV) centre favours the epoxidation reaction [29]. So, in this case, there is no remarkable effect on the catalytic activity of the silica support morphology and of the proximity (or not) of the surface silanol groups. A similar behaviour was observed in Ti(IV)-grafted silica catalysts where silanol groups were selectively removed by silylation and, in fact, the same

activity was recorded in Ti-silica catalysts in the presence or in the absence of neighbouring silanols [37]. Conversely, anchored systems presented a remarkably higher selectivity to endocyclic epoxide (1,2-epoxide) than titanocene-derived systems (*ca.* 80% vs. 60%, respectively), even at comparable conversions (at 12%). Also with this substrate, as for limonene, the higher acid character of grafted Ti-silica catalysts than in the anchored ones accounts for the formation of undesired acid-catalysed secondary products from carveol epoxide and the loss of *ca.* 20% in selectivity.

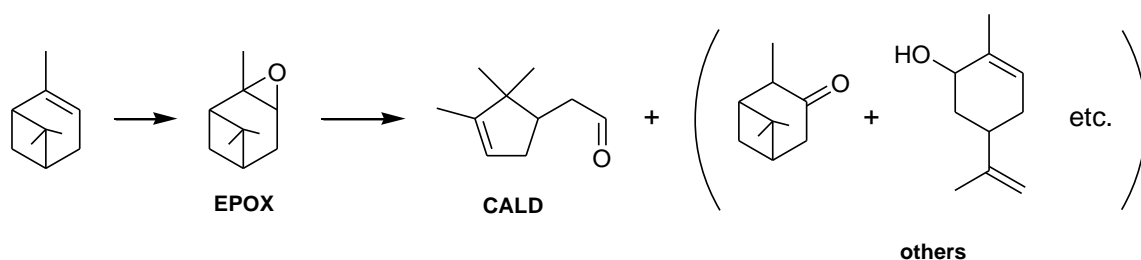
**Table 4.3.** Catalytic performance of the catalysts in carveol epoxidation

Catalyst	Ti content <sup>a</sup> (wt.%)	C <sup>b</sup> 24h (%)	TON <sup>c</sup> 24 h	S <sup>d</sup> 24h (%)	Select <sup>e</sup> isoconv. (%)
Ti-POSS-TSIPI/SBA-15	0.23	12	47	79	79
Ti-POSS-TSIPI/SiO <sub>2</sub>	0.33	19	52	80	83
Ti/SBA-15	0.24	12	48	57	57
Ti/SiO <sub>2</sub>	0.29	14	47	61	62
no catalyst	-	4	-	n.d. <sup>f</sup>	n.d.

Glass batch reactor; 10 mL AcOEt; 85°C; 24 h; 50 mg cat.; 1.2 mmol TBHP; 1.0 mmol carveol.

a: obtained by ICP-AES; b: carveol conversion after 24 h; c: after 24 h (mol converted substrate/ mol Ti); d: selectivity to endocyclic carveol monoepoxide after 24 h; e: selectivity to endocyclic carveol monoepoxide at 12% conversion; f: not determined.

Finally, the epoxidation of  $\alpha$ -pinene was chosen as a third test reaction, since the product of epoxidation,  $\alpha$ -pinene oxide, is a reactive molecule and can undergo further transformation by acid-catalysed rearrangement according to a two-step bifunctional pathway (Scheme 4.4). It is thus a tool to evaluate not only the oxidant activity of Ti(IV) sites, but also their acid properties [38].



**Scheme 4.4.** Two-step epoxidation of  $\alpha$ -pinene and acid-catalysed rearrangement of  $\alpha$ -pinene oxide.

The conversion and TON values are rather low for all the catalysts, even if they are roughly comparable to the values obtained in carveol epoxidation (Table 4.4). Nevertheless, in terms of selectivity (under isoconversion condition) to epoxidation and acid-catalysed rearrangement

products, a sharp difference was noted between anchored and grafted titanium-silica systems. In fact, over Ti-POSS/SBA-15 and Ti-POSS/SiO<sub>2</sub>,  $\alpha$ -pinene oxide was the major product recorded at the end of the reaction, whereas, over Ti/SBA-15 and Ti/SiO<sub>2</sub>, campholenic aldehyde, the compound obtained by bifunctional oxidation of  $\alpha$ -pinene plus acid-catalysed rearrangement of the intermediate  $\alpha$ -pinene oxide (Table 4.4), was the most abundant product. The rest of the products (from 15 to 30%) are carveol, pinocamphone, etc. and they are all obtained through via acid-catalysed rearrangement with different mechanisms.

Such product distribution is a further confirmation that grafted catalysts possess a higher acid character than the anchored ones [29,39] and the Lewis-acid nature of Ti(IV)-silica species is corroborated by the formation of campholenic aldehyde, that is commonly accepted to be formed mainly via a Lewis-acid catalysed rearrangement of  $\alpha$ -pinene oxide [40-42].

**Table 4.4.** Catalytic performance of the catalysts in  $\alpha$ -pinene epoxidation.

Catalyst	Ti content <sup>a</sup> (wt.%)	C <sup>b</sup> 24h (%)	TON <sup>c</sup> 24 h	S <sub>EPOX</sub> <sup>d</sup> (%)	S <sub>CALD</sub> <sup>d</sup> (%)	S <sub>others</sub> <sup>d</sup> (%)
Ti-POSS-TSIPI/SBA-15	0.23	13	47	59	14	27
Ti-POSS-TSIPI/SiO <sub>2</sub>	0.33	14	38	51	17	32
Ti/SBA-15	0.24	16	64	13	67	15
Ti/SiO <sub>2</sub>	0.29	8	26	12	72	10
no catalyst	-	3	-	n.d. <sup>f</sup>	n.d.	n.d.

Glass batch reactor; 10 mL AcOEt; 85°C; 24 h; 50 mg cat.; 1.2 mmol TBHP; 1.0 mmol pinene

a: obtained by ICP-AES; b: pinene conversion after 24 h; c: after 24 h (mol converted substrate/ mol Ti); d: selectivity to products EPOX, CALD and others (see Scheme 3) at 13% conversion; f: not determined.

## Conclusions

Ti-POSS precursors can be efficiently anchored via covalent bond, with good dispersion, on the surface of ordered and non-ordered silica supports. Owing to the peculiar size and reactivity of these precursors, Ti-POSS moieties are mainly accommodated as dinuclear dimer species on the external surface of ordered mesoporous silica or in the large mesopores of non-ordered silica supports. Ti-POSS/SBA-15 and Ti-POSS/SiO<sub>2</sub> are valid models of those solid systems where Ti(IV) centres are deposited onto a silica matrix and are not in close proximity of silanol groups. They can be used as heterogeneous catalytic models not only for generic Ti(IV)-catalysed oxidation reaction, but, more specifically, in those cases where a controlled chemical surroundings close to Ti(IV) sites (for instance, the presence or not of silanols moiety near the catalytic centre) is needed. Actually, these anchored Ti(IV) systems show, on average, a lower catalytic activity than their analogues obtained by post-synthesis grafting of simpler Ti(IV)

precursors. However, the different selectivity recorded over anchored catalysts, with respect to the grafted ones, can be potentially diagnostic about the mechanism or the molecular intermediates occurring at the surface during the oxidation reaction.

## Chapter 5. Use of Au in the epoxidation reactions with molecular O<sub>2</sub>

During decades the gold was supposed to be poorly active as a heterogeneous catalyst. However, the knowledge of poor activity comes from the chemistry of smooth gold surface or of relatively large gold particles with diameters above 10nm. In 1989 Haruta [1] found that when gold is deposited on selected metal oxides as ultra-fine particles, its chemistry dramatically changes. After this discovery, gold nanoparticles have been studied in many fields and, with particular efforts, in heterogeneous catalysis. It was found that dispersed gold particles are highly active in many important reactions for chemical industry, such as propene oxidation [2], CO oxidation at low temperatures [3], hydrochlorination of acetylene [4-6], oxidative coupling of methanol [7], epoxidation of propylene with H<sub>2</sub>/O<sub>2</sub> mixtures [8], oxidation of alcohols [9-13], and the direct synthesis of hydrogen peroxide [14, 15].

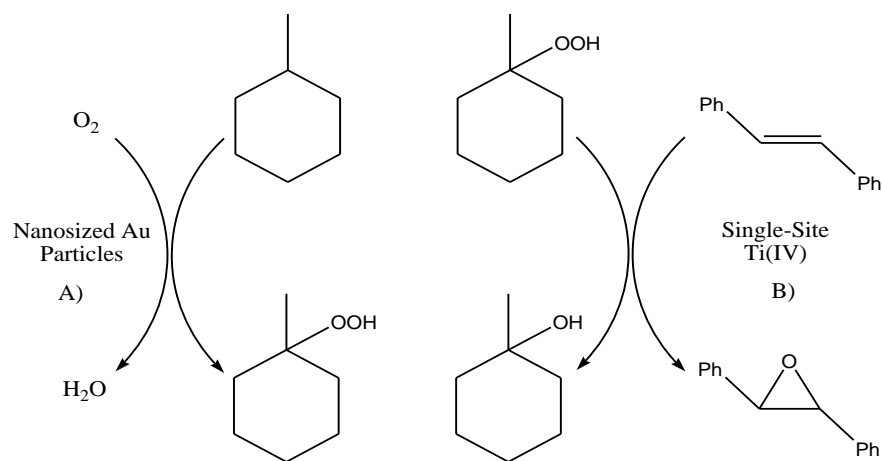
However, the adsorption of most molecules on gold surfaces is very weak at room temperature, and dissociative chemisorption of simple molecules such as O<sub>2</sub> is thermodynamically prohibited [16, 17]. This limitation, together with the already mentioned importance of oxidation reaction in the chemical industry, is at the bases of the big efforts devoted to promote oxygen activation over gold nanoparticles.

In particular, this part of the thesis, focused on the activation of molecular O<sub>2</sub>, was encouraged by a series of works by P. Lignier, where the stereoselective epoxidation of *trans*-stilbene using Au-based heterogeneous catalyst is performed. In such reactions methylcyclohexane (MCH) is used as a solvent, and TBHP as a radical initiator. It was shown that the use of methylcyclohexane as a solvent helps to reach the yield of 50% in *trans*-stilbene epoxide [18]. It was also discovered that Au/TiO<sub>2</sub> catalyst exhibits high selectivity for the aerobic epoxidation of stilbene [19].

In the epoxidation of cyclohexene, cyclooctene, styrene, *trans*-stilbene in the presence of catalytic amounts of TBHP and Au/C, under air at atmospheric pressure, it was shown that TBHP plays a role of an “initiator of a chain reaction sustained by oxygen” [20].

The hypothesis was the following: the combination of the gold ability to catalyze oxidations of C-H bonds in hydrocarbons, on one side, and the epoxidizing properties of Ti(IV), on the other side, could lead to an interesting catalyst for the epoxidation of bulky olefins in the liquid phase. Thus, the activation of molecular O<sub>2</sub> would proceed by means of gold nanosized particles, which are able to produce organic hydroperoxide from molecular O<sub>2</sub> and alkanes with a tertiary carbon atom (Scheme 5.1A). The *in situ* formation of the organic hydroperoxide can be therefore exploited to carry out the oxidation of the desired substrate molecule in the presence of a redox active Ti(IV) single-site centers (Scheme 5.1B).





**Scheme 5.1.** Mechanism for *trans*-stilbene epoxidation over the hybrid Au-Ti-based heterogeneous catalyst.

## Results and discussion

Gold nanoparticles with different loadings were deposited by three different methods: deposition precipitation (DP), impregnation and sol-gel immobilization (Table 5.1; See the Experimental part for the catalysts' preparation).

**Table 5.1.** Au-based catalysts used in the epoxidation reactions

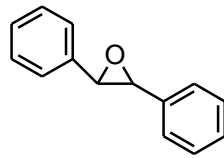
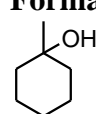
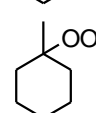
Catalyst	$D_p$ /nm	pH of preparation	Au content (wt.%)
Au/MgO	19.9	9	2
Au/TiO <sub>2</sub>		9	0.5
Au/SiO <sub>2</sub> (impregnation)	29.6	7	1
Au/SiO <sub>2</sub> 9732 (sol)	23.5	3	1
Au/SiO <sub>2</sub> DavC (sol)	9	3	1
Au/SiO <sub>2</sub> 9732 (impregnation)	33.6	3	1
Au/SiO <sub>2</sub> DavC (impregnation)	30.8	3	1
Au/SiO <sub>2</sub>	15.4	9	10
Au/C	<3		0.3
Au/SiO <sub>2</sub> Dav C	<3	3	0.5

The prepared materials were tested in the epoxidation of two substrates: *trans*-stilbene and limonene. In the literature, different solvents were tested in the epoxidation of *trans*-stilbene over Au/TiO<sub>2</sub> [21]. Amongst all the solvents investigated, only mono- and disubstituted cyclohexanes allow to achieve high yields of epoxide and high selectivity 1-methylpiperidine < piperidine < dimethylsulfoxide < benzylalcohol < dimethylformamide < cyclohexane < acetophenone < toluene < n-heptane < acetonitrile < propionitrile << methylcyclohexane ~ 1,4-dimethylcyclohexane ~ 1,3-dimethylcyclohexane. Methyl cyclohexane (MCH) showed to be the most appropriate solvent for the epoxidation of substrates chosen for our tests.

### Epoxidation of *trans*-stilbene

Epoxidation of *trans*-stilbene was chosen as a test reaction to avoid the undesired formation of allylic oxidation by-products. The preliminary results are demonstrated in the table 2.

**Table 5.2.** Epoxidation of *trans*-stilbene

Catalyst	Au or Ti (wt.%)	d <sub>Au</sub> (nm)	Formation of		Conversion of <i>trans</i> -stilbene (%)	Yield (%) of 
			 and 			
Au/SiO <sub>2</sub> 9732	10	15.4	Yes		23	6
Au/carbon	0.3	<3	Yes		40	9
Au/SiO <sub>2</sub> Aerosil	0.8	19.4	Yes		n.d.	n.d.
Au/TiO <sub>2</sub> (P25)	0.5		n.d.		n.d.	n.d.
Au/MgO	1	19.9	Yes		33	12
Ti/SiO <sub>2</sub> Dav.C <sup>a,c</sup>	1				27	8
Ti/SiO <sub>2</sub> Dav.C <sup>b,c</sup>	1				72	9
Au/SiO <sub>2</sub> coupled with Ti/SiO <sub>2</sub> Dav.C <sup>d</sup>			Yes		43	n.d.

Reaction conditions: magnetical stirring: 900 rpm, glass batch reactor, *trans*-stilbene: 0.5mmol, methylcyclohexane (MCH): 10 ml, catalyst: 150 mg, TBHP as co-oxidant: 0.025 mmol, O<sub>2</sub> pressure: 1atm, reaction T: 80 °C, 48 h, pretreatment of the catalyst at 250 °C for 4 h.

<sup>a</sup> solvent AcOEt

<sup>b</sup> solvent CH<sub>3</sub>CN

<sup>c</sup> H<sub>2</sub>O<sub>2</sub>

<sup>d</sup> addition of Ti/SiO<sub>2</sub> Davisil C was performed after 19 h of the reaction.

Au/SiO<sub>2</sub> (Au 10 wt.%) and Au/carbon (Au 0.3 wt.%) catalysts are active and selective catalysts, in terms of formation of stilbene oxide. It is worth noting, actually, that epoxide yields in the order of magnitude 10-20% represent promising results, with respect to the current state of the art. In addition, Au/SiO<sub>2</sub> (Au 0.8 wt.%) did not lead to the formation of epoxide, but the formation of tiny amounts of (methylcyclohexyl)hydroperoxide was observed. The formation of oxidized species was anyway higher than the initial quantity of TBHP, confirming an effective activation of molecular O<sub>2</sub> during the tests. The conversion of *trans*-stilbene reaches 40% in the case of Au/carbon (Au 0.3 wt.%) and 31% in the case of Au/SiO<sub>2</sub> (Au 10 wt.%).

Finally, the combination of Au and Ti based catalysts was tested by mechanical mixing the two materials, namely Au/SiO<sub>2</sub> and Ti/SiO<sub>2</sub>. Unexpectedly, the first test of coupling of Au activity and Ti epoxidation capacity did not show any activity of the system. A possible explanation could be the following: the presence of Ti-sites can suppress the formation of (methylcyclohexyl)hydroperoxide, and the present amount of TBHP can be not sufficient, since it was introduced in the reaction only as a free-radical chain initiator. Thus, the following strategy was adopted: 1) on the first step it is important to allow the formation of (methylcyclohexyl)hydroperoxide, 2) after 19 hours (it was seen that 19 hours is enough to have proper amount of (methylcyclohexyl)hydroperoxide in the system), the Ti/SiO<sub>2</sub> was added (Table 5.2, last line). Unfortunately, this strategy did not lead to any improved results. However, it is worth noting, that the set of data obtained so far are fully consistent with the best results described in the literature.

Further investigation to understand the effect of catalyst's pretreatment was followed (Table 5.3).

**Table 5.3.** Influence of the catalyst's pretreatment on the catalytic activity in *trans*-stilbene epoxidation.

Catalyst	Au (wt.%)	C 24h, (%)	Y 24h, (%)
Au/SiO <sub>2</sub> (non-pretreated)	10	32	13
Au/SiO <sub>2</sub> (pretreated)	10	23	23
Au/carbon (non-pretreated)	0.3	51	46
Au/carbon (pretreated)	0.3	40	34
Au/MgO (non-pretreated)	1	33 <sup>a</sup>	12 <sup>a</sup>
Au/MgO (pretreated)	2	n.d.	n.d.

Reaction conditions: magnetical stirring: 900 rpm, glass batch reactor, *trans*-stilbene: 0.5mmol, methylcyclohexane (MCH): 10 ml, catalyst: 150 mg, TBHP as co-oxidant: 0.025 mmol, O<sub>2</sub> pressure: 1atm, reaction T: 80 °C, 48 h, pretreatment of the catalyst at 250 °C for 4 h.

<sup>a</sup>Conversion of *trans*-stilbene after 48 h of the reaction

Note that the activity of the catalysts is higher when the materials are not pretreated. In addition, even though *trans*-stilbene epoxide was the only expected product of *trans*-stilbene epoxidation, other products, such as benzophenone, 2,2-diphenyl-acetaldehyde were also detected.

## Limonene epoxidation

Limonene was chosen as a further model for the epoxidation over Au-based systems using molecular O<sub>2</sub>. Several effects were studied, such as the Au nanoparticles' size, the solvent's nature, the presence of H<sub>2</sub>O, nature of radical initiator, the nature of the support, the pH during the catalyst preparation, and the reaction temperature.

### 1. The role of the Au particles' size

In this paragraph, the role of the Au nanoparticles' size in the epoxidation of limonene is analysed (Table 5.4).

**Table 5.4.** Influence of the Au particles' size on the conversion of limonene in limonene epoxidation.

Catalyst	Au (wt.%)	d(Au) nm	C limonene, %
Au/SiO <sub>2</sub> Dav. C	0.5	<3	13
Au/SiO <sub>2</sub> 9732	1	23.5	16
Au/SiO <sub>2</sub> Dav. C	1	30.8	26

Reaction conditions: glass batch reactor, 80°C, catalyst: 50 mg, limonene: 0.5 mmol, solvent: methyl cyclohexane (MCH), reaction time 48 h, oxidant: molecular O<sub>2</sub> 1 atm, co-oxidant: TBHP 0.03 mmol, catalysts pretreatment - 250°C in air for 4 h.

To compare the activity of the three catalysts having different Au loading (0.5 wt.% or 1 wt.%), the specific surface area of each material was calculated (nanoparticles were considered as being spherical):

$$S = (4\pi r^2) / (4\pi r^3 / 3) = 3/r$$

$$S1(\text{Au/SiO}_2 \text{ DavC, 0.5\%, } <3\text{nm}) = 2 \text{ nm}^{-1}$$

$$S2(\text{Au/SiO}_2 \text{ 9732, 1\%, } <23.5 \text{ nm}) = 0.3 \text{ nm}^{-1}$$

$$S3(\text{Au/SiO}_2 \text{ DavC, 1\%, } <30.8 \text{ nm}) = 0.2 \text{ nm}^{-1}$$

$$\rho(\text{Au}) = 19.30 \cdot 10^{-18} \text{ mg/nm}^3$$

$$m1 (\text{Au}) = 50 \text{ mg} \cdot 0.5\% / 100 = 0.25 \text{ mg Au}$$

$$V1 = m1/\rho = 12.9 \cdot 10^{15} \text{ nm}^3$$

$$\mathbf{A1 (\text{surface area}) = V1 \cdot S1 = 25.8 \cdot 10^{15} \text{ nm}^2}$$

$$m2 (\text{Au}) = 50 \text{ mg} \cdot 1\% / 100 = 0.5 \text{ mg Au}$$

$$V2 = m2/\rho = 25.9 \cdot 10^{15} \text{ nm}^3$$

$$\mathbf{A2 (\text{surface area}) = V2 \cdot S2 = 7.77 \cdot 10^{15} \text{ nm}^2}$$

$$m3 (\text{Au}) = 50 \text{ mg} \cdot 1\% / 100 = 0.5 \text{ mg Au}$$

$$V3 = m3/\rho = 25.9 \cdot 10^{15} \text{ nm}^3$$

$$\mathbf{A3 (\text{surface area}) = V3 \cdot S3 = 5.18 \cdot 10^{15} \text{ nm}^2}$$

Even though, the first material (Au/SiO<sub>2</sub> Dav. C) has the Au loading of 0.5%, the surface area (A1) is however higher than in other two materials with the Au loading of 1 wt.%. Notwithstanding only catalysts with particles size lower than 10 nm have always been considered as very active in oxidation reactions [1] Table 5.4 and calculations show unexpected results. Surprisingly, it was found that the catalyst with Au particle size of 30 nm is more active in the limonene epoxidation (limonene conversion 26%) than one with the nanoparticles' diameter of 3 nm (limonene conversion 13%). Perhaps, the optimal size of nanoparticles is not the same for all support types.

## 2. Effect of the solvent

The coupling of the Au activity with the epoxidation capacity of Ti has been performed also in this case. Since the presence of water can inhibit, in principle, the activity of Ti active sites (see chapter 1), anhydrous MCH was initially used as the solvent (Table 5.5). However, it was observed that anhydrous methyl cyclohexane does not lead to the improvement of the activity. On the contrary, the presence of water enhances the conversion of limonene and the yield of the limonene epoxide. This fact was as already observed in other oxidation reactions [22, 23]. The potential role of water and hydroxyls in catalysis over Au nanoparticles has been highlighted recently. It was shown that small amounts of water increase the catalytic activity in CO oxidation, which is partly attributed to activation of oxygen on the hydroxylated support. Analogously, the positive role of water suggests the need for free protonic species which may take part in the formation of the hydroperoxide intermediates. Further investigation is however needed to clarify the beneficial role of water and/or of protic solvents in this oxidation process.

**Table 5.5.** Influence of the solvent on the epoxidation of limonene

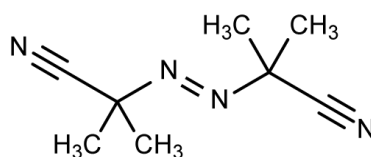
Catalyst	Solvent	C limonene (%)	Y limonene epoxide(%)
Au/MgO	MCH	29	n.d.
Au/MgO+Ti/SiO <sub>2</sub>	MCH	28	n.d.
Au/MgO+Ti/SiO <sub>2</sub>	MCH anhydrous	14	n.d.
Au/MgO+Ti/SiO <sub>2</sub>	MCH+20μl H <sub>2</sub> O MQ	43	7
Au/MgO+Ti/SiO <sub>2</sub>	5 mL MCH (anh.) + 5 mL TFT	14	n.d.

Reaction conditions: glass batch reactor, 80°C, limonene: 0.5 mmol, solvent: methyl cyclohexane (MCH): 10 mL, reaction time 48 h, T reaction: 80 °C, oxidant: molecular O<sub>2</sub>, 1 atm, co-oxidant: TBHP 0.03 mmol, catalysts pretreatment - 250°C in air for 4 h.

In order to verify the benefit of the presence of fluorinated solvents reported in the literature [24], that are ascribed to the increase of solubility of the dissolved oxygen and to the peculiar affinity of oxygen-donor species with fluorine-containing solvents, the role of trifluorotoluene as a co-solvent was evaluated. Unfortunately, no improvement was observed with respect to the use of pure MCH.

### 3. Influence of the radical's initiator nature

The role of different radical initiators was already deeply studied and many examples are present in the literature. In all cases O<sub>2</sub> was adopted as the oxidant. It was shown that the presence of catalytic amounts of TBHP leads to the production of epoxide, while di-*tert*-butylhydroperoxide (<sup>t</sup>BuO-OBu<sup>t</sup>) and hydrogen peroxide (HO-OH) are not suitable for epoxidation [21]. Moreover, the use of azobis-iso-butyronitrile, AIBN (Scheme 5.2), as radical initiator leads to high yields [25]. Here, the use of TBHP and AIBN was studied in the limonene epoxidation over Au/MgO catalyst (Table 5.6).

**Scheme 5.2.** Azobis-iso-butyronitrile, AIBN

**Table 5.6.** Influence of the radical initiator on the activity of Au/MgO in the limonene epoxidation.

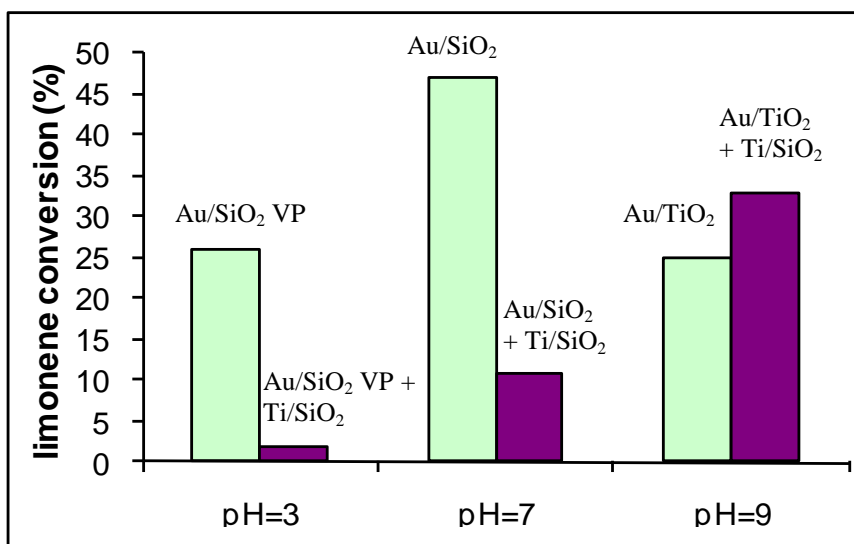
Catalyst	Radical Initiator	C limonene, %	Y limonene epoxide, %
Au/MgO	TBHP	41	10
Au/MgO	AIBN	36	5

Reaction conditions: glass batch reactor, 80°C, limonene 0.5 mmol, solvent: methyl cyclohexane (MCH), reaction time 48 h., oxidant: molecular O<sub>2</sub>, 1 atm, co-oxidant: 0.03 mmol, catalysts pretreatment – no pretreatment.

The use of AIBN as radical initiator does not lead to the improvement of the activity and selectivity of the catalyst. On the contrary, the yield to limonene epoxide is decreased (5%). Such difference in the behaviour can be ascribed to the difference pressure of O<sub>2</sub> adopted in the present work (1 atm) with the respect to the one used in the literature (12 atm) [3]. Moreover, the leaching of Au was observed together with a total decolouration of the the catalyst powder. In this case, the formation of soluble gold cyanocomplexes, derived from the decomposition of AIBN, and the leaching of the metal out from the support is probable.

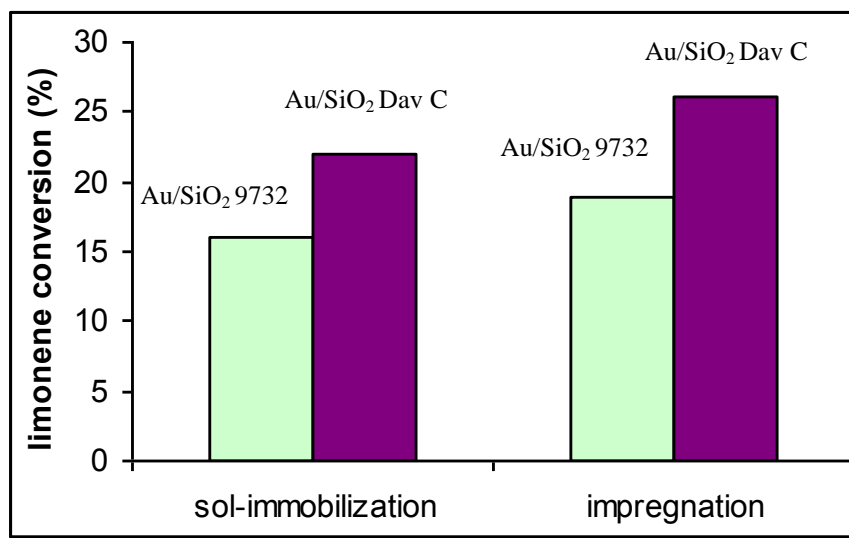
#### 4. Influence of pH and preparation method

The effect of pH during the catalyst synthesis was also investigated. In fact, preparation of the catalysts was performed at different pH values: 3, 7 and 9. These Au-containing catalysts were then tested without any co-catalyst or coupled with Ti-SiO<sub>2</sub> (Scheme 5.3). Au-based catalyst prepared at pH=7 shows high activity, but the activity decreases when the Au-based material is coupled with Ti-heterogeneous silica. On the other hand, Au-based catalyst prepared at pH=9 shows higher activity when coupled with Ti-heterogeneous silica. The Au-based material prepared at pH=3 has the same activity of the one prepared at pH=9, but its coupling with Ti leads to a drastic decrease of activity. The explanation of these effects is likely connected to the support PZC but the deep analysis of this factor is not a main aim of this work. Anyhow, these results are in accordance with the literature [26].



**Scheme 5.3.** Influence of the pH during the catalyst preparation on the catalytic behaviour in the limonene epoxidation.

In addition, the comparison of the two methods of the preparation of gold nanoparticles (sol immobilization and impregnation) was performed (Scheme 5.4).



**Scheme 5.4.** Different methods of the preparation of gold nanoparticles.

It was observed that Au/SiO<sub>2</sub> catalyst prepared by impregnation is more active than the one prepared by sol-immobilization. The activity reaches 48% in limonene conversion with the yield of 28% in limonene oxide.

To prove the hypothesis shown on Scheme 1, the ability of Au in O<sub>2</sub> activation has been coupled to the epoxidation capacity of Ti. First, the mechanical mixture of Au/SiO<sub>2</sub> and Ti/SiO<sub>2</sub> was prepared. Then, some bifunctional materials were obtained following the grafting of



TiCp<sub>2</sub>Cl<sub>2</sub> onto the surface of a pre-formed Au/SiO<sub>2</sub> mesoporous material. However, the expected synergistic effect was not achieved. Actually, the addition of titanium causes a dramatic loss of gold activity. Anyway, no clear-cut experimental evidences are available so far about the mechanism taking place at the Au centres and the work is still in progress in this topic.

## Conclusions

Gold with different loadings was deposited by two different methods: impregnation and sol-gel immobilization. The supporting materials were SiO<sub>2</sub>, MgO or Carbon and a common material was adopted while analyzing a certain factor. All composites were tested in the epoxidation of *trans*-stilbene and limonene. Molecular O<sub>2</sub> was used as oxidant and TBHP as a free-radical initiator. In the epoxidation of *trans*-stilbene the influence of the pretreatment of the catalyst was studied: it was observed that non-pretreated catalyst is more active in the epoxidation of *trans*-stilbene. The formation of side-products, such as benzophenone, 2,2-diphenyl-acetaldehyde was also detected, even though the expectations from the epoxidation of *trans*-stilbene were the formation of only *trans*-stilbene epoxide.

Limonene was chosen as another model for the epoxidation over Au-based systems. The effect of various factors, such as Au nanoparticles' size, the solvent's nature, the presence of H<sub>2</sub>O, nature of radical initiator, the pH during the catalyst preparation was studied. Surprisingly, it was found that the catalyst with Au particle size of 30 nm is more active in the limonene epoxidation (limonene conversion 26%) than one with the nanoparticles' diameter of 3 nm (limonene conversion 13%). Studying the influence of the solvent's nature, it was found that the presence of water enhances the conversion of limonene and the yield of the limonene epoxide, while the use of trifluorotoluene did not lead to improved performance.

Studying the nature of the radical initiator, it was observed that the use of AIBN does not lead to the improvement of the activity and selectivity of the catalyst, on the contrary, the yield to limonene epoxide is decreased (5%).

Au/SiO<sub>2</sub> catalyst prepared by impregnation method is more active than the one prepared by sol-immobilization technique in the epoxidation of limonene. The activity reaches 48% in limonene conversion with the yield of 28% in limonene oxide.

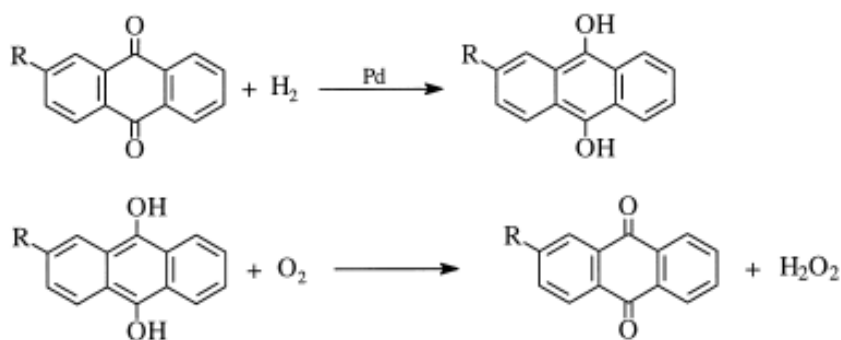
Finally, to prove the hypothesis shown on Scheme 5.1, the ability of Au in O<sub>2</sub> activation has been coupled to the epoxidation capacity of Ti. First, the mechanical mixture of Au/SiO<sub>2</sub> and Ti/SiO<sub>2</sub> was prepared. Then, bifunctional materials were obtained following the grafting of TiCp<sub>2</sub>Cl<sub>2</sub> onto the surface of a pre-formed Au/SiO<sub>2</sub> mesoporous material. However, the expected

synergistic effect was not achieved. Actually, the addition of titanium causes a dramatic loss of gold activity. Anyway, no clear-cut experimental evidences are available so far about the mechanism taking place at the Au centres and the work is still in progress in this topic.

## Chapter 6. Production of H<sub>2</sub>O<sub>2</sub> in-situ by means of (Glucose Oxidase) GOx in air

This part of the thesis was performed in Montpellier at *Laboratoire de Materiaux Catalytiques et Catalyse en Chimie Organique CNRS/ENSCM/UMI Ecole Nationale Supérieure de Chimie de Montpellier*.

The most common way for the industrial H<sub>2</sub>O<sub>2</sub> production is the anthraquinone process [1] (Scheme 6.1).



**Scheme 6.1.** Anthraquinone process for industrial H<sub>2</sub>O<sub>2</sub> production

Other methods for the H<sub>2</sub>O<sub>2</sub> production can be mentioned: hydrogenation of oxygen over the Pd-based heterogeneous catalyst [2], electrochemical ways [3], or enzymatic routes [4,5]. Here we will focus on the enzymatic route for in situ H<sub>2</sub>O<sub>2</sub> production.

Enzymes are very selective catalysts and may represent a suitable response for the challenges of the 21<sup>st</sup> century in catalysis with respect to improvement of the selectivity of the reactions [6]. Many industrial processes use enzymatic catalysis. For example, lactic acid, propane-1,3-diol, and many pharmaceutical intermediates can be synthesized by using either chemical or biochemical processes where catalytic steps are of great significance [7]. For instance, Glucose Oxidase (GOx) finds large application in chemical, pharmaceutical, food, beverage, clinical chemistry, biotechnology and other industries [8-10]. Novel applications of glucose oxidase in biosensors have increased the demand in recent years. Moreover, GOx promotes the H<sub>2</sub>O<sub>2</sub> production by catalyzing the oxidation of  $\beta$ -D-glucose to gluconic acid, by utilizing molecular oxygen as an electron acceptor.

However, there are some problems with the use of enzymes, such as their stability towards temperature, solvents, or pH. Thus, for industrial applications, a challenge is to find a way to increase the stability towards the factors mentioned above and to recover the biocatalyst from the medium after the reaction. The solution can be to heterogenize the biocatalyst by

immobilizing it into an inorganic matrix without deactivating it. There are different methods for immobilizing enzymes in inorganic supports such as covalent binding, adsorption and sol-gel encapsulation (Fig. 6.1) [11-13].

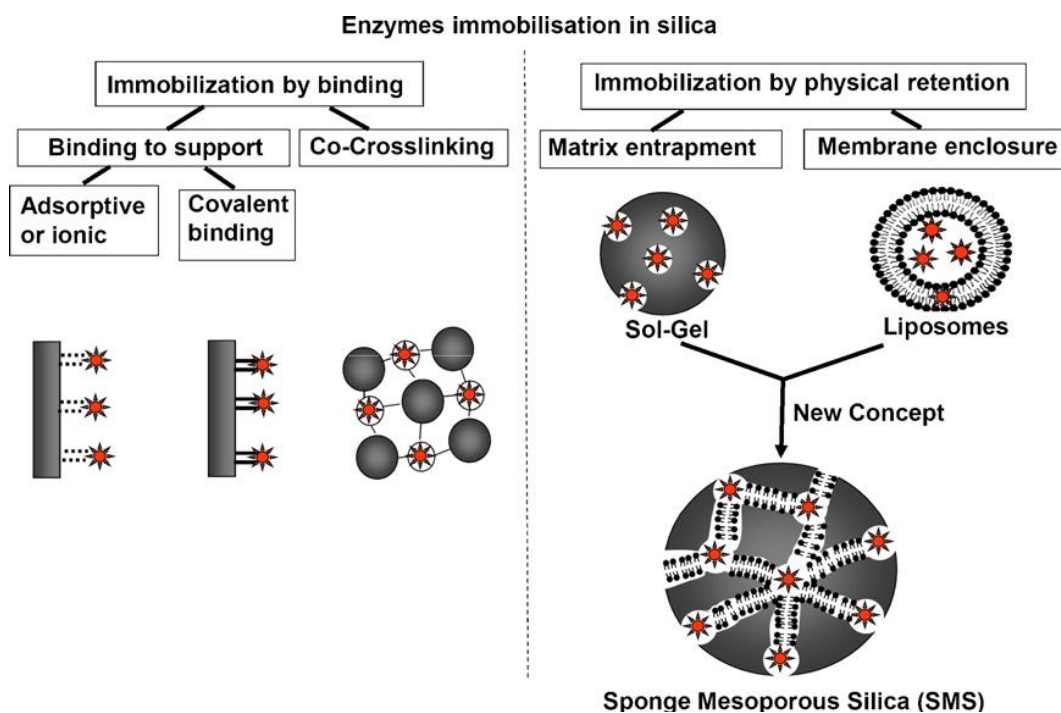


**Figure 6.1.** Schematic representation of the different ways to immobilize enzyme.

All these methods have advantages and disadvantages [14]. The adsorption of enzymes in an inorganic support is the cheapest and the easiest method, but is often susceptible to a progressive leaching. The grafting of enzymes onto a support avoids the leaching, but is more time consuming as it implies a previous functionalization of the support before to react with a part of the protein, which can sometimes lead to the denaturation of proteins. Silica sol-gel entrapment represents a good compromise. However, the direct interaction of proteins with silanols should be minimized to avoid protein deformation. For this purpose, soluble excipients are added to stabilize the correctly folded protein conformation. Additives help also to stabilize proteins against the denaturing stresses encountered upon sol-gel entrapment. Silica sol-gel allows maintaining activity of enzymes [14] or bacteria [15-17] by using additives such as sugars, glycerol, charged polymers (poly-vinylimidazole, -ethyleneimine, -ethyleneglycol) or gelatin. For lipases encapsulated in sol-gel, poly(vinyl alcohol) [18,19] has been used and the synthesis has been further developed commercially by Fluka. Nevertheless, in sol-gel encapsulation, the lack of controlled porosity limits the diffusivity of the substrates.

A new method developed by group of A. Galarneau for the encapsulation combines the sol-gel method with a templating process using bilayers of phospholipids to provide an organized

network of lecithine species inside the silica and, at the same time, to protect the embedded enzymes, as if they were entrapped in a biological membrane supported on silica [12]. This brings a porosity control to the classical sol-gel encapsulation and increases the accessibility of the substrate to a maximum of enzymes.

### Structure of Glucose Oxidase

GOx ( $\beta$ -D-glucose-oxygen 1-oxidoreductase) is a flavoprotein which catalyzes the oxidation of  $\beta$ -D-glucose to D-glucono- $\delta$ -lactone and hydrogen peroxide using molecular oxygen as an electron acceptor. GOx is a dimeric protein (Figure 6.2) with a molecular weight ranges from 130 to 1750 kDa, containing one tightly bound ( $K_a = 1 \times 10^{-10}$ ) flavin adenine dinucleotide (FAD) per monomer as cofactor (actually two FAD-sites per the enzyme). The FAD is not covalently bound and can be released from the holo-protein following partial unfolding of the protein. This process can be performed under mild conditions preventing full denaturation of the enzyme. The respective GOx apo-enzyme can be obtained after FAD extraction. The apo-enzyme missing the FAD cofactor is not biocatalytically active, but it can be reconstituted with native or artificially modified FAD cofactor. The enzyme is glycosylated with a carbohydrate content of 16% (w/w). The carbohydrate moiety is designated as high mannose type with 80% (w/w) of the carbohydrate being mannose. The mannose is N and O glycosidically linked to Asn, Thr and Ser.

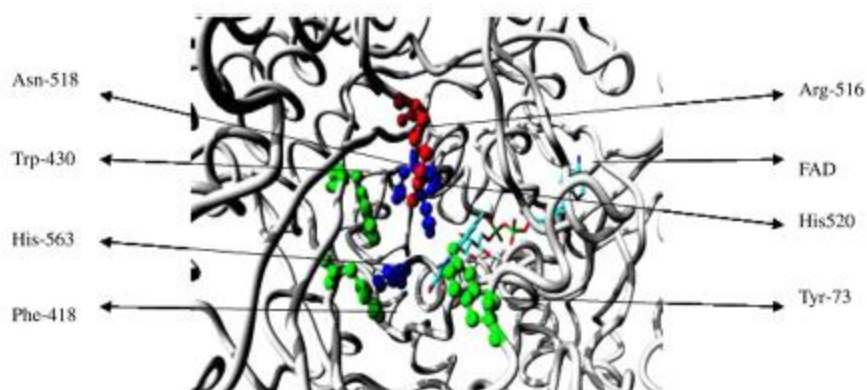


**Figure 6.2.** Glucose oxidase

Glucose oxidase (GOx) is purified from a range of different fungal sources, mainly from the genus *Aspergillus* and *Penicillium*, of which *A.niger* is the most commonly utilized for the production of GOx [20, 21].

It will be advantageous to combine chemo-, regio-, and stereoselectivity of enzymes with high oxidation ability of TS-1. In this chapter, the immobilization of GOx and its combined use with Ti(IV)-silica catalysts in the epoxidation reactions using *in situ* formed H<sub>2</sub>O<sub>2</sub> will be described.

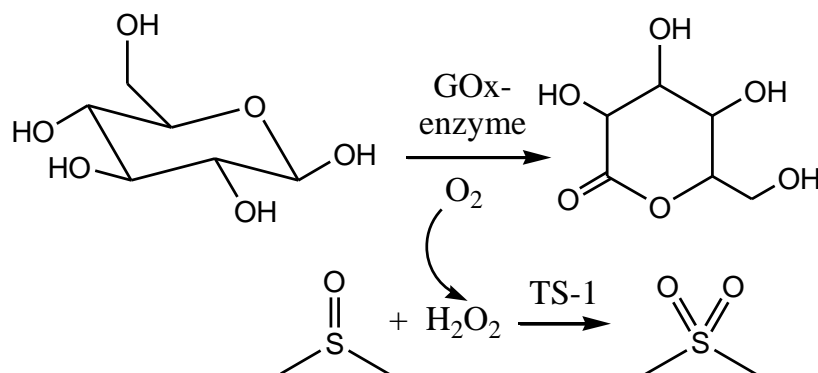
## Results and discussion

A hybrid enzymatic-inorganic system composed of glucose oxidase (GOx) and TS-1 was developed (see Experimental Part). This particular system in the presence of air and glucose allows one to perform oxidation reactions thanks to the *in situ* formation of H<sub>2</sub>O<sub>2</sub> [20,22].

### 1. DMSO oxidation

DMSO is widely used as a solvent. As a consequence, large amounts of DMSO-containing wastewater are generated. There are chemical and biological methods for treating wastewater containing organic contaminants. Among the chemical methods for DMSO removal, the oxidative degradation is particularly promising. Biological treatment is not applicable because DMSO is less biodegradable and during this process volatile and noxious products are formed. The combination of oxidation and biological processes could provide a valuable solution for the treatment of DMSO-containing wastewaters.

Here, the oxidation of DMSO is performed in liquid phase in water solution (Scheme 6.2). Encapsulated glucose oxidase (GOx-NPS) was used in the oxidation of DMSO in the presence of TS-1 in water solution at room temperature and it presented the first example of the use of hybrid enzyme-inorganic catalyst.



**Scheme 6.2.** In situ production of H<sub>2</sub>O<sub>2</sub> and its use in DMSO oxidation

The catalytic properties of TS-1 were initially investigated. For this, the reaction was performed with H<sub>2</sub>O<sub>2</sub> (50wt. % aqueous solution). The 100% conversion was reached in 15 minutes.

To perform the reaction with the hybrid enzyme-inorganic catalyst, it is crucial to determine the ratio between GOx and TS-1, since it is the first example of the use of hybrid enzyme-inorganic catalyst. Thus, different amounts of active free- and GOx-NPS were used. Obtained results are shown in Table 6.1.

**Table 6.1.** DMSO oxidation with GOx free and GOx-NPS hybrid enzyme-inorganic catalyst.

Amount of active GOx, mg	C <sub>DMSO</sub> at 24h, % Free GOx	C <sub>DMSO</sub> at 24h, % GOx-NPS
0	19	19
0.15	19	27
0.75	37	30
1.5	56	21
3.5	100	21
7.5	100	21
15	96	12
16.5	95	10

Reaction conditions: DMSO=2mmol, phosphate buffer =15 ml (pH=5.3), oxidant= bubbling air, biocatalyst=GOx free or GOx-NPS, catalyst= 50 mg TS-1, Glucose=4.5 g, reaction temperature=25°C.

The optimum amount of GOx free for DMSO oxidation (100% conversion) is 3.5 mg, corresponding to a GOx:Ti weight ratio of 5.4. Encapsulated glucose oxidase (GOx-NPS) was used in the oxidation of DMSO in the presence of TS-1 in water solution at room temperature. The maximum conversion for DMSO using encapsulated GOx was found to be 30% at the amount of active GOx 0.75 mg (Fig. 6.3).

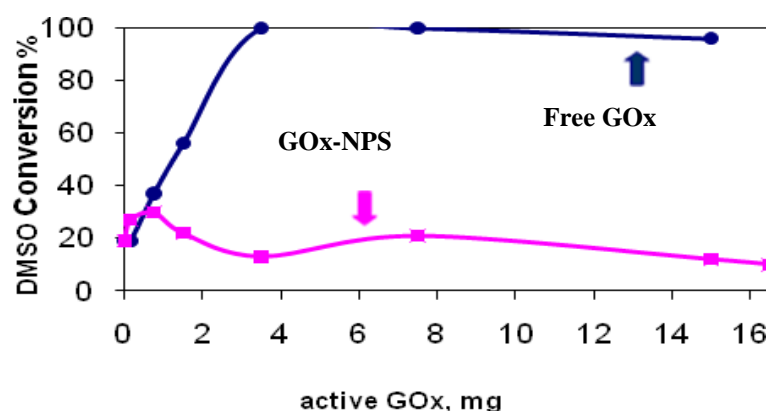


**Figure 6.3.** Conversion of DMSO vs. amount of active GOx:

## Determination of GOx activity

Since enzymes are particularly sensitive to environmental conditions such as temperature, pH, use of organic solvent, it is very important to measure the enzyme's activity if one of the parameters is changed. Different methods exist for measuring GOx activity. Most researchers use an analytical method for GOx that is based on the principle that GOx oxidizes  $\beta$ -D-glucose in the presence of oxygen to  $\beta$ -D-glucono- $\delta$ -lactone and  $H_2O_2$ . The  $H_2O_2$  is then utilized to oxidize a chromogenic substrate in a secondary reaction with horseradish peroxidase (HRP) with a resultant color change that is monitored spectrophotometrically.

Here, the activity of free GOx and of two batches of encapsulated GOx was determined by Trinder test (see Experimental part) [23]. Obtained results are demonstrated in the Table 6.2.

**Table 6.2.** Activity of the GOx free and encapsulated GOx (GOx-NPS)

Material	Activity
GOx free	8000 $\mu\text{mol}/\text{min}\cdot\text{g}$
GOx·NPS (EG020)	135 $\mu\text{mol}/\text{min}\cdot\text{g}$
GOx encapsulated (EG020) batch no. 1	16 mg active GOx/1g GOx·NPS
GOx·NPS (EG026)	90 $\mu\text{mol}/\text{min}\cdot\text{g}$
GOx encapsulated (EG026) batch no. 2	11 mg active GOx/1g GOx·NPS
GOx free <sup>a</sup>	8000 $\mu\text{mol}/\text{min}\cdot\text{g}$

<sup>a</sup>GOx activity measured in the presence of  $CH_3CN$  solvent.

To check the stability of free GOx in the presence of organic solvent, the activity was measured in the presence of  $CH_3CN$ . No change in activity was observed. The value of 8000  $\mu\text{mol}/\text{min}\cdot\text{g}$  confirmed that there is no influence of the organic solvent on the stability of free glucose oxidase.

## 2. Epoxidation of trans-stilbene

Free and encapsulated GOx were tested also in *trans*-stilbene epoxidation in organic media. The activity of free GOx in the presence of  $CH_3CN$  was measured and the value was not changed. Ti/SiO<sub>2</sub> catalyst was tested in the epoxidation of *trans*-stilbene with the slow dropwise addition



of H<sub>2</sub>O<sub>2</sub>. The conversion reached 50% after 3 hours with the yield to epoxide of 6%. The coupling of Ti(IV)-silica material with free GOx lead to the increase in the conversion (90%). Further coupling of the Ti-silica material with encapsulated GOx lead to the increase of the conversion up to 98% and the yield of the epoxide reached 12% after 3 hours of the reaction (Table 6.3).

**Table 6.3.** *trans*-stilbene epoxidation with H<sub>2</sub>O<sub>2</sub> formed in-situ from Glucose and GOx

Catalyst	Amount of active GOx	C 3h (%)	Y epoxide, 3h (%)
Ti/SiO <sub>2</sub> <sup>a</sup>	0	50	6
Ti/MCM-41	0.75 mg of GOx free	90	0
Ti/MCM-41	0.75 GOx-NPS	98	12

<sup>a</sup>oxidant=H<sub>2</sub>O<sub>2</sub>

Reaction conditions: *trans*-stilbene: 0.5mmol, solvent: 10 mL CH<sub>3</sub>CN, oxidant: slow addition of GOx in 15 ml of phosphate buffer, reaction temperature: 85°C

Thus, the coupling of Ti/MCM-41 with encapsulated GOx leads to the improvement of the activity and selectivity of the system. The conversion to *trans*-stilbene and the yield to epoxide enhance significantly, from 50% to 98% and from 6% to 12%, correspondingly. These promising results prompted us to go on with the tests about this topic and further unsaturated substrates will be tested soon.

## Conclusions

Encapsulation of glucose oxidase was performed by an efficient method combining the sol-gel technique with a templating process. The optimum amount of GOx free for DMSO oxidation is 3.5 mg, corresponding to a GOx:Ti weight ratio of 5.4 while for the encapsulated GOx the optimum amount was found to be 0.75 mg, and the maximum conversion was found to be 30%. The activity of encapsulated and free GOx was measured and the results show that the enzymes retain similar values when encapsulated in inorganic matrix and that the presence of organic solvent (CH<sub>3</sub>CN) does not change the activity of free glucose oxidase. Encapsulated and free GOx were also tested in the oxidation of *trans*-stilbene. The coupling of encapsulated GOx with Ti/MCM-41 led to very high activity of the system (*trans*-stilbene conversion reaches 98%) and the yield reached 12%. To our best knowledge, this is the first example of the combination of

enzyme and inorganic material used in the oxidation reactions both in aqueous and organic media. In other words, this is the proof of principle that such a combination leads to successful results. However, the set of data collected so far is still preliminary and the work is in progress.

## General Conclusions

The main following conclusions can be drawn:

- Ti(IV)-heterogeneous silicas were successfully synthesized by the grafting procedure;
- All Ti-containing catalysts are active in epoxidation reactions with aq.  $\text{H}_2\text{O}_2$  thanks to the applied slow dropwise addition protocol;
- The effect of Ti modification surrounding was studied;
- The model compound (Ti-POSS/ $\text{SiO}_2$ ) was synthesized. It can be a powerful tool for studying the mechanism of the epoxidation reaction;
- In-situ production of  $\text{H}_2\text{O}_2$  by means of GOx was performed;
- Activation of molecular  $\text{O}_2$  by means of Au-nanoparticles was studied.

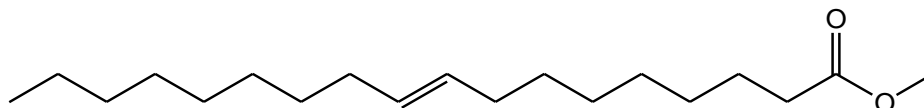
## Experimental Part

### Reagents

In the present work the following reagents were used:

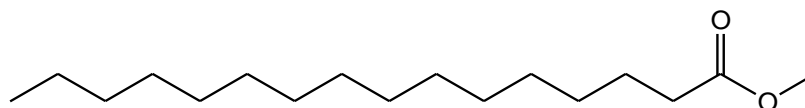
1. **9-octadecenoic acid methyl ester (methyl oleate)**

Sigma-Aldrich



2. **Methyl hexadecanoate (methyl palmitate)** - used as internal standard

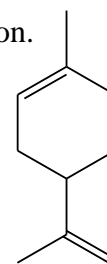
Sigma-Aldrich



3. **(R)-(+)-Limonene** – is a cyclic pentene used as a precursor in synthesis of carvone.

Limonene commercially is obtained from citrus fruits by centrifugation.

Sigma-Aldrich



4. **Cyclohexene** –Is a precursor to adipic acid. It is produced by the partial hydrogenation of benzene - Carlo-Erba
5. **Mesitylene** – Sigma-Aldrich - used as internal standard
6. **tert-butylhydroperoxide (TBHP 0.5-0.6 M in decane)** –Sigma-Aldrich
7. **Hydrogen peroxide (H<sub>2</sub>O<sub>2</sub>, 30% and 50% w/w)** – Sigma-Aldrich
8. **Molecular Oxygen**
9. **Acetonitrile** – is produced mainly as a byproduct of acrylonitrile manufacture.
10. **Ethyl Acetate** – is used in glues, nail polish removers. Is synthesized via Fischer esterification of ethanol and acetic acid.
11. **Dicloromethane** –
12. **Chloroform** – Sigma-Aldrich, stabilized with ethanol
13. **Pyridine** – Fluka
14. **Triethylamine** – Sigma-Aldrich

15. **Trifluorotoluene** – Sigma-Aldrich
16. **Titanocene dichloride (TiCp<sub>2</sub>Cl<sub>2</sub>)** – Fluka
17. **Glucose oxidase (GOx) from *Aspergillus niger* (E.C. 1.1.3.4. type X-S, 1000units/mg solid, 75% protein)**

## Materials used

The following materials were chosen as catalysts, reported in two different tables, in dependence on the nature of the active site.

**Table 1.** Ti-heterogeneous silicates

Catalyst	Ti content, wt. %	S <sub>BET</sub> /m <sup>2</sup> g <sup>-1</sup>	D <sub>p</sub> /nm
Ti/SBA-15	0.78		
Ti/Aerosil	0.64	262	n.d.
Ti/MCM-41	0.8	930	3.6
Ti/MCM-48	0.8	982	3.8
TS-1	1	346	
Ti-POSS-TSIPI/SBA-15	0.23	547	8.8-8.5
Ti-POSS-TSIPI/SiO <sub>2</sub>	0.33	210	10.0-32.5
Ti/SBA-15	0.24	n.d.	n.d.
Ti/SiO <sub>2</sub>	0.29	n.d.	n.d.

**Table 2.** Au-based catalysts

Catalyst	D <sub>p</sub> /nm	pH of preparation	Au content (wt. %)
Au/MgO	19.9	9	2
Au/TiO <sub>2</sub>		9	0.5
Au/SiO <sub>2</sub> (imp.)	29.6	7	1
Au/SiO <sub>2</sub> 9732 (sol)	23.5	3	1
Au/SiO <sub>2</sub> DavC (sol)	9	3	1
Au/SiO <sub>2</sub> 9732 (imp.)	33.6	3	1
Au/SiO <sub>2</sub> DavC (imp.)	30.8	3	1
Au/SiO <sub>2</sub>	15.4	9	10

## Preparation of the catalysts

The following supports were prepared in the laboratory of Anne Galarneau in Montpellier, France.

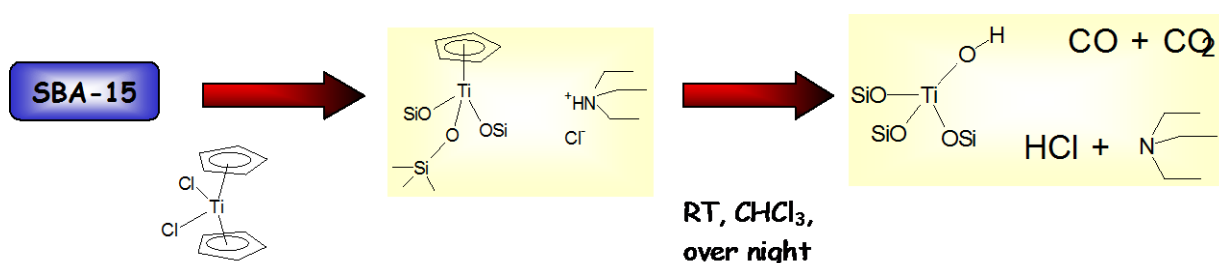
### Preparation of ordered mesoporous silicas

**MCM-41.** MCM-41 was prepared with the molar ratio, 1 SiO<sub>2</sub>/ 0.1 CTAB/ 0.27 NaOH/ 32 H<sub>2</sub>O. 19.06 g H<sub>2</sub>O, 0.356 g NaOH and 1.204 g cetyltrimethyl ammonium bromide (CTAB, Aldrich) were mixed at 50°C until an homogeneous solution was obtained and then 2 g of silica (Aerosil 200, Degussa) were added stepwise and stirred for 1 h. Then the mixture was put in an autoclave at 115°C for 24 h. The resulting slurry was filtered and washed until neutral pH and dried at 80°C overnight. The powder was then calcined at 550°C for 8h.

**MCM-48.** MCM-48 was prepared with the molar ratio, 1 SiO<sub>2</sub>/ 0.175 CTAB/ 0.38 NaOH/ 120 H<sub>2</sub>O. 214 g H<sub>2</sub>O, 1.54 g NaOH and 6.22 g cetyltrimethyl ammonium bromide (CTAB, Aldrich) were mixed at 50°C until an homogeneous solution was obtained and then 6 g of silica (Aerosil 200, Degussa) were added stepwise and stirred for 2 h. Then the mixture was put in an autoclave at 150°C for 15 h. The resulting slurry was filtered, without washing, and dried at 80°C overnight. The powder was poured again in an autoclave with water (7.5 g H<sub>2</sub>O per gram of solid), the mixture was stirred for 20 min and the autoclave was put at 130°C for 6 h. This post-treatment was repeated once again. The resulting slurry was filtered and washed until neutral pH and dried at 80°C overnight. The powder was then calcined at 550°C for 8h.

### Preparation of Ti-Silica Catalysts

Catalysts were prepared by grafting titanocene dichloride (TiCp<sub>2</sub>Cl<sub>2</sub>; Fluka) onto different silicas (MCM-41, MCM-48, Aerosil).



[32,42]

Before grafting, the supports were pretreated at 500°C for 2 hours in air and then in vacuo at the same temperature for 2 hours [T. Maschmeyer, F. Rey, G. Sankar, J.M. Thomas, *Nature*, 378,

**1995**, 159]. Titanocene dichloride was dissolved in anhydrous chloroform (Sigma-Aldrich) under argon and stirred for 2 hours at room temperature. Triethylamine (Sigma-Aldrich) or pyridine (Fluka) was then added to the suspension and left overnight under stirring to activate the surface silanols of the support (e.g. MCM-41). A weaker base, pyridine, was used in the grafting over MCM-41 and MCM-48 to protect the support. The colour of the suspension changed from red via orange to yellow, signifying that the well established substitution of chloride with alkoxide/siloxide ligands had occurred. After washing with chloroform, Ti(IV) active centers were obtained after calcination under dry oxygen at 550°C for 3h in the U-shaped reactor with a porous septum, leaving the white mesoporous catalyst. The last step is obligatory for removing the template, or the organic ligands of the organometallic precursor.



### **Preparation of TS-1**

The preparation of TS-1 was performed during the three months stay in Montpellier.

TS-1 was prepared by direct hydrothermal synthesis using tetraethoxysilane and titanium tetra-isopropoxide as Si and Ti sources, respectively. Alkali-free tetrapropylammonium hydroxide (TPAOH) was used as template. The initial molar composition of the gel was as follows:  $\text{SiO}_2:0.015 \text{ TiO}_2:0.4 \text{ TPAOH}:16 \text{ H}_2\text{O}$ . The gel was crystallized into a Teflon-lined autoclave at  $175^\circ\text{C}$  for 24 h. The resulting solid was recovered by centrifugation, extensively washed with deionised water until neutral pH and dried overnight at  $80^\circ\text{C}$ . The organic template was removed from the as-synthesized material by calcination under air flow at  $550^\circ\text{C}$  for 6 h.

The crystallinity of the samples prepared was measured by X-ray diffraction using Ni-filtered  $\text{Cu K}\alpha$  radiation (Philips, PW-1700), and the morphology of the samples was examined by SEM (Hitachi, X-650). FT-IR spectra were recorded in air at room temperature on a Bomem MB 104 spectrometer using a diffuse reflectance cell. UV-Vis diffuse reflectance spectroscopy was performed under ambient conditions using dehydrated MgO as a reference in the range of 190–800 nm on a Varian CARY 3E double-beam spectrometer.

## Characterization techniques

### N<sub>2</sub> adsorption/desorption:

The nitrogen adsorption/desorption isotherms (-196°C) were measured with a Micromeritics ASAP 2010 automatic analyzer.

TS-1 displayed an isotherm of type I, which revealed its microporous nature. The specific surface area and pore volume were 346 m<sup>2</sup>g<sup>-1</sup> and 0.1 cm<sup>3</sup>g<sup>-1</sup>, respectively.

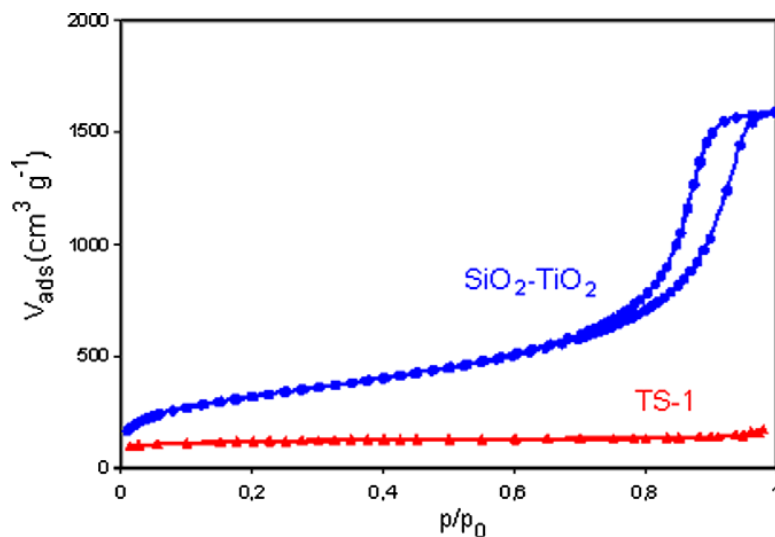


**Figure 1.** N<sub>2</sub> adsorption-desorption isotherm at -196°C of calcined TS-1

### UV-VIS analysis

The Diffuse Reflectance UV-Vis (DRUV-Vis) spectroscopic analysis is a tool to evaluate the coordination environment of Ti atoms in the catalyst. DRUV-vis spectra was recorded on a Varian Cary 05 E UV-vis-NIR spectrometer equipped with an integrating sphere using BaSO<sub>4</sub> powder as the reflectance standard. TS-1 showed a well-defined band at 210-215 nm attributed to oxygen-to-metal charge transfer at isolated tetrahedral Ti(IV) centers.

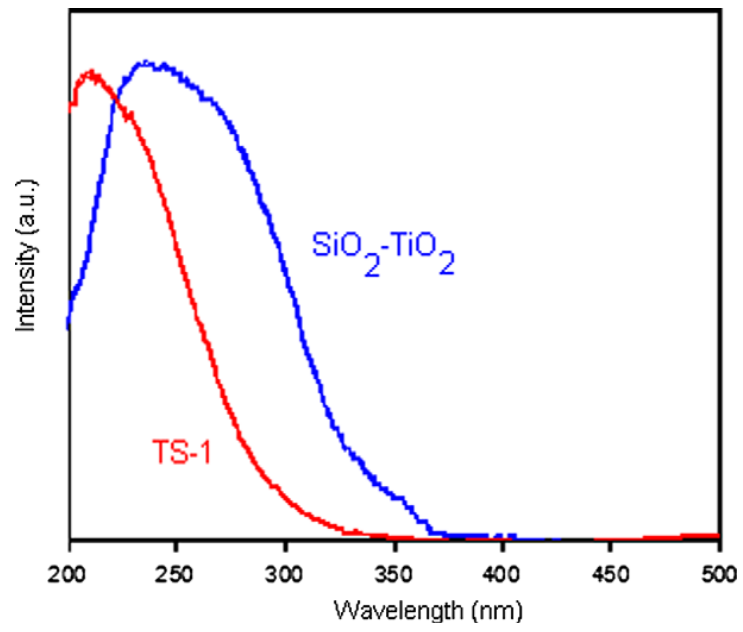


**Figure 2.** DRUV-Vis spectra of TS-1.

## **Ti-content determination**

Ti-content determination was performed via inductively coupled plasma atomic emission spectroscopy (ICP-AES). Samples have to be mineralized with HF since the materials' matrix contains insoluble silica. Thus, the mineralization is occurred in teflon beaker. The concentration of HF has to be maintained as slow as possible in order to not to damage the quartz parts of spectrophotometer, the concentration of HF has to be maintained low. Thus, the final concentration of HF of the solutions to analyze was ca. 0.01 ppm.

### **Sample's mineralization:**

Beaker in teflon

Automatic micropipette P1000 (1000  $\mu$ l)

Flask 0.5 L in polipropilene

Standard solution of Ti (1020  $\mu$ g/mL Fluka)

*The mineralization procedure was the following:*

25 mg of the sample were transferred into the teflon beaker with the following addition (under the hood) of 0.3 mL of HF (40% aqueous solution) using the automatic micropipette. After the careful agitation, 50 mL of deionized water MilliQ. The solution is transferred into the flask of polipropilene of 0.5 L and necessary amount of water MilliQ is added.

*Preparation of standard solution:*

Using the standard solution of Ti (1020  $\mu$ g/mL) three standard solutions are prepared in the flask of 0.5 L with water MilliQ and HF (40%): 0.5 ppm, 1 ppm and 2 ppm. In the same manner, the blank standard is prepared, using water MilliQ and HF (40%) using the same flask of 0.5 L.

*Calculation of the Ti content:*

The intensity is registered at Ti **334.9 nm**. Concentration values are obtained using linear regression of 3 standards + blank standard.

The SiO<sub>2</sub>-TiO<sub>2</sub> Grace (1.40% Ti p/p), being a commercial sample, was always used in the analysis as a reference material.

## Gas-Chromatography (GC-FID)

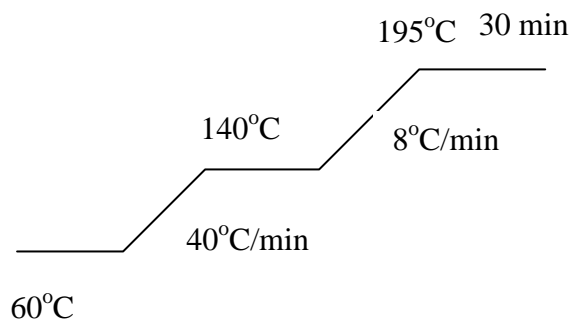
HP5890; HP-5 column, 30m x 0.25mm; FID detector, head pressure 165 kPa. Split ratio of the injector was 17.7 and the characteristics of the flows are the following:

- ❖ Column flow: 6.1 mL min<sup>-1</sup>;
- ❖ H<sub>2</sub> flow: 30 mL min<sup>-1</sup>;
- ❖ Makeup flow: 25 mL min<sup>-1</sup>;
- ❖ Air flow: 410 mL min<sup>-1</sup>;
- ❖ Split: 80 mL min<sup>-1</sup>;
- ❖ Septum purge: 3 mL min<sup>-1</sup>.

For the analysis of methyl epoxystearate the following temperature program was used:

- initial temperature: 60°C
- temperature rate of 40°C min<sup>-1</sup> until 140°C
- temperature rate of 8°C min<sup>-1</sup> until 195°C
- final temperature: 150°C for 30 min.

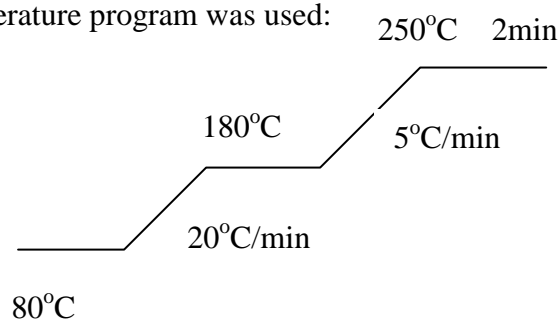
Total time = 38.87 min



For the analysis of *trans*-stilbene the following temperature program was used:

- initial temperature: 80°C
- temperature rate of 20°C min<sup>-1</sup> until 180°C
- temperature rate of 5°C min<sup>-1</sup> until 250°C
- final temperature 250°C for 2 min.

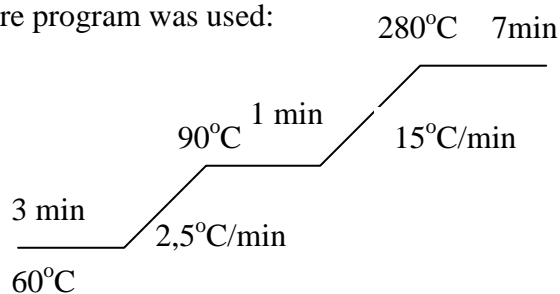
Total time = 21 min



For the analysis of limonene the following temperature program was used:

- initial temperature: 60°C for 3 min
- temperature rate of 2.5°C min<sup>-1</sup> until 90°C for 1 min
- temperature rate of 15°C min<sup>-1</sup> until 280°C
- final temperature 280°C for 7 min.

Total time = 35.33 min



For the analysis of cyclohexene the following temperature program was used:

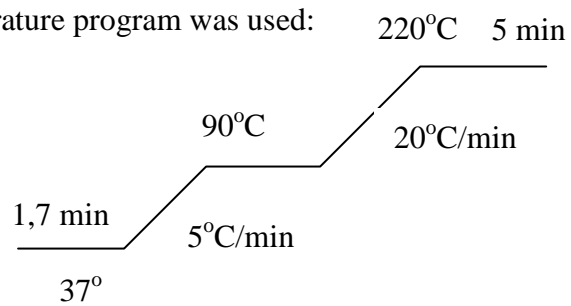
-initial temperature: 37°C for 1,7 min

-temperature rate of 5°C min<sup>-1</sup> until 90°C

-temperature rate of 20°C min<sup>-1</sup> until 220°C

-final temperature 220°C for 5 min.

Total time=23,8 min



## **Preparation of anhydrous solvents**

The preparation of anhydrous solvents was performed over the molecular sieves (Siliporite A) activated at 180°C for 2h in air and for 2h in *vacuum*. The solvent of interest was added to the pretreated molecular sieves in the Ar flow by the help of a syringe, letting bubble the solvent in the syringe first. Prepared solvent was conserved under the Ar atmosphere.

## Experimental part for Chapter 1

### *Preparation of Ti-Silica Catalysts*

Catalysts were prepared by grafting titanocene dichloride ( $\text{TiCp}_2\text{Cl}_2$ ; Fluka) onto different silicas (SBA-15, Aerosil, MCM-41, MCM-48), as previously described [32, 42]. Aerosil 380 is commercially available from Degussa. Before grafting, the supports were pretreated at  $500^\circ\text{C}$  for 2 hours in air and then in vacuo at the same temperature for 2 hours. Titanocene dichloride was dissolved in anhydrous chloroform (Sigma-Aldrich) under argon and stirred for 2 hours at room temperature. Triethylamine (Sigma-Aldrich) or pyridine (Fluka) was then added to the suspension and left overnight under stirring to activate the nucleophilic substitution of surface silanols onto titanocene. A weaker base, pyridine, was used in the grafting over MCM-41 and MCM-48 to protect the support. After filtering, Ti(IV) active centres were obtained after calcination under dry oxygen at  $550^\circ\text{C}$  for 3h.

### *Catalytic test*

All catalysts were pretreated at  $500^\circ\text{C}$  in dry air for 1 h prior to use. The epoxidation tests were carried out in a glass batch reactor under inert atmosphere at  $85^\circ\text{C}$ . Typically, the solution of cyclohexene (2.5 mmol; Aldrich) in 5 ml of acetonitrile was added to the catalyst (50 mg). A solution of 1.2 ml of hydrogen peroxide (30% aqueous solution) in 20 ml acetonitrile (1 mmol  $\text{H}_2\text{O}_2$  in 1.8 mL of solution) was slowly added ( $0.01 \text{ ml min}^{-1}$  over 3h) with an automatic dosimetric apparatus. Hot filtration tests followed by separation of the solid catalyst were performed and the resulting solution was tested in catalysis to evaluate the leaching and confirm the heterogeneous nature of the catalytic reaction. During recycling tests, the catalyst was filtered off, washed with methanol and acetonitrile, calcined at  $500^\circ\text{C}$  (this high-temperature calcination step is essential to have a complete and thorough removal of the adsorbed heavy organic by-products) for 3 hours under dry air, cooled in vacuo and reused under the same conditions.

Catalytic performance was determined on GC analysis (HP6890; HP-5 30m – column; FID detector). Mesitylene was added as internal standard. All data were obtained from an average of at least three catalytic tests. Cyclohexene conversion was computed considering the substrate as the limiting agent. Epoxide yield was computed according to the relation:

$$Y_{\text{epox}} = [\text{mol (obtained epoxide)}/\text{mol (H}_2\text{O}_2)] \times 100$$

At the end of each reaction, minimal amounts of the oxidant were detected by potassium iodide colorimetric tests. Standard deviations on conversion and selectivity values are  $\pm 2\%$  and  $\pm 4\%$ , respectively.



### **TGA analysis**

To calculate the surface concentration of hydroxyl groups ( $\text{OH}/\text{nm}^2$ ) TGA analysis were performed. In a typical procedure 10-20 mg of the sample were transferred in air in the pan hanging from the balance. The samples were heated in programmable manner ( $5.0^\circ\text{C min}^{-1}$ ) in air from 50 to  $1000^\circ\text{C}$ . Air flow was  $35 \text{ mL min}^{-1}$ , oxygen flow was  $35 \text{ mL min}^{-1}$ .

The TGA pattern of Ti/SBA-15 shows a weight loss in two steps at  $120^\circ\text{C}$  and  $700^\circ\text{C}$ . The first step is due to the removal of physically adsorbed water. The weight loss between  $120^\circ\text{C}$  and  $700^\circ\text{C}$  is due to the decomposition of organic groups and condensation of silanols.

## Experimental part for Chapter 2

### *Preparation of ordered mesoporous silicas*

MCM-41. MCM-41 was prepared with the molar ratio, 1 SiO<sub>2</sub>/ 0.1 CTAB/ 0.27 NaOH/ 32 H<sub>2</sub>O. 19.06 g H<sub>2</sub>O, 0.356 g NaOH and 1.204 g cetyltrimethyl ammonium bromide (CTAB, Aldrich) were mixed at 50°C until an homogeneous solution was obtained and then 2 g of silica (Aerosil 200, Degussa) were added stepwise and stirred for 1 h. Then the mixture was put in an autoclave at 115°C for 24 h. The resulting slurry was filtered and washed until neutral pH and dried at 80°C overnight. The powder was then calcined at 550°C for 8h.

MCM-48. MCM-48 was prepared with the molar ratio, 1 SiO<sub>2</sub>/ 0.175 CTAB/ 0.38 NaOH/ 120 H<sub>2</sub>O. 214 g H<sub>2</sub>O, 1.54 g NaOH and 6.22 g cetyltrimethyl ammonium bromide (CTAB, Aldrich) were mixed at 50°C until an homogeneous solution was obtained and then 6 g of silica (Aerosil 200, Degussa) were added stepwise and stirred for 2 h. Then the mixture was put in an autoclave at 150°C for 15 h. The resulting slurry was filtered, without washing, and dried at 80°C overnight. The powder was poured again in an autoclave with water (7.5 g H<sub>2</sub>O per gram of solid), the mixture was stirred for 20 min and the autoclave was put at 130°C for 6 h. This post-treatment was repeated once again. The resulting slurry was filtered and washed until neutral pH and dried at 80°C overnight. The powder was then calcined at 550°C for 8h.

### *Preparation of Ti-Silica Catalysts*

Catalysts were prepared by grafting titanocene dichloride (TiCp<sub>2</sub>Cl<sub>2</sub>; Fluka) onto different silicas (MCM-41, MCM-48, Aerosil), as previously described [32,42]. Aerosil 380 is commercially available from Degussa. Before grafting, the supports were pretreated at 500°C for 2 hours in air and then in vacuo at the same temperature for 2 hours. Titanocene dichloride was dissolved in anhydrous chloroform (Sigma-Aldrich) under argon and stirred for 2 hours at room temperature. Triethylamine (Sigma-Aldrich) or pyridine (Fluka) was then added to the suspension and left overnight under stirring to activate the nucleophilic substitution of surface silanols onto titanocene. A weaker base, pyridine, was used in the grafting over MCM-41 and MCM-48 to protect the support. After filtering, Ti(IV) active centres were obtained after calcination under dry oxygen at 550°C for 3h.

### *Textural and spectroscopic characterization*

Nitrogen adsorption/desorption isotherms of materials were measured using a Micromeritics ASAP 2010 instrument. The calcined samples were outgassed at 250°C and titanocene-

containing samples at 120°C until stable static vacuum of  $3 \times 10^{-3}$  Torr was reached. Mesopore diameters were calculated from the desorption branch of the nitrogen isotherms by the Broekhoff and de Boer (BdB) method,<sup>45</sup> which has been shown to provide reliable results for MCM-41 materials [46].

UV-Vis diffuse reflectance spectra were obtained in a Varian Cary 05E UV-Vis-NIR spectrophotometer using BaSO<sub>4</sub> as background standard. Titanium content was determined by ICP-AES on an Intrepid Iris instrument (Thermo Elemental).

### *Catalytic tests*

All catalysts were pretreated at 500°C in dry air for 1 h prior to use. The epoxidation tests were carried out in a glass batch reactor under inert atmosphere at 85°C. Typically, the solution of methyl oleate (1.5 mmol; Aldrich) in 5 ml of acetonitrile was added to the catalyst (50 mg). A solution of hydrogen peroxide (50% aqueous solution) in solvent (2 mmol H<sub>2</sub>O<sub>2</sub> in 2.4 mL of solution) was slowly added (0.01 ml min<sup>-1</sup> over 4h) with an automatic dosimetric apparatus. Hot filtration tests followed by separation of the solid catalyst were performed and the resulting solution was tested in catalysis to evaluate the leaching and confirm the heterogeneous nature of the catalytic reaction. During recycling tests, the catalyst was filtered off, washed with methanol and acetonitrile, calcined at 500°C for 3 hours under dry air, cooled in vacuo and reused under the same conditions.

Catalytic performance was determined on GC analysis (HP6890; HP-5 30m – column; FID detector). Methyl palmitate was added as internal standard. All data were obtained from an average of at least three catalytic tests. Methyl oleate conversion was computed considering the substrate as the limiting agent. At the end of each reaction, minimal amounts of the oxidant were detected by potassium iodide colorimetric tests. For this reason, oxidant efficiency (Ox Eff) was calculated, as follows:

$$\text{Ox Eff (\%)} = 100\% \times (\sum \text{mol}_{\text{oxidised products}}) / (\text{mol}_{\text{H}_2\text{O}_2 \text{ consumed}})$$

considering the full consumption of the initial hydrogen peroxide after 24 h. Standard deviations on conversion and selectivity values are  $\pm 2\%$  and  $\pm 4\%$ , respectively.

### *GC-MS analysis*

Reaction products were also analysed by Gas-Chromatography interfaced with mass spectroscopy.

The chromatograms of the reaction mixture after 24 hours shown in the Spectrum 1 (GC) and Spectrum 2 (GC-MS) represent four principle compounds with the following retention time (first value is from GC, the second is from GC-MS):

Internal standard – methyl palmitate - retention time 8.89 min (11.6 min);

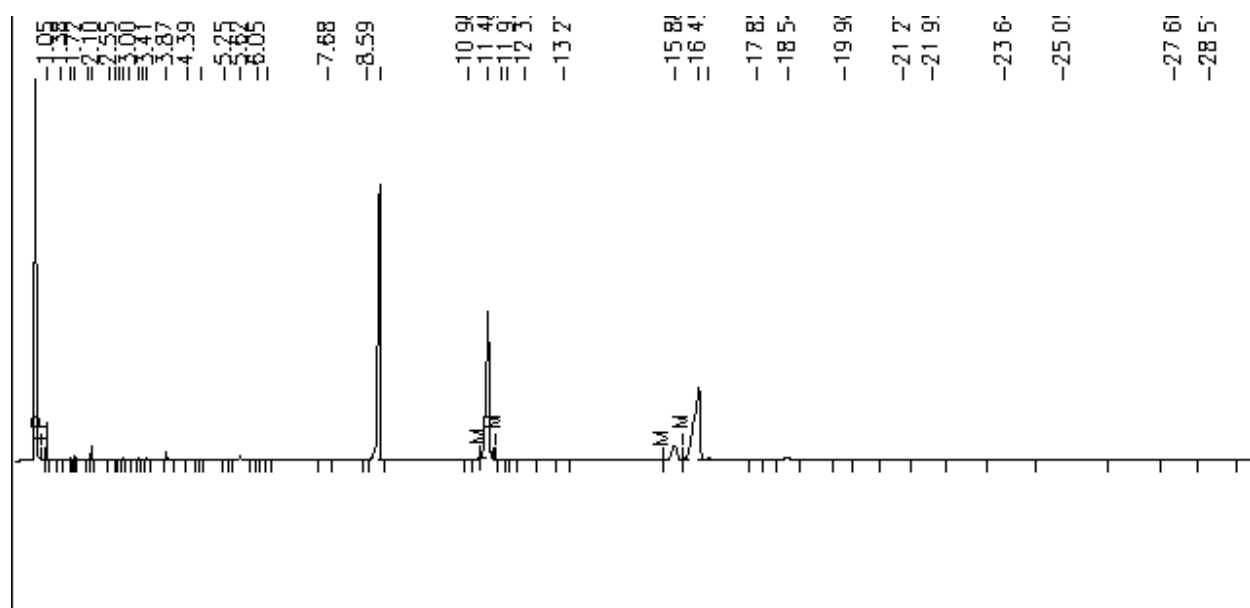
Methyl oleate non-reacted - retention time 11.5 min (15.9 min);

*trans*-methyl epoxystearate - retention time 15.8 min (23.94 min);

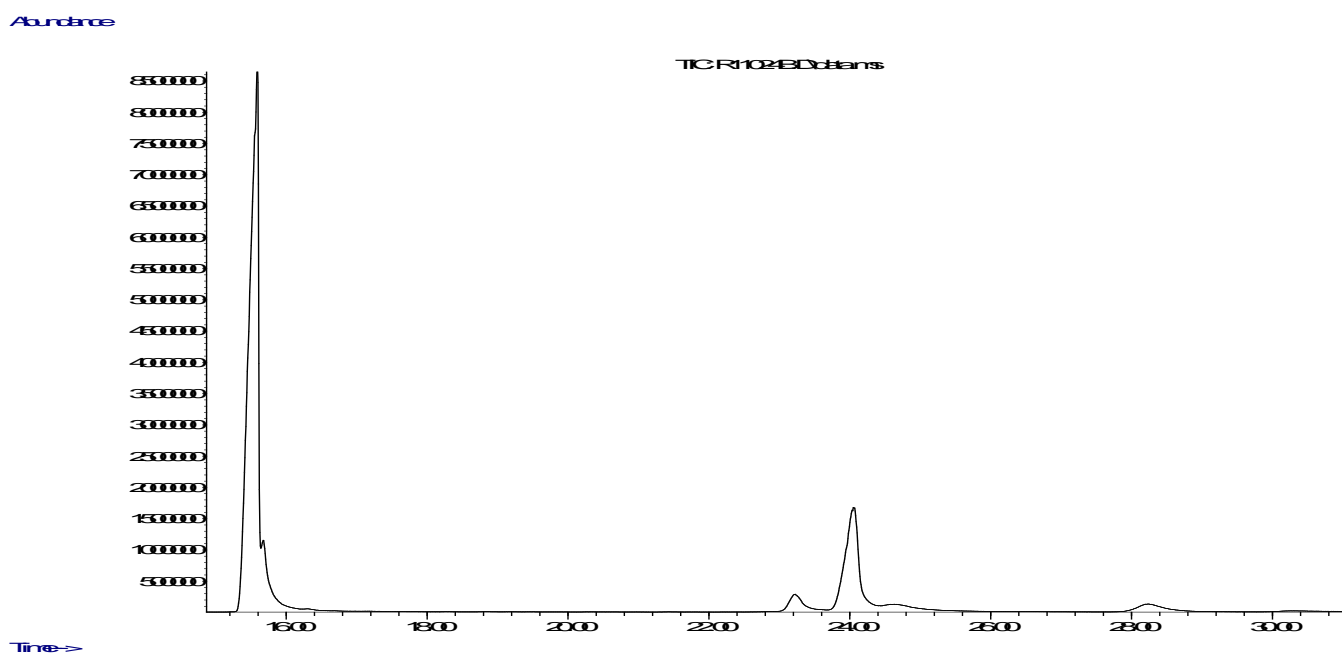
*cis*-methyl epoxystearate - retention time 16.4 min (24.85 min);

Methyl oxooctadecanoate (KETO; a mixture of methyl 9-oxooctadecanoate and methyl 10-oxooctadecanoate) - retention time 16.5 min (24.65 min);

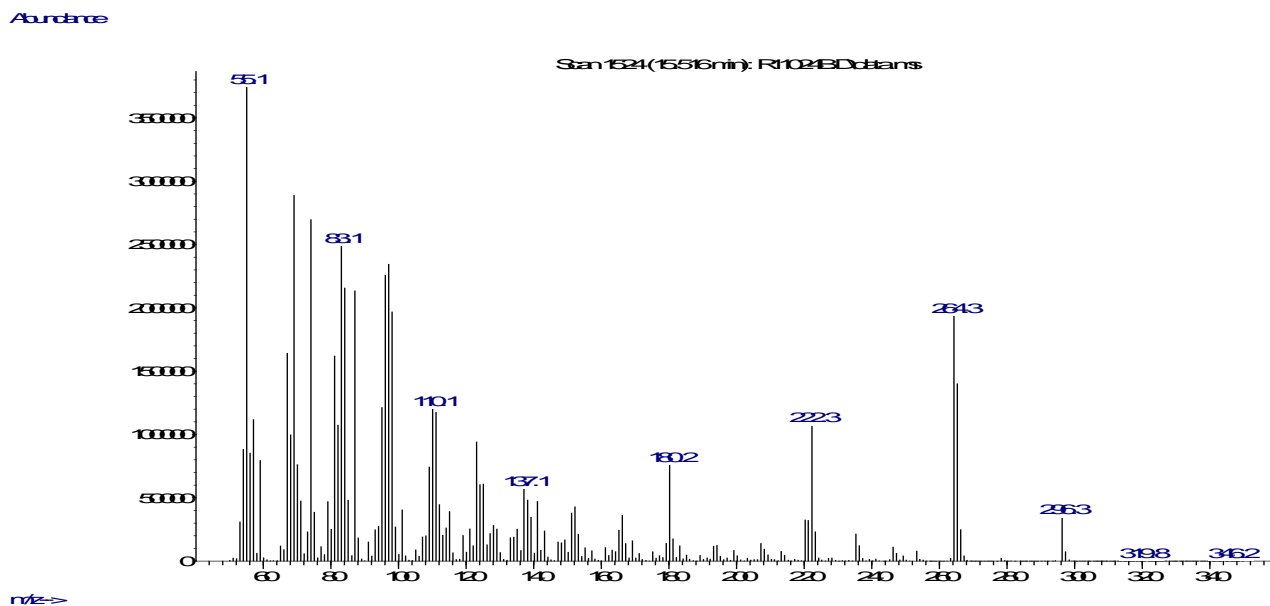
Methyl oxooctadecenoate (ENON; a mixture of methyl 8-oxooctadec-9-enoate and methyl 11-oxooctadec-9-enoate) - retention time 18.5 min (28.24 min).



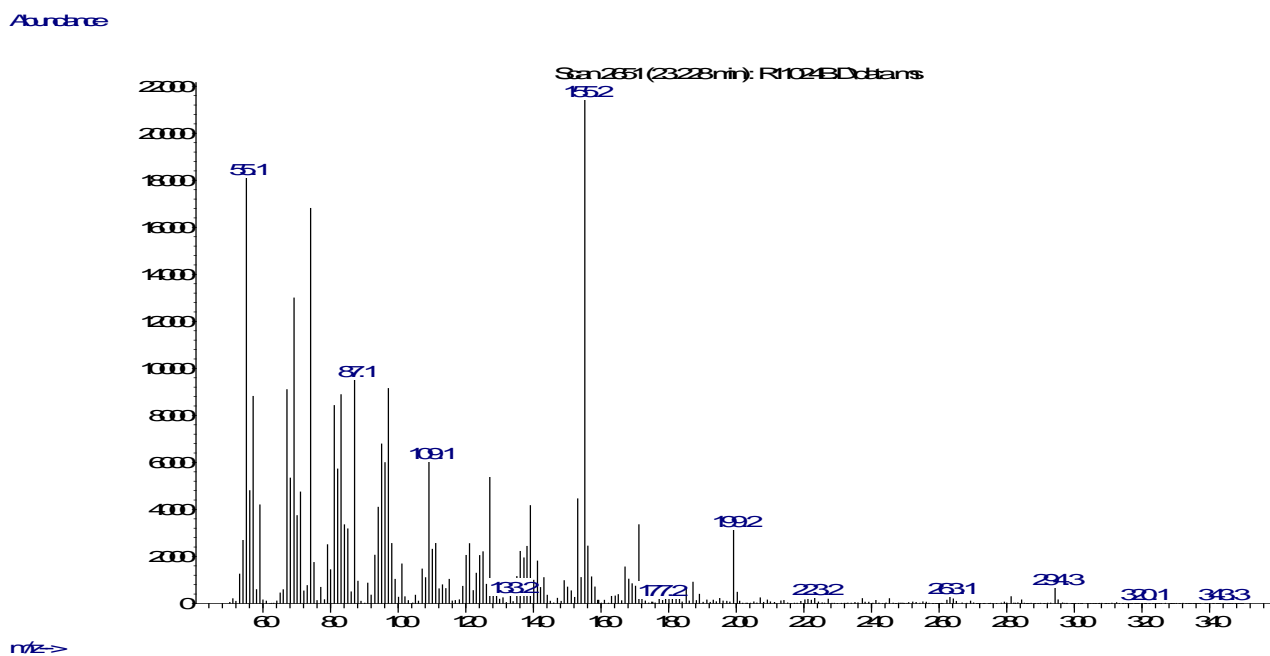
**Spectrum 1.** Chromatogram of the reaction mixture after 24h (analysed by GC)



**Spectrum 2.** Chromatogram of the reaction mixture after 24h (analysed by GC-MS)

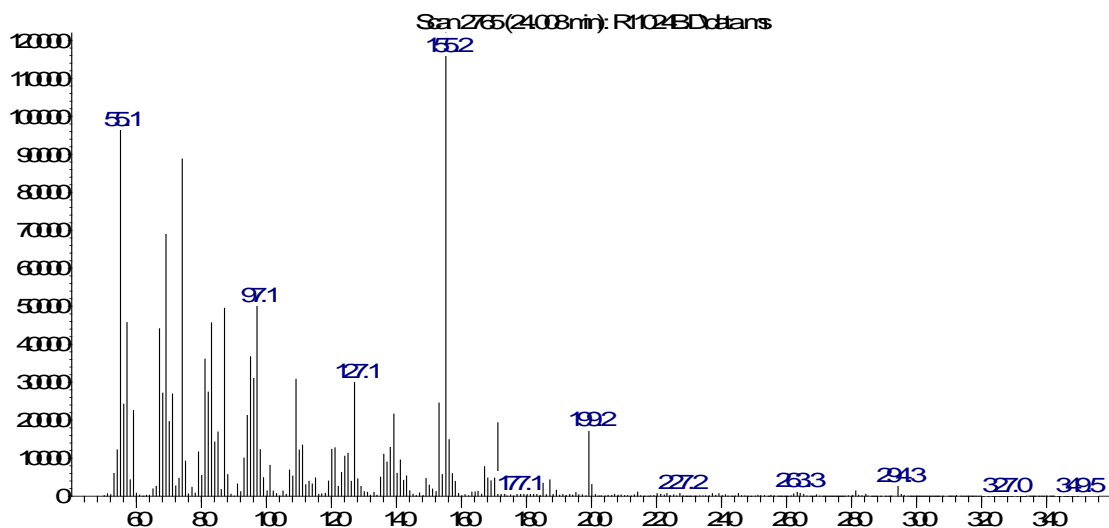


**Spectrum 3.** Mass-spectra of methyl oleate



**Spectrum 4.** Mass-spectra of cis- methyl epoxystearate (cis-EPOX)

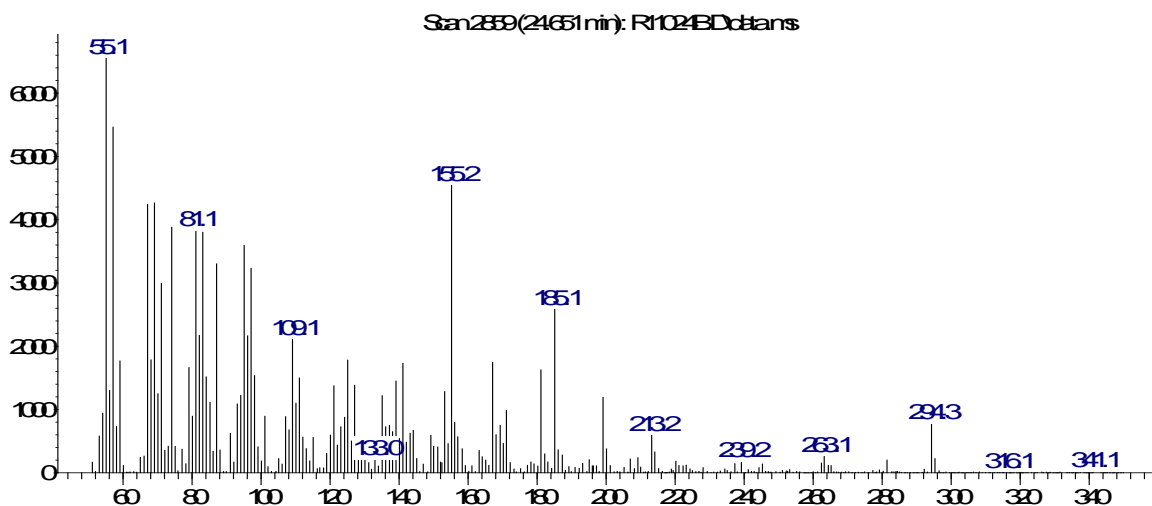
Abundance



m/z->

**Spectrum 5.** Mass-spectra of *trans*-methyl epoxystearate (trans-EPOX)

Abundance

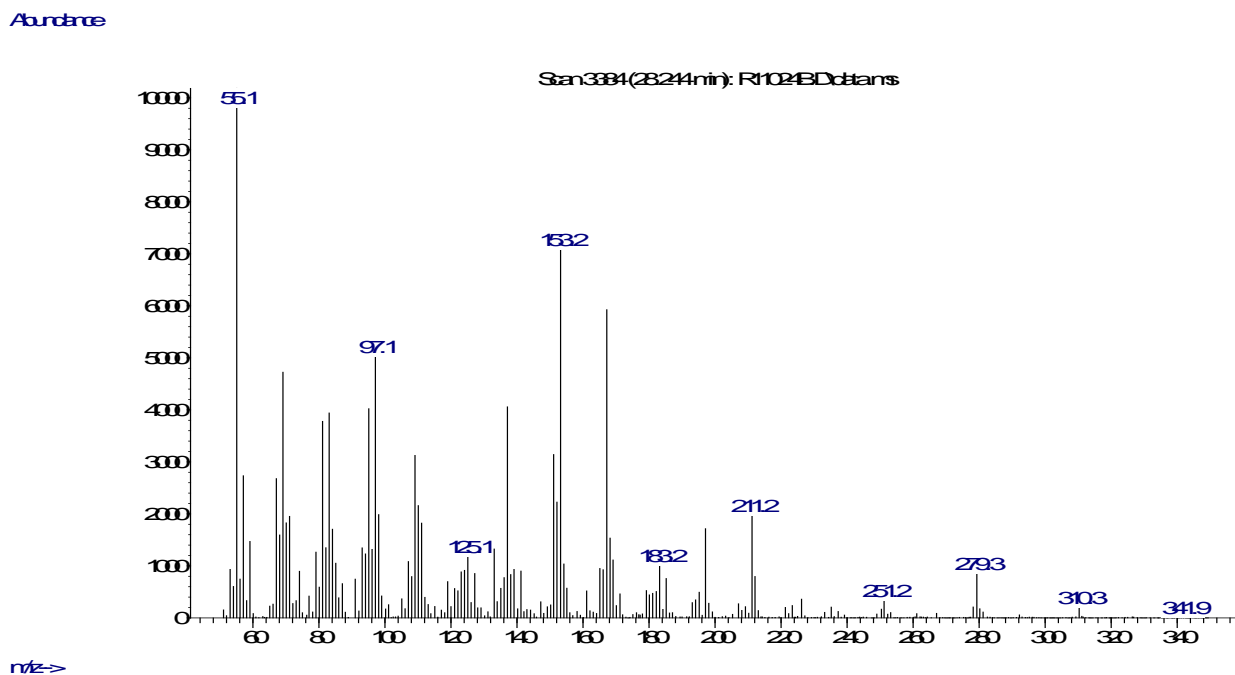


m/z->

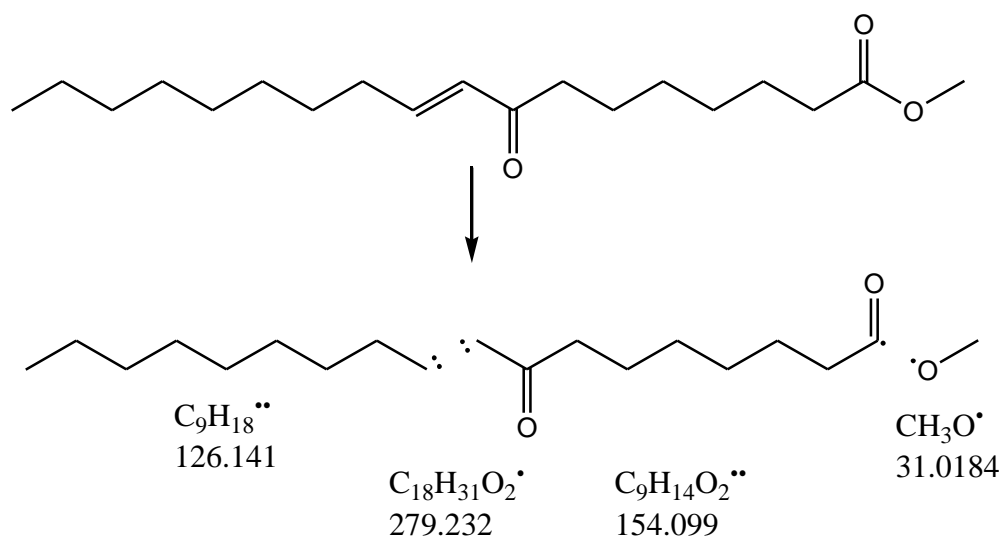
**Spectrum 6.** Mass-spectra of Methyl oxooctadecanoate (KETO; a mixture of methyl 9-oxooctadecanoate and methyl 10-oxooctadecanoate)

### Determination of ENON and KETO

To determine two unknown peaks, we have performed the defragmentation analysis of the mass-spectra were performed. On the spectrum 6, the mass-spectra of the compound X (ENON) is present.

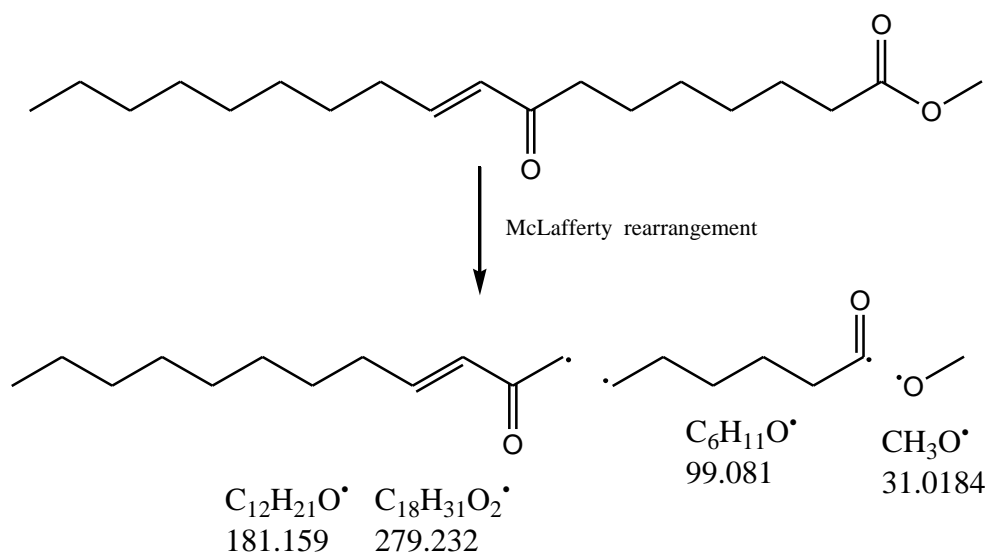


**Spectrum 7.** Mass-spectra of ENON (oxooctadecenoate)



**Scheme 1.** Fragmentations of the ENON

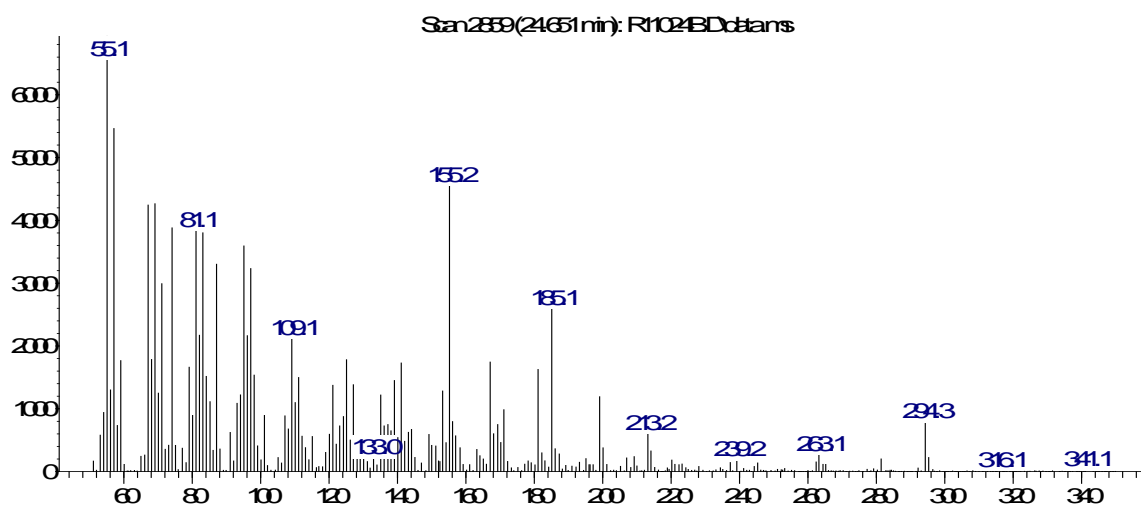
McLafferty rearrangement is observed in mass-spectrometry. A molecule containing a double bond, a keto-group undergoes  $\beta$ -cleavage with the gain of the  $\gamma$ -H atom (Scheme 2).



**Scheme 2.** McLafferty rearrangement of ENON

Determination of the product Y (KETO)

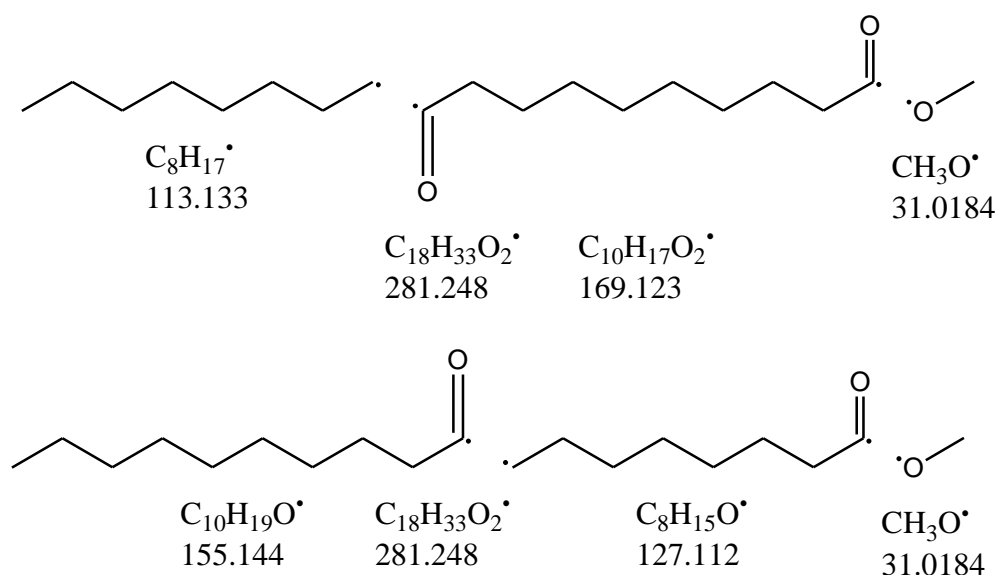
*Abundance*



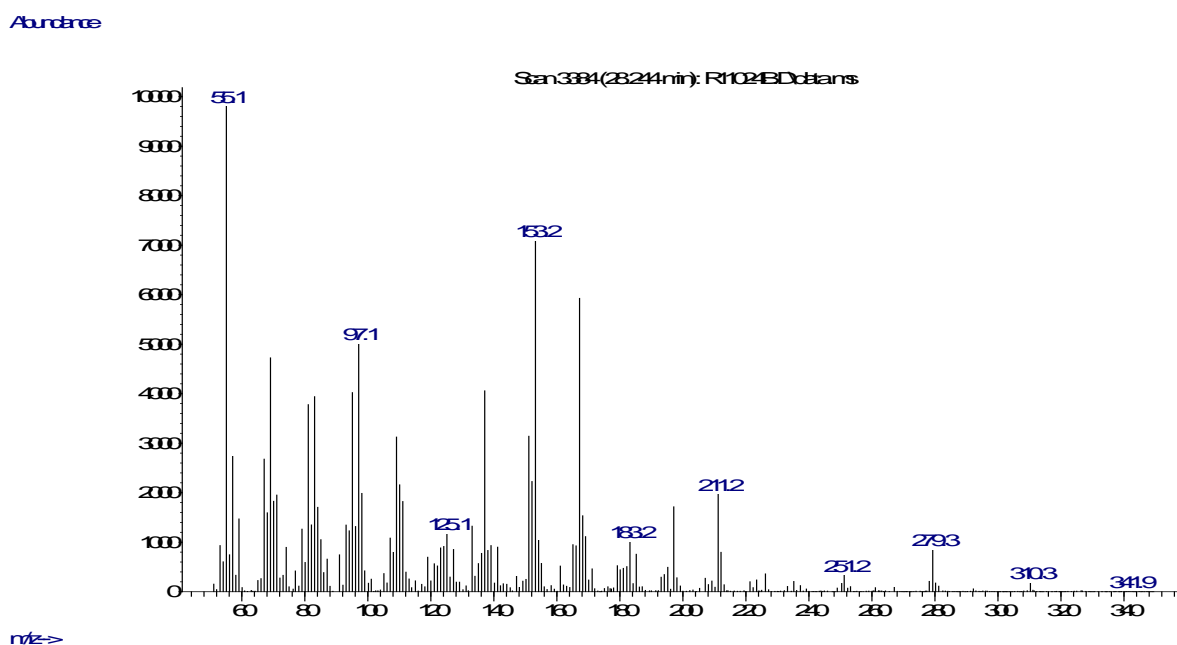
*m/z* →

**Spectrum 8.** Mass-Spectra of the Methyl oxooctadecanoate (KETO; a mixture of methyl 9-oxooctadecanoate and methyl 10-oxooctadecanoate)





**Scheme 3.** Fragmentations of the KETO.



**Spectrum 9.** Mass-spectra of Methyl oxooctadecenoate (ENON; a mixture of methyl 8-oxooctadec-9-enoate and methyl 11-oxooctadec-9-enoate)

## Experimental part for Chapter 3

### *Materials:*

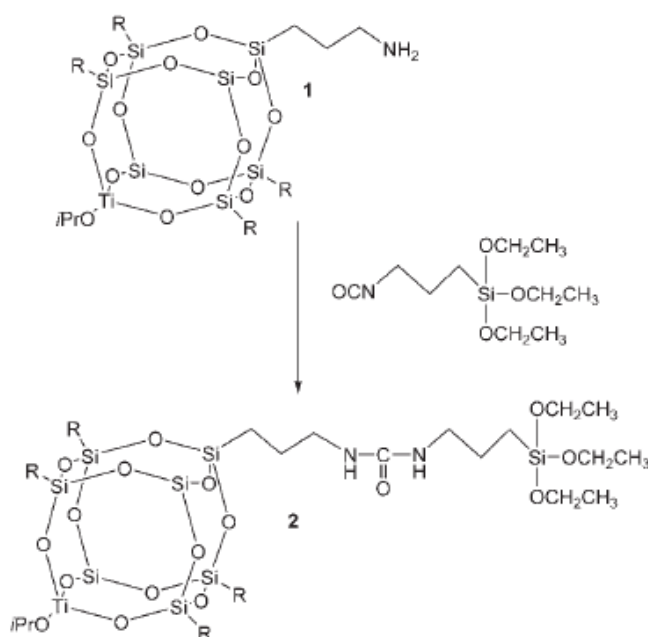
Ti-MCM-41 was prepared by grafting  $\text{Ti}(\text{Cp})_2\text{Cl}_2$  (Fluka) onto a purely siliceous mesoporous MCM-41 [7,24]. Limonene (R-(+)-limonene; 97%) was used as received from Aldrich. The titanium-containing catalysts were modified by calcining the sample at 573 K for 1 h in air and for 2 h in vacuo. The solids were treated with a solution of hexamethyldisilazane (HMDS, Aldrich) in anhydrous toluene (20 mL; dried on molecular sieves) under argon at 383 K during 2 h. Silylation was performed using different of HMDS to catalyst molar ratios (computed as mol HMDS / mol  $\text{SiO}_2$ ) (see Tab. 1). The silylated catalysts were filtered, washed with dry toluene (40 mL) and finally dried at 373 K. The catalysts were pretreated at 573 K in vacuo prior their use.

The epoxidation tests were carried out in a glass batch reactor (stirring rate 500 rpm) at 363 K using the pretreated catalyst (25 mg), ethyl acetate (AcOEt, Carlo Erba), as solvent (5 mL), previously dried on 3A molecular sieves, limonene (0.5 mmol) and mesitylene (Fluka) as internal standard. Anhydrous tert-butylhydroperoxide (TBHP; Aldrich, 5 M solution in decane) was used as oxidant (TBHP/limonene molar ratio = 1.10). The presence of the oxidant at the end of each reaction was systematically confirmed by means of GC analysis or iodometric titration. The catalyst to substrate weight ratio was 33 wt.%. Samples were analysed by GC analysis (HP5890; HP-5 column, 30m x 0.25mm; FID or MS detectors, head pressure 160 kPa). Standard deviation is  $\pm 2\%$  and  $\pm 3\%$  in conversion and selectivity values, respectively. Carbon content analyses were performed on a Thermoquest NA2100 analyzer. A blank experiment was carried out mixing the reactants in the absence of the catalyst. A substrate conversion of 2% was recorded and was then subtracted to all the other conversion data in the presence of catalyst. Specific activity ( $A_{\text{Ti}}$ ) was calculated after 1h with respect to the total number of Ti sites:  $[\text{mol}_{\text{converted limonene}}]/[\text{mol}_{\text{Ti}}\cdot\text{h}]$ .

## Experimental part for Chapter 4

### Materials

Ti-POSS suitable to be anchored on the silica materials was prepared following a synthetic methodology developed and optimized by some of us [24]. Ti-NH<sub>2</sub>POSS [25] (1g; 1.1•10<sup>-3</sup> mol) was dissolved in 40 mL of chloroform (by Sigma Aldrich) and stirred at room temperature for few minutes. Triethylamine (153 μL) and 3-isocyanatopropyl triethoxysilane (272 μL; 1.1 •10<sup>-3</sup> mol) were added to the solution under dry nitrogen flow. The reaction was stirred at room temperature for 20 h. Finally, the solvent was removed under vacuum until to obtain a powder product (700 mg).

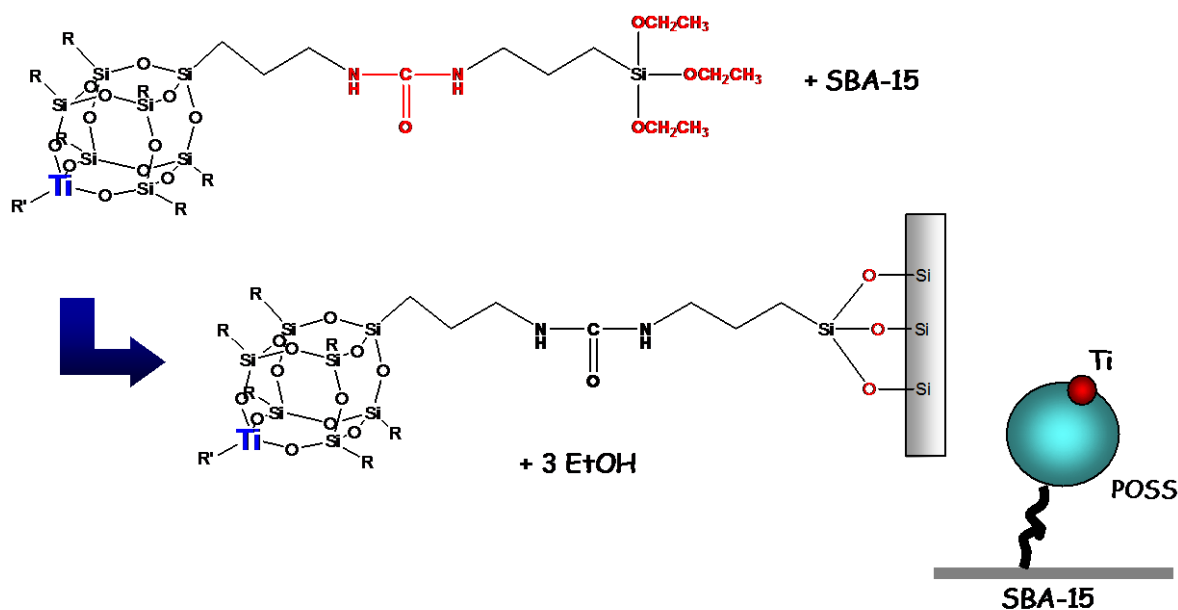


**Scheme 1.** Reaction between Ti-NH<sub>2</sub>POSS and (1) 3-isocyanatopropyl triethoxysilane for the preparation of Ti-POSS-TSIPI (2); R=isobutyl group.

<sup>1</sup>H NMR (400 MHz) spectrum of Ti-POSS in CDCl<sub>3</sub> solvent: 3.9 ppm [2H, NH, ureic group], 3.7 ppm [6H, CH<sub>2</sub>, OEt], 3.6 ppm [1H CH, OiPr], 2.9 [4H, CH<sub>2</sub> of ureic group], 1.85 ppm [6H, CH], 1.20 ppm [15H, CH<sub>3</sub> of OEt and OiPr groups and], 0.93 ppm [36 H, CH<sub>3</sub> of isobutyl groups], 0.59 ppm [20H, CH<sub>2</sub>].

SBA-15 mesoporous silica was prepared according to the literature [26] and non-ordered amorphous SiO<sub>2</sub> Davison was a commercial sample obtained from Grace Davison. The anchoring of Ti-POSS on the surface of both SBA-15 and SiO<sub>2</sub> Davison was carried out by using the following approach. The silica supports were previously activated by treating them in vacuum at 500°C for 4h. Ti-POSS (200 mg) was then added to a suspension of activated silica (1

g in 50 mL of toluene) during 24 h at room temperature. The final anchored solids, namely Ti-POSS/SBA-15 and Ti-POSS/SiO<sub>2</sub>, were obtained by filtration and washing in toluene.



**Scheme 1.** – Preparation of the systems Me-POSS anchored on inorganic oxides, one-step pathway

Ti/SBA-15 and Ti/SiO<sub>2</sub> catalysts were prepared by grafting titanocene dichloride onto the surface of SBA-15 and SiO<sub>2</sub> Davison, respectively, adapting the method developed by Maschmeyer et al. [27,28]. Titanocene dichloride (Ti(Cp)<sub>2</sub>Cl<sub>2</sub>; Fluka) was dissolved in anhydrous chloroform (Sigma-Aldrich) under argon and stirred for 2 hours at room temperature. Triethylamine (Sigma-Aldrich) was then added to the suspension and left overnight under stirring to activate the covalent grafting. After filtering and washing, the final catalysts were obtained by calcining the solids under dry oxygen at 550°C for 3h.

### Characterization

- N<sub>2</sub> physisorption measurements were carried out at 77 K in the relative pressure range from 1÷10<sup>-6</sup> to 1 P/P<sub>0</sub> by using a Quantachrome Autosorb1MP/TCD instrument. Prior to the analysis the samples were outgassed at 373 K for 3 h (residual pressure lower than 10<sup>-6</sup> Torr). Apparent surface areas were determined by using Brunauer-Emmett-Teller equation, in the relative pressure range from 0.01 to 0.1 P/P<sub>0</sub>. Pore size distributions were obtained by applying NLDFT method (N<sub>2</sub> silica kernel based on a cylindrical pore model applied to the desorption branch).
- Thermogravimetric analyses (TGA/DTG) were performed under oxygen flow (100 mL min<sup>-1</sup>) with a SETSYS Evolution TGA-DTA/DSC thermobalance, heating from 50°C to 800°C at 10 °C min<sup>-1</sup>.

- DR-UV-Visible spectra were recorded using a Perkin Elmer Lambda 900 spectrometer equipped with a diffuse reflectance sphere accessory (DR-UV-Vis). Prior to the analysis, the powdered samples were dispersed in anhydrous BaSO<sub>4</sub> matrix (10 wt%) and treated at 100°C in vacuum for 1h in order to remove physisorbed water coordinated to the metal centre.
- XAFS characterization was performed at the XAFS beamline of the Elettra Synchrotron facility in Trieste. EXAFS-XANES spectra of pure and supported Ti complex and of Ti reference systems (Ti foil for calibration in energy, TiO<sub>2</sub>, Ti(*i*PrO)<sub>4</sub> for octahedral and tetrahedral Ti(IV)) were collected at the Ti K edge (4966 eV) in transmission mode at both room and liquid nitrogen temperature at the end of both in-situ and ex-situ treatments (in-situ treatments have been carried out inside our EXAFS-catalysis cell, designed to work in transmission mode under controlled gas flow and temperature, permanently located at the beamline available to users). The very low Ti loading of some of the samples required integration time of several hours per EXAFS spectrum, getting spectra of satisfactory signal-to-noise ratio even in transmission mode. The use of the Si(311) monochromator, with the high accuracy of the encoder, allowed to obtain XANES spectra with excellent resolution.

#### *Catalytic tests*

The catalysts (50 mg) were pre-treated at 140°C in vacuum for 12 h prior to use. At this temperature and in the absence of oxygen no degradation of the organic moiety in Ti-POSS-anchored samples occurs. The substrates ((+)-limonene, (-)-carveol and (-)- $\alpha$ -pinene; Aldrich; 1.0 mmol), internal standard (1.0 mmol; mesitylene; Fluka) and the oxidant (1.2 mmol; TBHP 5.5 M in decane; Aldrich) were added to the solid in anhydrous ethyl acetate (Fluka) under dry nitrogen. The reaction was performed in a glass batch reactor, at 85°C during 24 h and the mixture was analysed by GC-FID and GC-MS. Titanium contents were determined by mineralization of the solids and elemental analysis by ICP-AES as described in the literature [29].

## Experimental part for Chapter 5

Materials were prepared by the group of Prof. M. Rossi at the Dept. of Inorganic, Metallorganic and Analytical Chemistry of the University of Milan.

### *Synthesis of the materials*

Gold with different loadings was deposited by three different methods: deposition precipitation (DP), impregnation, sol-gel immobilization.

*1%Au/MgO (Ref7)* preparation: 2 g of MgO are dissolved in 40 mL of water with the following addition of 0.5 mL of Au 40mg/mL (HAuCl<sub>4</sub>) solution. The initial pH=9.3 is raised to 10.6 with NH<sub>3</sub> 6N. Following dropwise addition of NaBH<sub>4</sub> (Au: NaBH<sub>4</sub>=1:1 w/w) reduces the Au<sup>3+</sup> to a metal state. After the deposition for 30 min, the catalyst was filtered with distilled water to remove chlorine contaminants and dried at 170°C.

*10%Au/SiO<sub>2</sub>9732-0.5%Au/SiO<sub>2</sub>9732 (Ref 9)* preparation: 1 g of SiO<sub>2</sub> is dissolved in 20 mL of water with the following addition of 2 mL (0.1 mL) of Au 50mg/mL (HAuCl<sub>4</sub>) solution and 1 mL of NH<sub>3</sub> 6N and left for stirring for some minutes. Following dropwise addition of NaBH<sub>4</sub> (Au: NaBH<sub>4</sub>=1:1 w/w) reduces the Au<sup>3+</sup> to a metal state. After the deposition for 30 min, the catalyst was filtered with distilled water to remove chlorine contaminants and dried at 170°C.

*1%Au/SiO<sub>2</sub>Davisill-sol and 0.5% Au/SiO<sub>2</sub>Davisil-sol, 1%Au/SiO<sub>2</sub>9732-sol and 0.5% Au/SiO<sub>2</sub>9732sol, sol-gel immobilization.* First, the preparation of 400 ml (200 ml) of sol of Au 25 mg/L is done as follows:

400 mL (200 mL) of water milliQ is added to the 1 mL (0.5 mL) of the solution of Au 10 mg/mL (HAuCl<sub>4</sub>), glucose (glucose/Au=50, molar ratio) and the solution of NaBH<sub>4</sub> (Au: NaBH<sub>4</sub>=1:1 w/w) with the following addition of SiO<sub>2</sub>, and the pH is changed to 2.3 by the addition of HCl 1 M. The mixture is left for stirring for 1h, then the catalyst is filtered with distilled water and dried at 170°C.

*1%Au/SiO<sub>2</sub>9732 VP-0.5% Au/SiO<sub>2</sub>9732 VP, 1%Au/SiO<sub>2</sub>Davisil VP-0.5% Au/SiO<sub>2</sub>Davisil VP*

### *Impregnation:*

1 mL (0.5 mL) of Au 10 mg/mL solution are added to the 0.7 mL (1.2 mL) of water milliQ, with the following addition of 1 g of SiO<sub>2</sub>. The catalyst is reduced at 300°C for 3h in H<sub>2</sub> flow.

### Catalytic tests

The catalytic tests were carried out in a magnetically stirred glass batch reactor containing substrate (0.5mmol), solvent (10 ml), oxidant (TBHP, 0.03 mmol, molecular O<sub>2</sub>, 1 bar). The temperature of the reaction was 80°C. Catalytic performance was determined by GC analysis (HP6890; HP-5 30m – column; FID detector). All data were obtained from an average of at least three catalytic tests. Substrate conversion is calculated as [initial concentration of substrate - final concentration of substrate]/[initial concentration of substrate]\*100.

### GC/ GC-MS analysis

Oxidation of limonene over Au/MgO (1%) with TBHP as radical initiator and molecular O<sub>2</sub>

Reaction products were also analysed by Gas-Chromatography interfaced with mass spectroscopy.

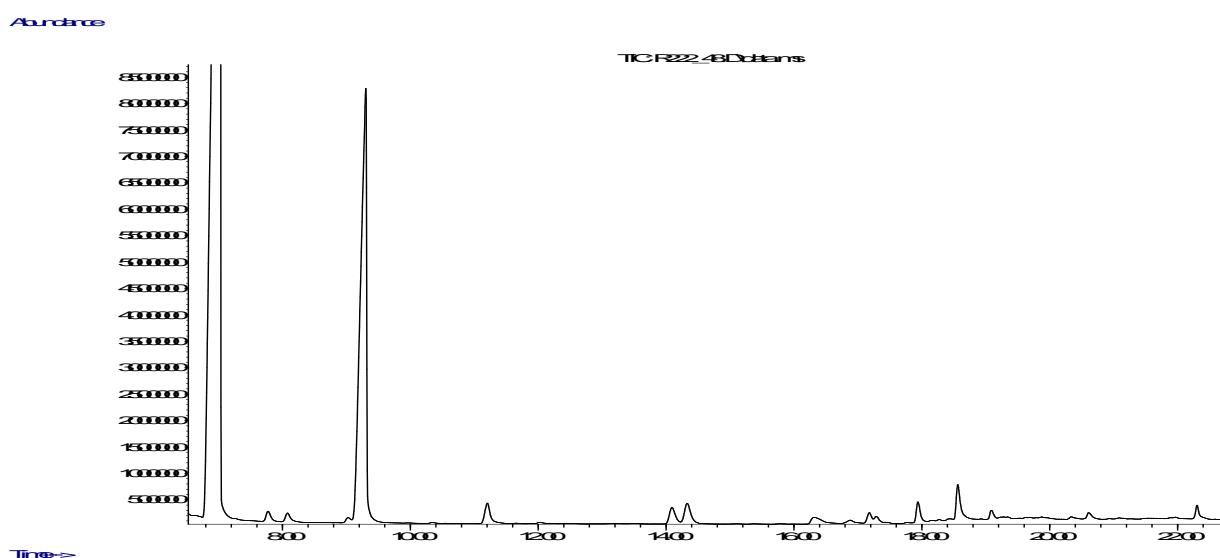
The chromatograms of the reaction mixture after 24 hours shown in the Spectrum 1 (GC) and Spectrum 2 (GC-MS) represent four principle compounds with the following retention time (first value is from GC, the second is from GC-MS):

Internal standard – mesitylene - retention time 3.6 min (6.87 min);

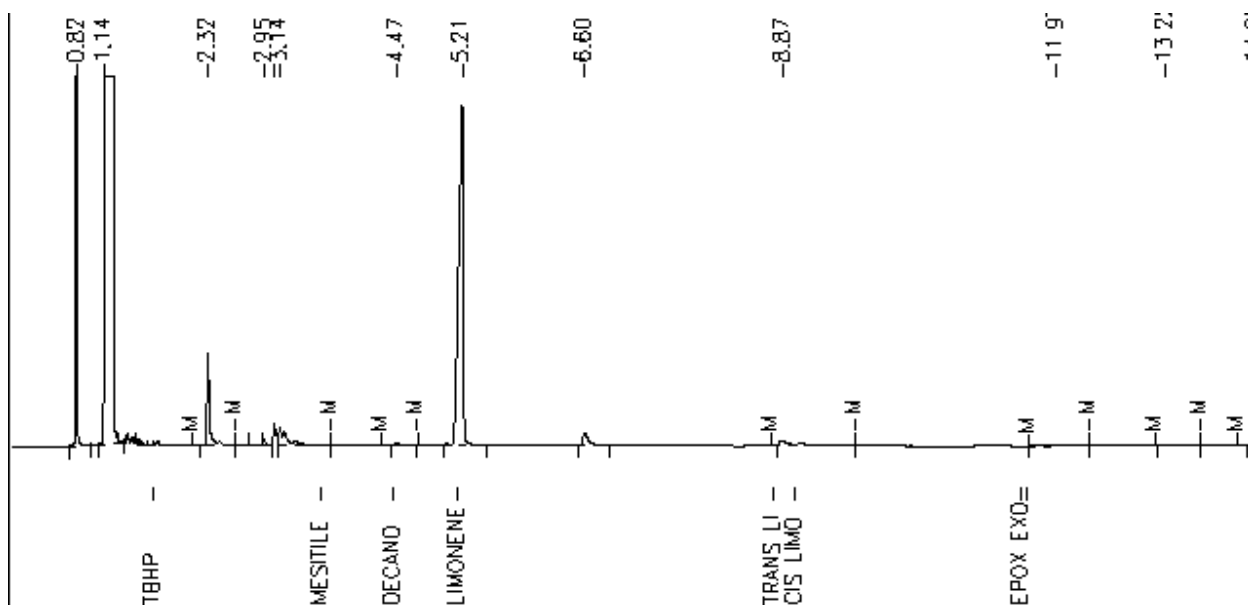
limonene - retention time 5.21 min (9.26 min);

*trans*-limonene oxide - retention time 8.87 (14.32 min);

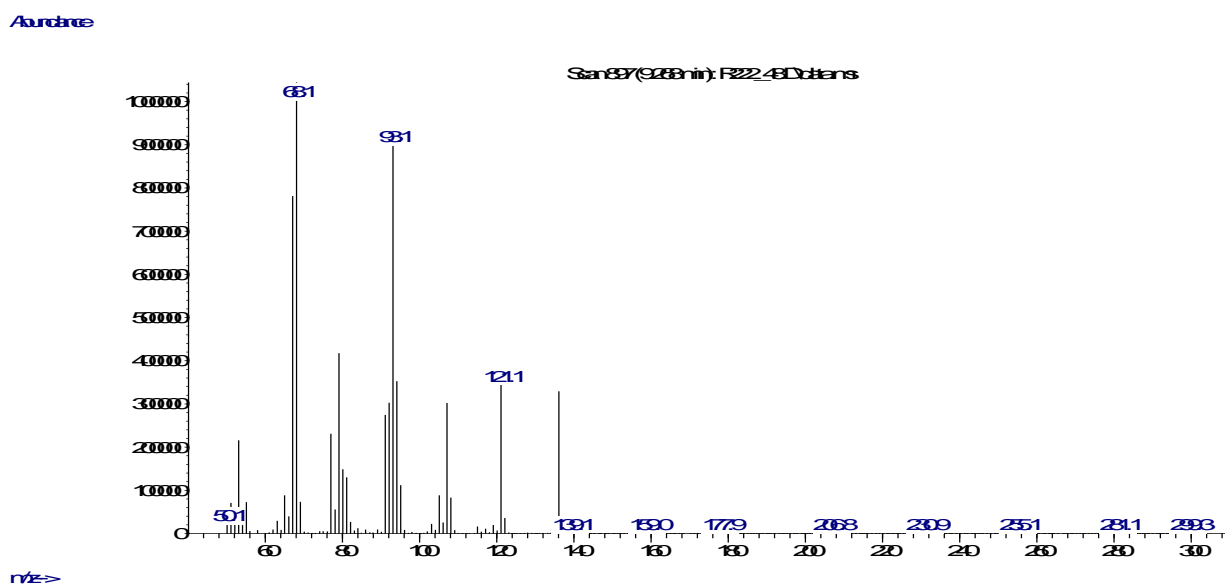
*cis*-limonene oxide - retention time 16.4 min (14.09 min);



Spectrum 1. Chromatogram of the reaction mixture after 48h (analysed by GC-MS)

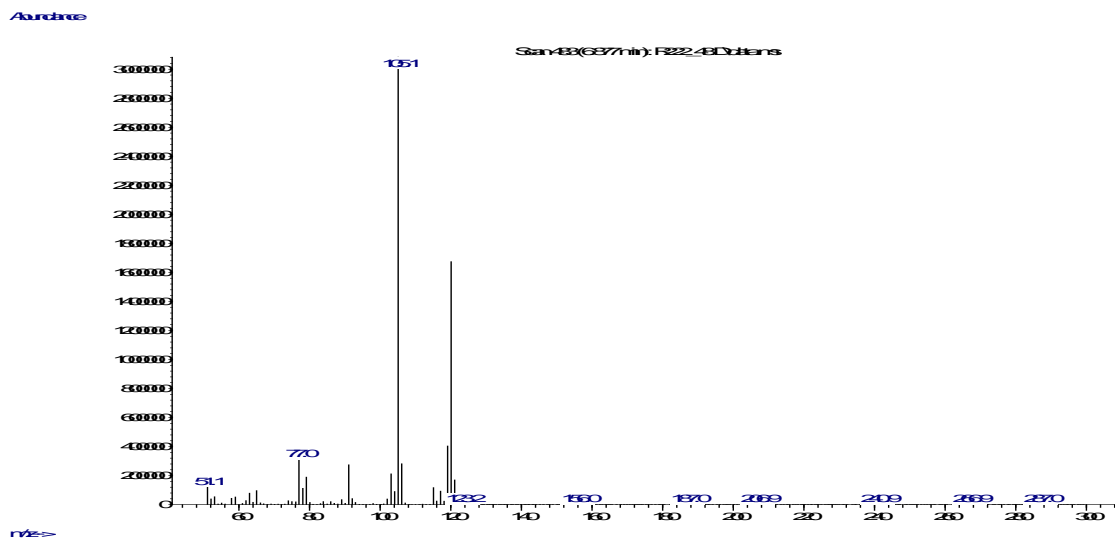


Spectrum 2. Chromatogram of the reaction mixture after 48h (analysed by GC)

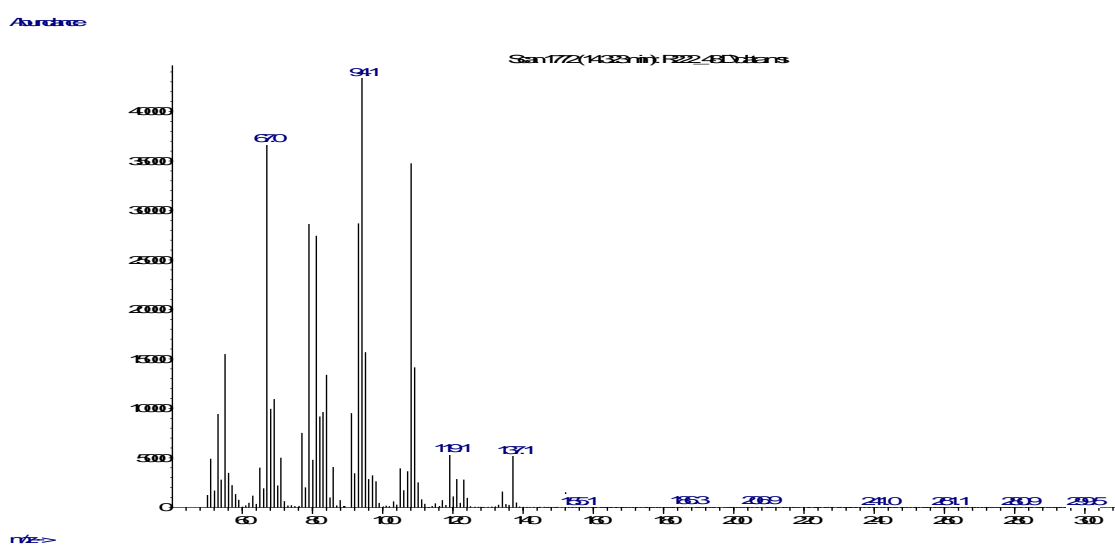


Spectrum 3. Limonene

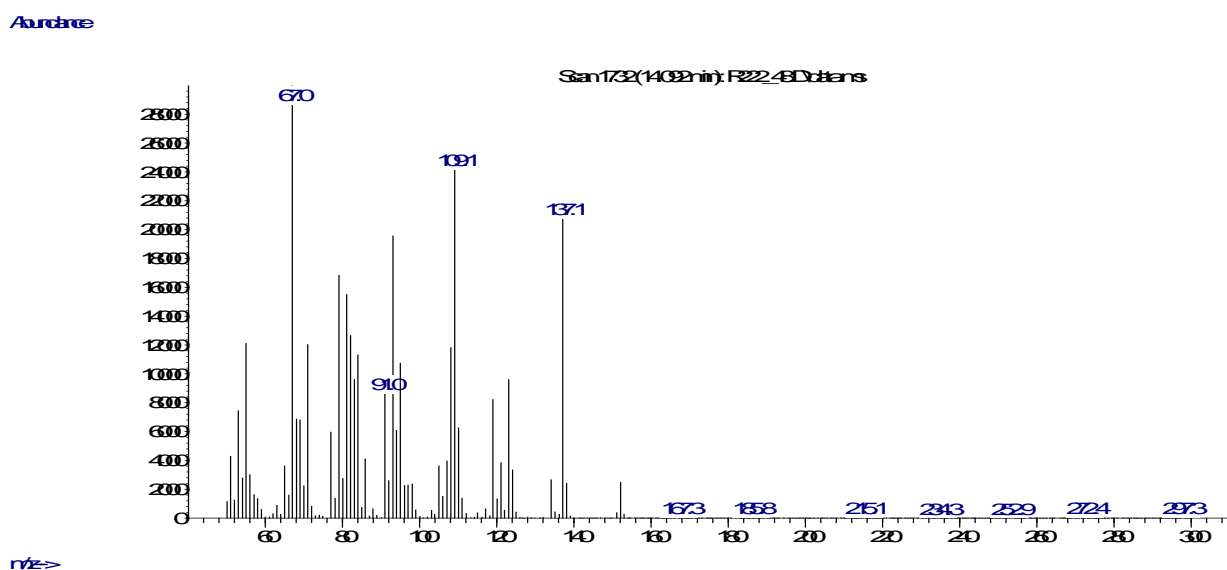




Spectrum 4. Mesitylene



Spectrum 5. *trans* - limonene oxide



Spectrum 6. *cis*-limonene oxide

## Measuring the oxygen consumption in limonene oxidation with molecular O<sub>2</sub> and TBHP used as radical initiator.

The apparatus to measure the oxygen consumption in the reaction of limonene epoxidation over Au-based catalyst is shown on the Figure 1: a barometric tube of glass of 60 cm was connected to the mercury vessel at one end and to the reactor at the other end. First, the test with empty reactor was performed at the temperature of 20°C. For this, the reactor and the tube were filled with molecular O<sub>2</sub>, compensated to air and after that, the reactor was closed (closing the stop-cock 1). The initial level of mercury in the barometric tube was 4.15. After 2 hours it was changed to 4.8, After 24 h the value was 4.36. Second test, the blank reaction without catalyst, was performed at the temperature 80°C. The following reagents were added into the reactor at the room temperature: methyl cyclohexane (MCH), TBHP, limonene, mesitylene. The reactor was filled with O<sub>2</sub> and the stop-cock 1 was closed. The barometric tube was filled with molecular O<sub>2</sub>, the stop-cock 1 was opened, and the mercury level was set up to the sign of 4.5 mL on the barometric tube. The reactor was put in the oil bath at 80°C. The stop-cock was closed and the reactor was left for 2 hours. After 2 hours, before measuring the level of O<sub>2</sub>, the reactor was cooled to room temperature. The level was changed from 4.5 mL to 3.95 mL. After 22 h the level was 2.08 mL. However, even though the temperature difference, the dead volume of the system were considered, it is clear that the sensitivity of this technique does not allow to evaluate the quantitative consumption of O<sub>2</sub> in the reaction of limonene epoxidation.

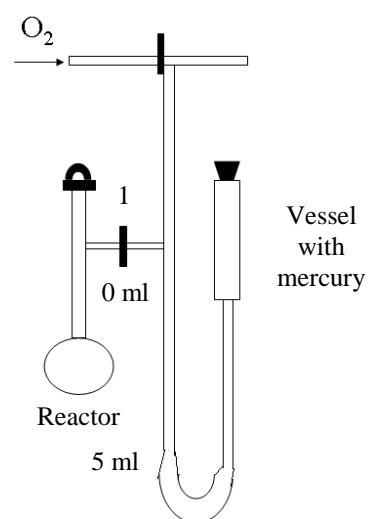


**Figure 1**

## Experimental part for Chapter 6

### Encapsulation of glucose oxidase (GOx)

Nanoporous silica capsules (NPS) were synthesized during the three months stage in Montpellier by using lecithin/dodecylamine/lactose as templates in an ethanol/aqueous media and are suitable for enzyme encapsulation.

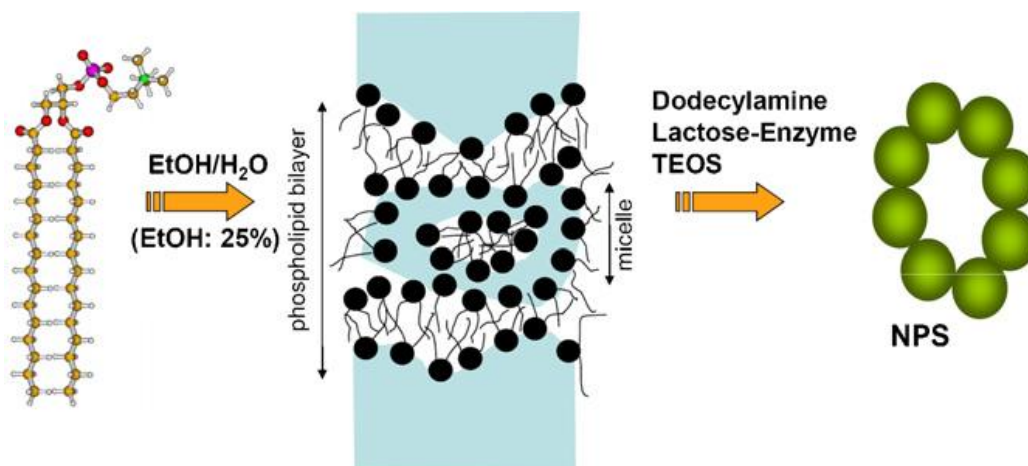


**Figure 1.** Schematic representation of porous nanoporous silica capsules (NPS) formation, from phospholipids and formation of micelles of phospholipids inside lipids bilayer.

NPS encapsulation combines the sol-gel method with a templating process using bilayers of phospholipid to provide an organized network of phospholipids inside the silica and in the same time protect the embedded enzymes (Fig. 1). The role of each reagent in the synthesis is described below. Lecithin (Fig. 2) belongs to the phospholipids family, which forms the lipid matrix of biological membranes. Because of its nearly cylindrical molecular shape, lecithin can not grow micelles by itself in aqueous media. Its tendency to curve, described in terms of its spontaneous curvature, is very low, and therefore it induces the formation of lamellar bilayer phospholipids structures, described as membranes, vesicles or liposomes (Fig. 3). By addition of surfactant, which is dodecylamine in our case, the transition of vesicles to micelles is possible due to the spontaneous curvature induced by mixed-micelles formation. Thus, dodecylamine stabilizes the structure of the resulting mesophase by maintaining the space between lipid heads. At the same time, dodecylamine catalyzes the polymerization of the alkoxyde of silica (TEOS) around this mesophase to lead to the NPS material. The addition of ethanol facilitates the water penetration in the membrane interior as well as the migration of phospholipids.

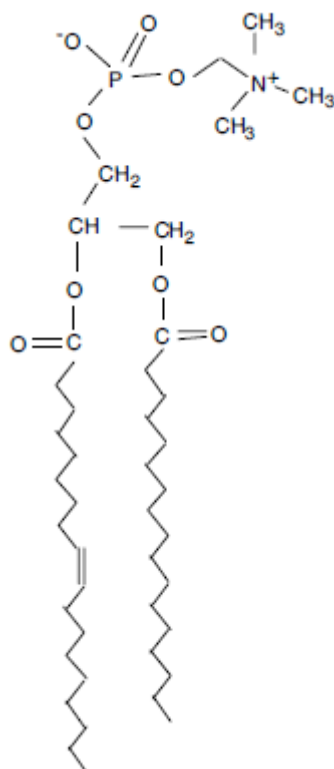


**Figure 2.** Schematic model of lecithin.

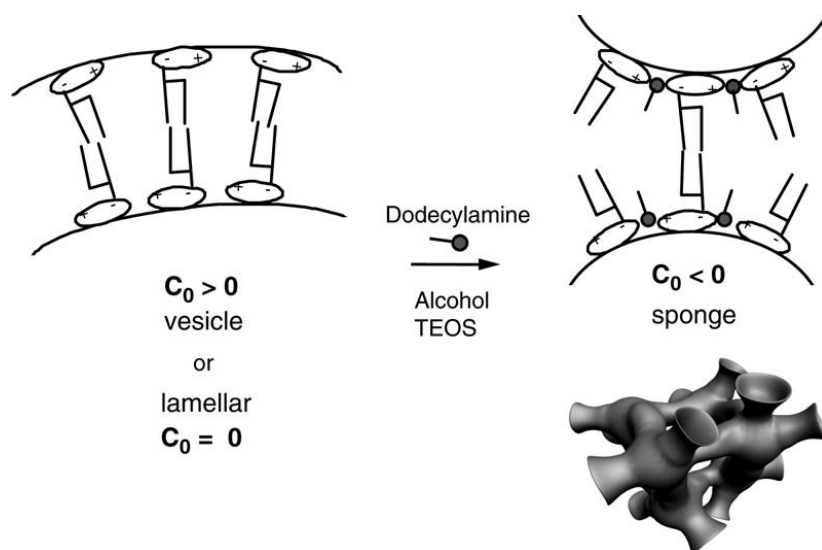


**Figure 3.** Vesicle to sponge-like phase transition by addition of dodecylamine/ethanol and silica source to lecithin vesicles.  $C_0$  is a spontaneous curvature of each phase.

Encapsulation of GOx was performed as following: the first solution was prepared with 7.2 mL of phosphate buffer (pH=7), 50 mg GOx, 50 mg  $\beta$ -lactose. The second solution with 2g ethanol, 0.7g lecithin and 50 mg of dodecylamine was prepared. The two solutions were mixed under stirring for 30 min and then 1 g of TEOS was added. The mixture was then left in static for 24 hours in a water bath at 37°C. The solution was then centrifugated and washed 3 times with

phosphate buffer at pH=7 and then 3 times with ethanol. The solids were dried by lyophilisation and kept in fridge at 4°C before use.

### **Measurements of the activity of GOx free and encapsulated GOx by Trinder test.**

The activity of GOx was measured by Trinder test (Fig. 4). The Trinder test is a reaction between H<sub>2</sub>O<sub>2</sub>, phenol and aminoantipyrine with the formation of a quinone (quinoneimine), catalyzed by the presence of a horseradish peroxidase. For this purpose, the following solutions were prepared:

- 1) Solution of 4-aminoantipyrine 0.5 mM (4-AAP) and phenol (31.25 mM) in phosphate buffer (0.1 M, pH=7)
- 2) solution of horseradish peroxidase (HRP) 10 mg L<sup>-1</sup>
- 3) solution of GOx 5 mg L<sup>-1</sup>
- 4) solution of glucose 2.5 M

All solutions for GOx activity determination were prepared in phosphate buffer. Phosphate buffer solution (0.1 M) was prepared by mixing appropriate amounts of Na<sub>2</sub>HPO<sub>4</sub> in water MQ, then adjusting the solution to the pH value needed with HCl or NaOH.

### **Measurements of free GOx activity:**

In the cuve of Quartz of 3 mL 1600 µL of the solution of 4-AAP and phenol were added. The following addition of 150 µL HRP, 200 µL glucose was performed. By the addition of 50 µL of the solution of glucose we start the kinetic measurements. Augmentation of optical density occurs at 508 nm. The test lasts 4 min (Fig. 5). The temperature of the measurement procedure was 25°C.



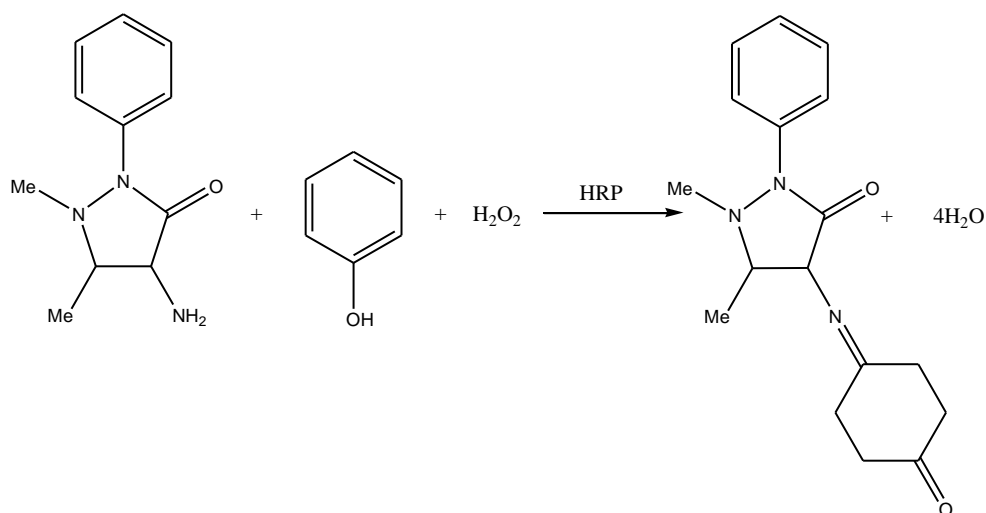


**Figure 4.** Trinder test

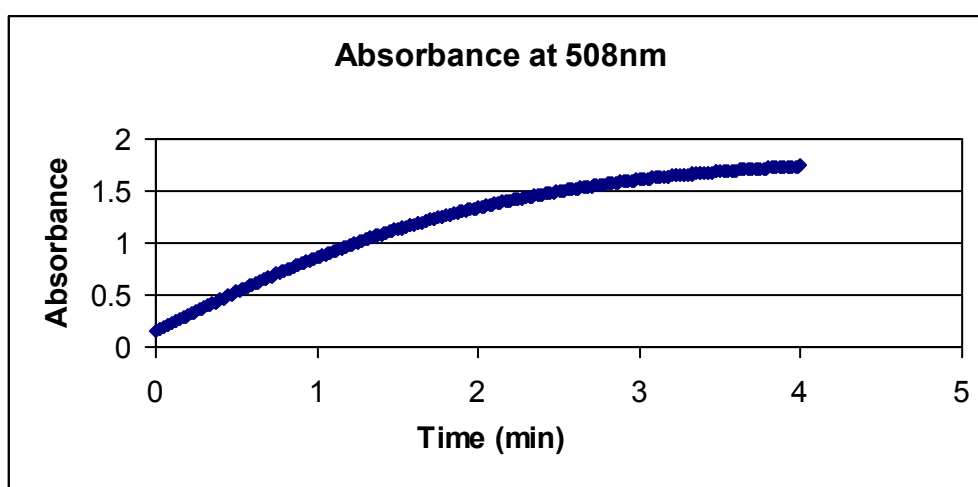


**Figure 5.** Absorbance versus time for GOx free

A series of three experiments with different concentration of glucose (1.5 M, 1 M, 5 M) was performed. The activity was calculated from the Beer-Lambert law:

$$[\text{Product}] = \text{Absorbance} / \epsilon \cdot l$$

#### Measurements of encapsulated GOx

Into the reactor of 40 mL equipped with a glass filter (Fig. 6) the solution of 4-AAP and phenol was added. The following addition of 50  $\mu\text{L}$  of HRP, 5 mL of glucose solution was occurred. With the addition of 10 mg of encapsulated GOx the reaction was started. The agitation of the solution was kept on 200 tours  $\text{min}^{-1}$ . The peristaltic pump (40 mL  $\text{min}^{-1}$ ) was used to induce the flow. The reagents from the reactor were introduced into the capillaries using typical flow-rated tubes, using the filter Interchim (PVDF, 0.45  $\mu\text{m}$ , NM770). Measurements were performed at 508 nm. A series of three experiments with different concentration of glucose (1.5 M, 1 M, 5 M) was performed.



**Figure 6.** Picture of the reactor, peristaltic pump and UV-spectrophotometer.

### **Catalytic test:**

In a typical catalytic test 50 mg of TS-1, 2 mmol DMSO, 15 mL phosphate buffer (pH=5.5), 10  $\mu$ L GO<sub>x</sub>, 4.5 g of glucose were added into the reactor. The syringe with the attached compressed air was inserted into the reactor allowing air to bubble.

### **HPLC analysis**

High pressure liquid chromatography (HPLC) was used for the analysis of the DMSO oxidation reaction. The characteristics are the following:

Column: Rezex – RHM – Monosaccharide H<sup>+</sup> (8%) (contains sulfonated styrene – divinylbenzene spheres in 8% cross-link forms).

Mobile phase: H<sub>2</sub>O MQ

Flow rate: 1ml min<sup>-1</sup>

Detection: RI (refractive index)

T=85°C

Back pressure: 265 psi

## APPENDIX I

### Ab-initio DFT calculations results

Ab-initio DFT calculations were performed in the collaboration with Dr. Tzonka Mineva, *Laboratoire de Materiaux Catalytiques et Catalyse en Chimie Organique CNRS/ENSCM/UMI Ecole Nationale Supérieure de Chimie de Montpellier*.

The idea was to study the role of the silicate curvatures (plan and pores) on the geometrical properties and energies of grafted  $\text{Ti}(\text{OH})_x$  ( $x=2$  and  $3$ ) species from ab-initio DFT calculations.

Four stable structures of  $\text{Ti}(\text{OH})_x / \text{SiOH}$  were obtained. These structures represent  $\text{Ti}(\text{OH})_2$  and  $\text{Ti}(\text{OH})_3$  species, bound to two or one oxygen, respectively, of the silicate surface. The two surfaces are models of a SiOH plane and pore walls. Only one  $\text{Ti}(\text{OH})_x$  species per surface model have been considered. The interaction energies of  $\text{Ti}(\text{OH})_x$  have been computed from the relation:

$\Delta E = E(\text{Ti}(\text{OH})_x / \text{SiOH}) - [E(\text{SiOH}) + E(\text{Ti}^{n+}(\text{OH})_x) - x \cdot E(\text{H})]$ , where  $n$  is the charge on the  $\text{Ti}^{n+}(\text{OH})_x$ , i.e. for  $x = 2$  and  $3 \rightarrow n = 2$  and  $1$ . The interaction energies per Ti – O bonds to the surface oxygens are summarized in Table 1, together with characteristic geometrical parameters. An on-top view of the optimized structures is given in Figures 1 - 4.

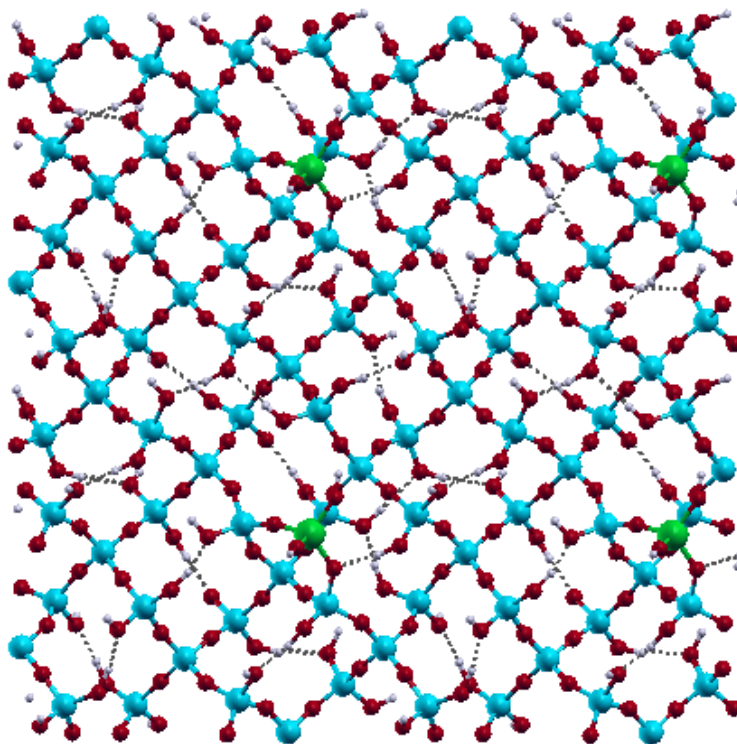




**Figure 1.** On top view of the fully optimized  $\text{Ti}(\text{OH})_2 / \text{SiOH}$  plane model. Red, blue, green and gray balls represent O, Si, Ti and H atoms, respectively. Same is used in Figure 2, 3 and 4. The H-bonds are shown as dotted lines.

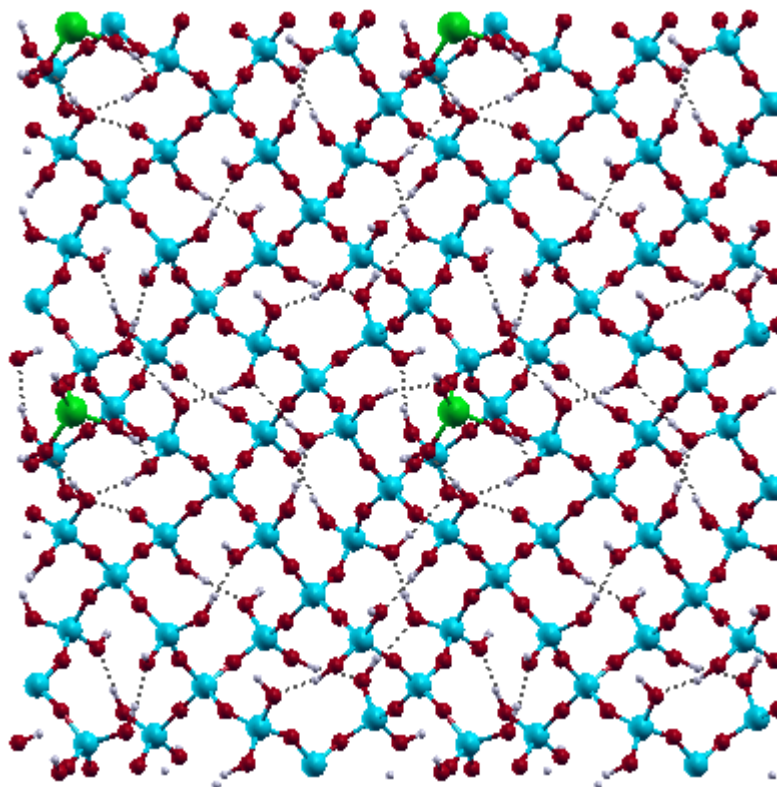


**Figure 2.** On top view of the fully optimized  $\text{Ti}(\text{OH})_3 / \text{SiOH}$  plane model.

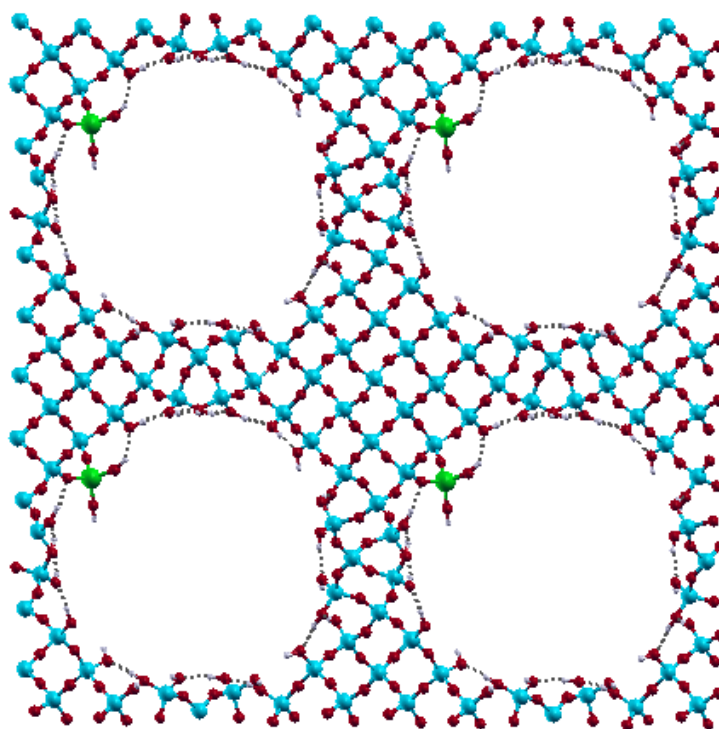


**Figure 3.** On top view of the fully optimized  $\text{Ti(OH)}_2 / \text{SiOH}$  pore model

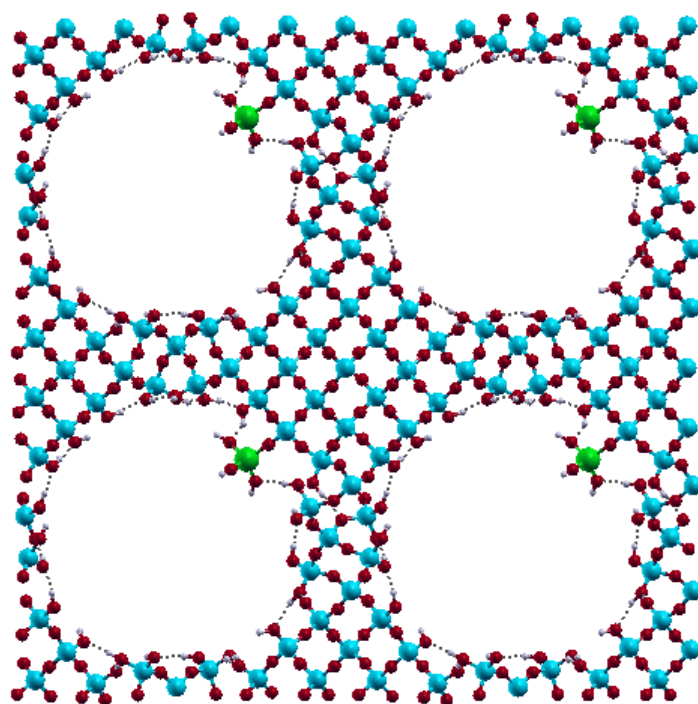


**Figure 4.** On top view of the fully optimized  $\text{Ti(OH)}_3 / \text{SiOH}$  pore model.

**Table 1:** Interaction energies,  $\Delta E$ , in eV, selected bond distances in Å and atomic charges (Mulliken evaluation scheme) in electrons as obtained for the four minimum energy  $\text{Ti(OH)}_x /$

SiOH models. The error bars of the bond lengths are within 0.005 Å and of the  $\Delta E$  within few kcal/mol. The Basis Set Superposition Error is not considered, but it will be similar in the four models.

System	$\Delta E$	Ti – O(Si)	Ti-O(H)	q (Ti)	q (O(Ti))
Ti(OH) <sub>2</sub> / SiOH (plane)	-8.67	1.81 1.87	1.77	+1.5	-1.0
Ti(OH) <sub>3</sub> / SiOH (plane)	-7.03	1.83	1.78; 1.76 1.82 (H...O-Si)	+1.5	-1.0
Ti(OH) <sub>2</sub> / SiOH (pore)	-10.00	1.81 1.86	1.75	+1.5	-1.0
Ti(OH) <sub>3</sub> / SiOH (pore)	-6.49	1.80	1.81; 1.77 1.82 (H...O-Si)	+1.5	-1.0

### Conclusion

- On both surface models, Ti(OH)<sub>2</sub> species bound stronger than Ti(OH)<sub>3</sub>;
- Almost no difference in the geometrical parameters and atomic charges computed in the 4 models.
- This leads to a hypothesis that the confinement potentials influence the binding energies and not geometrical differences due to the surface curvatures.

## References Chapter 1

- [1] J.M. Fraile, J.I. Garcia, J.A. Mayoral, E. Vispe, *J. Catal.*, 204, **2001**, 146
- [2] J.M. Thomas, R. Raja, *Aust. J. Chem.*, 54, **2001**, 551
- [3] K. Sato, M. Aoki, R. Noyori, *Science*, 281, **1998**, 1646
- [4] D.P. Das, K.M. Parida, *Catal. Lett.*, 128, **2009**, 111
- [5] Y. Usui, K. Sato, *Green Chem.*, 5, **2003**, 373
- [6] A.R. Ravishankara, J.S. Daniel, R.W. Portmann, *Science*, 326, **2009**, 123
- [7] S. Ren, Z. Xie, L. Cao, X. Xie, G. Qin, Wang, *J. Catal. Commun.*, 10, **2009**, 464
- [8] R. Sever, R. Alcalá, J. Dumesic, T. Root, *Microp. Mesop. Mat.*, 66, **2003**, 53.
- [9] A. Hagen, K. Schuelerb, F. Roessner, *Microp. Mesop. Mat.*, 51, **2002**, 23.
- [10] S. Laha, R. Kumar, *Microp. Mesop. Mat.*, 53, **2002**, 163.
- [11] F. Chiker, J.P. Nogier, F. Launay, J.L. Bonardet, *Appl. Catal. A: Gen.*, 259, **2004**, 153
- [12] H. Kochkar, F. Figueras, *J. Catal.*, 171, **1997**, 420
- [13] M.A. Camblor, A. Corma, P. Esteve, A. Martinez, S. Valencia, *Chem. Commun.*, **1997**, 795
- [14] L.Y. Chen, G.K. Chuah, S. Jaenicke, *J. Catal.*, 171, **1997**, 420
- [15] F. Chiker, F. Launay, J.P. Nogier, J.L. Bonardet, *Green Chem.*, 5, **2003**, 318
- [16] A. Welch, N.R. Shiju, I.D. Watts, G. Sankar, S. Nikitenko, W. Bras, *Catal. Lett.*, 105, **2005**, 179
- [17] E. Gianotti, C. Bisio, L. Marchese, M. Guidotti, N. Ravasio, R. Psaro, S. Coluccia, *J. Phys. Chem. C.*, 111, **2007**, 5083
- [18] S.A. Holmes, F. Quignard, A. Choplin, R. Teissier, J. Kervennal, *J. Catal.*, 176, **1998**, 173
- [19] S.B. Kumar, S.P. Mirajkar, G.C.G. Pais, P. Kumar, R. Kumar, *J. Catal.*, 156, **1995**, 163
- [20] A. Holmes, F. Quignard, A. Choplin, R. Teissier, J. Kervennal, *J. Catal.*, 176, **1998**, 182
- [21] M.C. Capel-Sanchez, J.M. Campos-Martin, J.L.G. Fierro, M.P. de Frutos, A. Padilla Polo, *Chem. Commun.*, **2000**, 855
- [22] A. Corma, M.J. Diaz-Cabanas, M.E. Domine, F. Rey, *Chem. Commun.*, **2000**, 1725
- [23] J.M. Fraile, J.I. Garcia, J.A. Mayoral, E. Vispe, *Appl. Catal. A: General* 245, **2003**, 363
- [24] C.K. Jorgensen, S.J. Lippard (Eds.), *Prog. Inorg. Chem.*, Wiley, New York, **1970**, 12
- [25] M. Boccuti, K.M. Rao, A. Zecchina, G. Leofanti, G. Petrini, C. Morterra, A. Zecchina, G. Costa (Eds.), *Structure and Reactivity of Surfaces*, Elsevier, Amsterdam, **1989**, 133
- [26] A. Zecchina, G. Spoto, S. Bordiga, M. Padovan, G. Leofanti, G. Petrini, *Proceedings of the Zeocat 90*, Leipzig, Elsevier, Amsterdam. **1990**

- [27] G.J. Wanga, G.Q. Liu, M.X. Xu, Z.X. Yang, Z.W. Liu, Y.W. Liu, S.F. Chen, L. Wanga, *Appl. Surf. Science*, 255, **2008**, 2632
- [28] Q. Zou, S. Nourbakhsh, J. Kim, *Mater. Lett.*, 40, **1999**, 240

## References Chapter 2

- [1] K.M. Doll, B.R. Moser and S.Z. Erhan, *Energy Fuels*, 21, **2007**, 3044.
- [2] K.M. Doll, B.K. Sharma and S.Z. Erhan, *Clean*, 36 (8), **2008**, 700.
- [3] H. Schuster, L.A. Rios, P.P. Weckes and W.F. Hoelderich, *Appl. Catal. A: Gen.*, 348, **2008**, 266.
- [4] J. Salimon, N. Salih and E. Yousif, *Eur. J. Lipid Sci. Technol.*, 112, **2010**, 519.
- [5] A. Kleinova, P. Fodran, L. Brncalova and J. Cvengros, *Biomass Bioenergy*, 32, **2008**, 366.
- [6] P.Czub, *Macromol Symp.*, 242, **2006**, 60.
- [7] J.O. Metzger, *Eur. J. Lipid Sci. Technol.*, 111, **2009**, 865.
- [8] H. Endres, H. Fischer, F. Loeffelholz, P. Wedl, K. Worchech, A. Hansen and G. Geismar, DE Pat. 4,117,034, **1991**.
- [9] M.T. Benaniba, N. Belhanceche-Bensemra and G.Gelbard, *Polym. Degrad. Stabil.*, 82, **2003**, 245.
- [10] M.S. Reisch, *Chem. Eng. News*, 85, **2007**, 15.
- [11] I.Scheuffsen and A. Meffert, DE Pat. 3,326,455, **1983**.
- [12] S. Grinberg, N. Kipnis, C. Linder, V. Kolota and E. Heldman, *Eur. J. Lipid Sci. Technol.*, 112, **2010**, 137.
- [13] B.K. Sharma, K.M. Doll and S.Z. Erhan, *Green Chem.*, 9, **2007**, 469.
- [14] Z.S. Petrovic, A. Zlatanovic, C.C. Lava and S. Sinadinovic-Fiser, *Eur. J. Lipid Sci. Technol.*, 104, **2002**, 293.
- [15] U. Biermann, W. Friedt, S. Lang, W. Luhs, G. Machmuller, J.O. Metzger, M. Rusch gen. Klaas, H.J. Schafer and M. Schneider, *Angew. Chem., Int. Ed.*, 39, **2000**, 2206.
- [16] M.A. Cambor, A Corma, P. Esteve, A. Martinez and A. Valencia, *Chem. Commun.*, **1997**, 795.
- [17] J. Sepulveda, S. Teixeira and U. Schuchardt, *Appl. Cat. A: Gen.*, 318, **2007**, 213.
- [18] P.A.Z. Suarez, M.S.C. Pereira, K.M. Doll, B.K. Sharma and S.Z. Erhan, *Ind. Eng. Chem. Res.*, 48, **2009**, 3268.
- [19] E. Poli, J-M. Clacens, J. Barraulta and Y. Pouilloux, *Catal. Today*, 140, **2009**, 19.
- [20] P. Jiang, M. Chen, Y. Dong, Y. Lu, X. Ye and W. Zhang, *J. Am. Oil Chem. Soc.*, 87, **2010**, 83.
- [21] A. Campanella, M. A. Baltanas, M.C. Capel-Sanchez, J.M. Campos-Martin and J. L. G. Fierro, *Green Chem.*, 6, **2004**, 330.
- [22] S. Warwel and M. Ruesch gen. Klaas, *J. Mol. Catal. B: Enzym.*, 1, **1995**, 29.

- [23] W. S. D. Silva, A. A. M. Lapis, P. A. Z. Suarez and B. A. D. Neto, *J. Mol. Catal. B: Enzym.*, 68, **2011**, 98.
- [24] M. Guidotti, R. Psaro, N. Ravasio, M. Sgobba, E. Gianotti and S. Grinberg, *Catal. Lett.*, 122, **2008**, 53.
- [25] M. Guidotti, N. Ravasio, R. Psaro, E. Gianotti, K. Marchese and S. Coluccia, *Green Chem.*, 5, **2003**, 421.
- [26] J. S. Rafelt and J. H. Clark, *Catal. Today*, 57, **2000**, 33.
- [27] R.A. Sheldon and J. Dakka, *Catal. Today*, 19, **1994**, 215.
- [28] M. Ziolk, *Catal. Today*, 90, **2004**, 145.
- [29] E. Gianotti, C. Bisio, L. Marchese, M. Guidotti, N. Ravasio, R. Psaro and S. Coluccia, *J. Phys. Chem. C*, 111, **2007**, 5083.
- [30] M. Guidotti, C. Pirovano, N. Ravasio, B. Lázaro, J. M. Fraile, J. A. Mayoral, B. Coq and A. Galarneau, *Green Chem.*, 11, **2009**, 1421.
- [31] J. M. Fraile, J. I. Garcia, J. A. Mayoral and E. Vispe, *Appl. Catal. A: Gen.*, 245, **2003**, 363.
- [32] T. Maschmeyer, F. Rey, G. Sankar and J. M. Thomas, *Nature*, 378, **1995**, 159.
- [33] M. Guidotti, L. Conti, A. Fusi, N. Ravasio and R. Psaro, *J. Mol. Catal. A*, 149, **2002**, 182.
- [34] M. Guidotti, R. Psaro, M. Sgobba and N. Ravasio, "Catalytic Processes for the Selective Epoxidation of Fatty Acids: More Environmentally Benign Routes", in "Catalysis for Renewables: From Feedstock to Energy Production", G. Centi and R. A. van Santen (Eds.), WILEY-VCH, **2007**, Weinheim, p. 257.
- [35] E. Jorda, A. Tuel, R. Teissier and J. Kervennal, *J. Catal.*, 175, **1998**, 93.
- [36] F. Carniato, C. Bisio, G. Gatti, M. Guidotti, L. Sordelli and L. Marchese, *Chem. Asian J.*, 6, **2011**, 914.
- [37] R. D. Oldroyd, J. M. Thomas, T. Maschmeyer, P. A. MacFaul, D. W. Snelgrove, K. U. Ingold and D. D. M. Wayner, *Angew. Chem., Int. Ed. Eng.*, 35, **1996**, 2787.
- [38] A. O. Bouh, J. H. Espenson, *J. Mol. Catal. A: Chem.*, 200, **2003**, 43.
- [39] (a) G. B. Payne and P. H. Williams, *J. Org. Chem.*, 26, **1961**, 251; (b) G. B. Payne, *Tetrahedron*, 18, **1962**, 763.
- [40] G. W. Huber, S. Iborra and A. Corma, *Chem. Rev.*, 106, **2006**, 4044.
- [40] (a) K. Neimamm, R. Neumann, *Org. Lett.*, 2, **2000**, 2861; (b) A. Berkessel, J.A. Adrio, D. Huttenhain, J.M. Neudorfl, *J. Am. Chem. Soc.*, 128, **2006**, 8421.
- [41] C. Berlini, M. Guidotti, G. Moretti, R. Psaro and N. Ravasio, *Catal. Today*, 60, **2000**, 219.
- [42] M. Guidotti, N. Ravasio, R. Psaro, G. Ferraris and G. Moretti, *J. Catal.*, 214, **2003**, 242.

- [43] A. Galarneau, M. Nader, F. Guenneau, F. Di Renzo and A. Gedeon, *J. Phys. Chem. C*, 111(23), **2007**, 8268.
- [44] A. Galarneau, M. F. Driole, C. Petitto, B. Chiche, B. Bonelli, M. Armandi, B. Onida, E. Garrone, F. Di Renzo and F. Fajula, *Microp. Mesop. Mater.*, 83, **2005**, 172.
- [45] J. C. P. Broekhoff and J.H. De Boer, *J. Catal.*, 10, **1968**, 377.
- [46] A. Galarneau, D. Desplantier, R. Dutartre and F. Di Renzo, *Microp. Mesop. Mater.*, 27, **1999**, 297.



### References Chapter 3

- [1] K. Bauer, D. Garbe, H. Surbury, *Common Fragrance and Flavor Materials: Preparation, Properties and Uses*, Wiley-VCH, Holzminden, Germany, **1997**, 177-238.
- [2] R. H. Deboukian, P. J. Weldon, Patent WO2007025197, **2007**.
- [3] F. Smith, J. Jankauskas, O. Messerschmidt, Patent WO2006094126, **2006**.
- [4] C. M. Byrne, S. D. Allen, E. B. Lobkovsky, G. W. Coates, *J. Am. Chem. Soc.*, **2004**, 126, 11404.
- [5] R. C. Jeske, A. M. Diciccio, G. W. Coates, *J. Am. Chem. Soc.*, **2007**, 129, 11330.
- [6] A. Corma, S. Iborra, A. Velty, *Chem. Rev.*, **2007**, 107, 2411.
- [7] M. Guidotti, N. Ravasio, R. Psaro, G. Ferraris, G. Moretti, *J. Catal.*, **2003**, 214, 247.
- [8] D. Marino, N. G. Gallegos, J. F. Bengoa, A. M. Alvarez, M. V. Cagnoli, S. G. Casuscelli, E. R. Herrero, S. G. Marchetti, *Catal. Today*, **2008**, 133-135, 632.
- [9] W. F. Maier, J. A. Martens, S. Klein, J. Heilmann, R. Parton, K. Vercruyse, P. A. Jacobs, *Angew. Chem. Int. Ed.*, **1996**, 35(2), 180.
- [10] T. Tatsumi, K. A. Koyano, N. Igarashi, *Chem. Commun.*, 1998, 325.
- [11] K. Lin, L. Wang, F. Meng, Z. Sun, Q. Yang, Y. Cui, D. Jiang, F-S. Xiao, *J. Catal.*, **2005**, 235, 423
- [12] M. Guidotti, I. Batonneau-Gener, E. Gianotti, L. Marchese, S. Mignard, R. Psaro, M. Sgobba, N. Ravasio, *Microp. Mesop. Mater.*, **2008**, 111, 39.
- [13] M. R. Prasad, M. S. Hamdy, G. Mul, E. Bouwman, E. Drent, *J. Catal.*, **2008**, 260, 288
- [14] M.C. Capel-Sanchez, J.M. Campos-Martin, J.L.G. Fierro, *Catal. Today*, **2010**, 158, 103
- [15] T. Maschmeyer, F. Rey, G. Sankar, J. M. Thomas, *Nature*, **1995**, 378, 159.
- [16] A. Corma, M. Domine, J. A. Gaona, J. L. Jordà, M. T. Navarro, F. Rey, J. Pérez-Pariente, J. Tsuji, B. McCulloch, L. T. Nemeth, *Chem. Commun.*, **1998**, 2211.
- [17] M. L. Pena, V. Dellarocca, F. Rey, A. Corma, S. Coluccia, L. Marchese, *Microp. Mesop. Mater.*, **2001**, 44-45, 345.
- [18] H. Barthel, E. Nikitina, *Silicon Chem.*, **2002**, 1, 249
- [19] I. Batonneau-Gener, A. Yonli, A. Trouvé, S. Mignard, M. Guidotti, M. Sgobba, *Separ. Sci. Techn.*, **2010**, 45(6), 768.
- [20] M. V. Cagnoli, S. G. Casuscelli, A. M. Alvarez, J. F. Bengoa, N. G. Gallegos, M. E. Crivello, E. R. Herrero, S. G. Marchetti, *Catal. Today*, **2005**, 107-108, 397.
- [21] N. Ravasio, F. Zaccheria, M. Guidotti, R. Psaro, *Topics Catal.*, **2004**, 27(1-4), 157.

- [22] M. V. Cagnoli, S.G. Casuscelli, A. M. Alvarez, J. F. Bengoa, N. G. Gallegos, N. M. Samaniego, M. E. Crivello, G. E. Ghione, C. F. Perez, E. R. Herrero, S. G. Marchetti, *Appl. Catal. A: Gen.*, **2005**, 287, 227.
- [23] R. Hutter, T. Mallat, A. Baiker, *J. Catal.*, **1995**, 153, 177.
- [24] M. Guidotti, L. Conti, A. Fusi, N. Ravasio, R. Psaro, *J. Mol. Catal. A*, **2002**, 182–183, 151.

## References Chapter 4

- [1] G. Bellussi, M.S. Rigutto, *Stud. Surf. Sci. Catal.* 85, **1994**, 177.
- [2] M. G. Clerici, in: S. D. Jackson, J.S.J. Hargreaves (Eds.), *Metal Oxide Catalysis*. Wiley-VCH, Weinheim, **2009**, p. 705.
- [3] J. P. M. Niederer, W. F. Hölderich, *Appl. Catal. A: Gen.*, 229, **2002**, 51.
- [4] R. J. Saxton, *Top. Catal.*, 9, **1999**, 43.
- [5] P. Wu, T. Komatsu, T. Yashima, *J. Phys. Chem. B*, 102, **1998**, 9297.
- [6] P. Ratnasamy, D. Srinivas, H. Knözinger, *Adv. Catal.*, 48, **2004**, 1.
- [7] A. Hagen, K. Schuelerb, F. Roessner, *Micropor. Mesopor. Mater.*, 51, **2002**, 23.
- [8] F. Berube, A. Khadhraoui, M. T. Janicke, F. Kleitz, S. Kaliaguine, *Ind. Eng. Chem. Res.*, 49, **2010**, 6977.
- [9] N. Igarashi, K. Hashimoto, T. Tatsumi, *Micropor. Mesopor. Mater.*, 104, **2007**, 269.
- [10] F. Carniato, C. Bisio, G. Gatti, M. Guidotti, L. Sordelli, L. Marchese, *Chem. Asian J.*, 6(3), **2011**, 914.
- [11] F. Carniato, C. Bisio, G. Gatti, E. Boccaleri, L. Bertinetti, S. Coluccia, O. Monticelli, L. Marchese, *Angew. Chem. Int. Ed.*, 48, **2009**, 6059.
- [12] H. C. L. Abbenhuis, S. Krijnen, R. A. van Santen, *Chem. Commun.*, **1997**, 331.
- [13] T. Maschmeyer, M. Klunduk, C. C. M. Martin, D. S. Shephard, J. M. Thomas, B. F. G. Johnson, *Chem. Commun.*, **1997**, 1847.
- [14] M. Crocker, R. H. M. Herold, A. G. Orpen, M. T. A. Overgaag, *J. Chem. Soc. Dalton Trans.*, 21, **1999**, 3791.
- [15] P. P. Pescarmona, J. C. van der Waal, I. E. Maxwell, T. Maschmeyer, *Angew. Chem. Int. Ed.*, 40, **2001**, 740.
- [16] K. Wada, T. Mitsudo, *Catal. Surv. Asia*, 9, **2005**, 229.
- [17] E. A. Quadrelli, in: J. M. Basset, R. Psaro, D. Roberto, R. Ugo (Eds.), *Modern surface organometallic chemistry*, Wiley-VCH, Weinheim, **2009**, p. 557.
- [18] J. M. Fraile, J. I. García, J. A. Mayoral, E. Vispe, *J. Catal.*, 233, **2005**, 90.
- [19] S. Krijnen, H. C. L. Abbenhuis, R. W. J. M. Hanssen, J. H. C. Van Hooff, R. A. Van Santen, *Angew. Chem. Int. Ed.*, 37, **1998**, 356.
- [20] L. Zhang, H. C. L. Abbenhuis, G. Gerritsen, N. N. Bhriain, P. C. M. M. Magusin, B. Mezari, W. Han, R. A. van Santen, Q. Yang, C. Li, *Chem. Eur. J.*, 13, **2007**, 1210.
- [21] S. Krijnen, B. L. Mojet, H. C. L. Abbenhuis, J. H. C. Van Hooff, R. A. Van Santen, *Phys. Chem. Chem. Phys.*, 1, **1999**, 361.

- [22] P. Smet, J. Riondato, T. Pauwels, L. Moens, L. Verdonck, *Inorg. Chem. Commun.*, **3**, 2000, 557.
- [23] M. D. Skowronska-Ptasinska, M. L. W. Vorstenbosch, R. A. Van Santen, H. C. L. Abbenhuis, *Angew. Chem. Int. Ed.*, **41**, 2002, 637.
- [24] F. Carniato, C. Bisio, E. Boccaleri, M. Guidotti, E. Gavrilova, L. Marchese, *Chem. Eur. J.*, **14**, **2008**, 8098.
- [25] F. Carniato, E. Boccaleri, L. Marchese, *Dalton Trans.*, **2008**, 36.
- [26] D. Zhao, J. Feng, Q. Huo, N. Melosh, G. H. Fredrickson, B. F. Chmelka, G. D. Stucky, *Science*, **279**, **1998**, 548.
- [27] T. Maschmeyer, F. Rey, G. Sankar, J.M. Thomas, *Nature*, **378**, **1995**, 159.
- [28] M. Guidotti, L. Conti, A. Fusi, N. Ravasio, R. Psaro, *J. Mol. Catal. A*, 182–183, **2002**, 151.
- [29] C. Berline, M. Guidotti, G. Moretti, R. Psaro, N. Ravasio, *Catal. Today*, **60**, **2000**, 219.
- [30] E. Gianotti, A. Frache, S. Coluccia, J.M. Thomas, T. Maschmeyer, L. Marchese, *J. Mol. Catal. A*, 204-205, **2003**, 483.
- [31] L. Marchese, E. Gianotti, V. Dellarocca, T. Maschmeyer, F. Rey, S. Coluccia, J. M. Thomas, *Phys. Chem. Chem. Phys.*, **1**, **1999**, 585.
- [32] O. A. Kholdeeva, I. D. Ivanchikova, M. Guidotti, C. Pirovano, N. Ravasio, M. V. Barmatova, Y. A. Chesalov, *Adv. Synth. Catal.*, 351, **2009**, 1877.
- [33] I. W. C. E. Arends, R. A. Sheldon, *Appl. Catal. A: Gen.*, 212, **2001**, 175.
- [34] T. Giovenzana, M. Guidotti, E. Lucenti, A. Orbelli Biroli, L. Sordelli, A. Sironi, R. Ugo, *Organometallics*, **29**, **2010**, 6687.
- [35] A. Bhaumik, T. Tatsumi, *J. Catal.*, 182, **1999**, 349.
- [36] A. Bhaumik and T. Tatsumi, *J. Catal.*, 189, **2000**, 31.
- [37] M. Guidotti, I. Batonneau-Gener, E. Gianotti, L. Marchese, S. Mignard, R. Psaro, M. Sgobba, N. Ravasio, *Microp. Mesop. Mater.*, 111, **2008**, 39.
- [38] C. Bisio, G. Gatti, L. Marchese, M. Guidotti, R. Psaro, in: G. Rios, N. Kannelopoulos, G. Centi (Eds.), *Nanoporous materials for energy and the environment*, ISBN: 978-981-4267-17-5, Pan Stanford Publishing Pte Ltd, **2011**, in the press.
- [39] M. Guidotti, N. Ravasio, R. Psaro, G. Ferraris, G. Moretti, *J. Catal.*, 214, **2003**, 247.
- [40] K. Arata, K. Tanabe, *Chem. Lett.*, **8**, **1979**, 1017.
- [41] A.T. Liebens, C. Mahaim, W.F. Holderich, *Stud. Surf. Sci. Catal.*, 108, **1997**, 587.
- [42] N. Ravasio, F. Zaccheria, M. Guidotti, R. Psaro, *Topics Catal.*, 27(1-4), **2004**, 157.

## References Chapter 5

- [1] M. Haruta, N. Yamada, T. Kobayashi, S. Iijima, *J. Catal.*, 115, **1989**, 301
- [2] E. Sacaliuc-Parvulescu, H. Friedrich, R. Palkovits, B. M. Weckhuysen, T. A. Nijhuis, *J. Catal.*, 259, **2008**, 43-53
- [3] M. Haruta, T. Koyabashi, H. Sano, N. Yamada, *Chem. Lett.*, 16, **1987**, 405-408
- [4] G. J. Hutchings, *J. Catal.*, 96, **1985**, 292-295
- [5] B. Nkosi, M. D. Adams, N. J. Coville, G. J. Hutchings, *J. Catal.*, 128, **1991**, 333
- [6] G. J. Hutchings, *Gold Bull.*, 29, **1996**, 123
- [7] A. Eittstick, V. Zielasek, J. Bieener, C. M. Friend, M. Baumer, *Science*, 327, 2010, 319-322
- [8] T. Hayashi, K. Tanaka, M. Haruta, *J. Catal.*, 178, **1998**, 566-575
- [9] S. Carrettin, P. McMorn, P. Johnston, K. Griffin, C. J. Kiely, G. J. Hutchings, *Phys. Chem. Chem. Phys.*, 5, **2003**, 1329-1336
- [10] L. Prati, F. Porta, *Appl. Catal. A*, 291, **2005**, 199
- [11] M. Comotti, C. Della Pina, R. Matarrese, M. Rossi, A. Siani, *Appl. Catal. A*, 291, **2005**, 204
- [12] M. Comotti, C. Della Pina, R. Mataresse, M. Rossi, *Angew. Chem. Int. Ed.*, 43, **2004**, 5812
- [13] S. Biella, G. L. Castiglioni, C. Fumagalli, L. Prati, M. Rossi, *Catal. Today*, 72, **2002**, 43
- [14] P. Landon, P. J. Collier, A. J. Papworth, C. J. Kiey, G. J. Hutchings, *Chem. Commun.*, **2002**, 2058-2059
- [15] J.K. Edwards, A.F. Carley, A.A. Herzing, C. Kiely and J. G. J. Hutchings, *Faraday Discuss.*, **2008**, 138, 225
- [16] T.V.W. Janssens, B.S. Clausen, B. Hvolbæk, H. Falsig, C.H. Christensen, T. Bligaard, J.K. Nørskov, *Top. Catal.*, 44, 1-2, **2007**, 15-26
- [17] T. Bligaard, J.K. Nørskov, S. Dahl, J. Matthiesen, C.H. Christensen, J. Sehested, *J. Catal.* 224, **2004**, 206.
- [18] G. C. Bond, D. T. Thompson, *Catal. Rev. Sci. Eng.*, 41, **1999**, 319
- [19] P. Lignier, F. Morfin, S. Mangematin, L. Massin, J.-L. Rousset, V. Caps, *Chem. Commun.*, **2007**, 186
- [20] M. D. Hughes, Y.-J. Xu, P. Jenkins, P. McCorn, P. Landon, D. I. Enache, A. F. Carley, G. A. Attard, G. J. Hutchings, F. King, E. H. Stitt, P. Johnston, K. Griffin, C. J. Kiely, *Nature*, 437, **2005**, 1132
- [21] P. Lignier, S. Mangematin, F. Morfin, J.L. Rousset, V. Caps, *Catal. Today*, 138, **2008**, 50

- [22] M. A. Brown, Y. Fujimori, F. Ringleb, X. Shao, F. Stavale, N. Nilius, M. Sterrer, H.-J. Freund, *J. Am. Chem. Soc.*, 133, **2011**, 10668
- [23] C.-J. Jia, Y. Liu, H. Bongard, F. Schuth, *J. Am. Chem. Soc.*, 132, **2010**, 1520
- [24] K. Neimann, R. Neumann, *Org. Lett.*, 2(18), **2000**, 2861
- [25] C. Aprile, A. Corma, M.E. Domine, H. Garcia, C. Mitchell, *J. Of Catal.*, 264, **2009**, 44
- [26] S. Tsubota, D.A.H. Cunningham, Y. Bando, M. Haruta, *Stud. Surf. Sci. Catal.*, 91, **1995**, 227

## References Chapter 6

- [1] W.T. Hess, Kirk-Othmer Encyclopedia of Chemical Technology, Vol. 13, 4th ed., Wiley, New York, **1995**, 961
- [2] L.W. Gosser, U.S. Pat., 4.681.751, **1987**
- [3] S. Yuan, Y. Fan, Y. Zhang, M. Tong, P. Liao, Environm. Sci. Technol., 45, **2011**, 8514
- [4] P.J. Brumm, Biotech. Lett., 10(4), **1988**, 237
- [5] R. Montgomery, U.S.Pat., 5176889, **1991**
- [6] P. Laveille, L. Truong Phuoc, J. Drone, F. Fajula, G. Renard, A. Galarneau, *Cat. Today*, 157, **2010**, 94
- [7] P. Beltrame, M. Comotti, C. Della Pina, M. Rossi, *J. Catal.*, 228, **2004**, 282
- [8] M. Petruccioli, F. Federici, C. Bucke, T. Keshavarz, *Enzyme Macrob. Technol.*, 24, **1999**, 397
- [9] S. Pluschkell, K.Hellmuth, U. Rinas, *Biotechnol. Bioeng.*, 51, **1996**, 215
- [10] M. Gerritsen, A. Kros, J. Lutterman, R. Nolte, J. Jansen, *J. Mater. Sci. Mater. Med.*, 12(2), **2001**, 129
- [11] M. Mureseanu, A. Galarneau, G. Renard, F. Fajula, *Langmuir*, 21, **2005**, 4648
- [12] A. Galarneau, M. Mureseanu, S. Atger, G. Renard, F. Fajula, *New. J. Chem.*, 30, **2006**, 562
- [13] Y.S. Chaudhary, S.K. Manna, S. Mazumdar, D. Khushalani, *Micropor. Mesopor. Mater.*, 109, **2008**, 535
- [14] L.H. Zhou, Y.H. Tao, J. Hu, X. Han, H. L. Liu, Y. Hu, *J. Porous Mater.*, 15, **2008**, 653
- [15] N. Nassif, C. Roux, T. Coradin, M. N. Rager, O. M. M. Bouvet, J. Livage, *J. Mater. Chem.*, 13, **2003**, 203
- [16] N. Nassif, O. Bouvet, M. N. Rager, C. Roux, T. Coradin, J. Livage, *Nat. Mater.*, 1, **2002**, 42
- [17] N. Nasiff, A. Coiffier, T. Coradin, C. Roux, J. Livage, O. Bouvet, *J. Sol-Gel Sci. Technol.*, 26, **2003**, 1141
- [18] M. T. Reetz, *Tetrahedron*, 58, **2002**, 6595
- [19] M. T. Reetz, P. Tielmann, W. Wisenhofer, W. konen, A. Zonta, *Adv. Synth. Catal.*, 345, **2003**, 717
- [20] D.G. Hatzinikolaou, O.C. Hansen, B.J. Macris, A. Tingey, D. Kekos, P. Goodenough, *Appl. Microbiol. Biotechnol.*, 46, **1996**, 371

- [21] H.M. Kalisz, H.J. Hecht, D. Schomburg, R.D. Schmid, *Biochim. Biophys. Acta*, 1080(2), **1991**, 138
- [22] S. Pluschkell, K. Hellmuth, U. Rinas, *Biotechnol. Bioeng.*, 51, **1996**, 215
- [23] A. Kaplan, *Methods in Clinical Chemistry*, A.J. Pesco, L.A. Kaplan (Eds.), Part III, Glucose, **1987**, The C.V. Mosby Company, MO, USA, 105



## List of Publications

The work carried out during the three-year Ph.D. period led to the following publications:

1. F. Carniato, C. Bisio, E. Boccaleri, M. Guidotti, E. Gavrilova, L. Marchese, *Chemistry: a European Journal*, 14, **2008**, 8098-8101
2. M. Guidotti, E. Gavrilova, A. Galarneau, B. Coq, R. Psaro, N. Ravasio, *Green Chemistry*, 13, **2011**, 1806-1811.
3. M. Guidotti, R. Psaro, I. Batonneau-Gener, E. Gavrilova, *Chemical Engineering & Technology*, 34 (11), **2011**, 1924-1927
4. F. Carniato, C. Bisio, L. Sordelli, E. Gavrilova, M. Guidotti, "Ti-POSS covalently immobilized onto mesoporous silica. A model for active sites in heterogeneous catalytic epoxidation", *Inorg. Chem. Acta*, DOI. 10.1016/j.ica.2011.11.051 accepted.

...and to the following oral or poster contributions at international congresses

1. E. Gavrilova, M. Guidotti, R. Psaro, A. Galarneau, N. Ravasio, "Epoxidation of methyl oleate over Ti(IV) -grafted silica catalysts with hydrogen peroxide", 4th Workshop on Fats and Oils as Renewable Feedstock for the Chemical Industry, Karlsruhe (Germany), March 20-22, 2011; oral L32, p. 51.
2. E. Gavrilova, M. Guidotti, R. Psaro, N. Ravasio, B. Coq, A. Galarneau, "Sustainable production of methyl epoxystearate from methyl oleate with hydrogen peroxide over heterogeneous titanium-silica catalysts", Convegno Nazionale "Chimica Verde, Chimica Sicura", II edition, Pavia (Italy), June 23-24, 2011; oral O2; p. 19.
3. E. Gavrilova, M. Guidotti, E. Falletta, C. Della Pina, R. Psaro, "Epoxidation of limonene over Au-deposited materials with in-situ formed alkyl hydroperoxide from molecular oxygen", Convegno Nazionale "Chimica Verde, Chimica Sicura", II edition, Pavia (Italy), June 23-24, 2011; poster P8, p. 41.
4. E. Gavrilova, M. Guidotti, R. Psaro, A. Galarneau, "Titanium-silica catalysts in methyl oleate epoxidation with hydrogen peroxide", NANO-HOST Workshop, Design of Hierarchically Ordered Materials for Catalysis, Montpellier (France), 4-6 October 2010, oral.
5. E. Gavrilova, M. Guidotti, R. Psaro, A. Galarneau, "Epoxidation of methyl oleate over Ti(IV) -grafted silica catalysts with hydrogen peroxide", 10th Italian Seminar on Catalysis (GIC 2010), 15 - 18 September 2010, Palermo, Italy; (POSTER AWARD).
6. B. Lázaro, J. M. Fraile, J. A. Mayoral, E. Gavrilova, M. Guidotti, R. Psaro, A. Galarneau, "Stability of Ti(IV)-grafted catalysts for the epoxidation of alkenes in the presence of hydrogen peroxide", 9th Congress on Catalysis Applied to Fine Chemicals (CAFC-9), 13-16 September 2010, Zaragoza (Spain), pres. poster P-49.

7. E. Gavrilova, M. Guidotti, R. Psaro, L. Sordelli, C. Bisio, F. Carniato, L. Marchese, "Ti-POSS covalently immobilized onto mesoporous silica as model catalyst for epoxidation reactions", 16th International Zeolite Congress and 7th International Mesostructured Materials Symposium, IZC- IMMS2010, Sorrento (Italy), 4-9 July 2010, pres. orale, no. 959.
8. E. Gavrilova, M. Guidotti, L. Sordelli, R. Psaro, "Immobilization of Ti-POSS species via covalent anchoring approach. Ti(IV) sites with a controlled chemical environment" ISHHC-XIV – International Symposium on Relations between Homogeneous and Heterogeneous Catalysis, Stockholm, Sweden, 13-18 September 2009, poster.
9. European Network of Doctoral Studies in Chemical Sciences, Milan, Italy, 20-22 May 2009
10. E. Gavrilova, M. Guidotti, NanoHost Workshop "Single Sites in Heterogeneous Catalysis" Milan, Italy, 28-29 September 2009, oral
11. E. Gavrilova, New insights in the adipic acid production: design of heterogeneous catalysts for epoxidation reactions using sustainable oxidants Marie Curie Conference, Turin, Italy, 1-2 July 2010, poster
12. ESOF, Turin, Italy, 1-2 July, 2010

## Acknowledgements

First of all, I owe my deepest gratitude to my co-tutor Dr. Matteo Guidotti. I appreciate his patience and immense knowledge, and all his contribution of ideas and time that he gave me. I'm really thankful for encouraging me and guiding me during these three years of Ph.D. I could not imagine a better tutor than him. I would also like to thank Prof. Francesco Sannicolò for the kind support.

I would like to show my gratitude to Rinaldo Psaro for his great help and for giving me the opportunity to work in his lab.

I am grateful to:

Dr. Anne Galarneau (*Laboratoire de Matériaux Catalytiques et Catalyse en Chimie Organique CNRS/ENSCM/UMI Ecole Nationale Supérieure de Chimie de Montpellier*) for the prepared mesoporous silicas and performed UV-Vis spectra and also, for giving me opportunity to spend three months period in Montpellier and all guys from that lab. Also, I thank Dr. Tzonka Mineva for performed ab-initio DFT calculations.

Fabio Carniato and Chiara Bisio (Nano-SISTEMI Centre, Univ. Eastern Piedmont, Alessandria) for the prepared TiPOSS-TSIPI moieties. Laura Sordelli for the performed XAS analysis.

The group of Prof. Rossi (Dept. of Inorganic, Metallorganic and Analytical Chemistry of the University of Milan) for the provided Au-based materials.

Dr. Pierluigi Barbaro and Serena Orsi.

I would like to thank my lab girlfriends for their friendliness and tea-time giggles.

I would like to thank my family for their love, encouragement and support during all the time. Also, I would like to thank my husband's parents for their support.

And a big thank you to my husband Django Junior Junior Junior...

The work was financially supported by the European Community's Seventh Framework Programme through the Marie Curie Initial Training Network NANO-HOST, (Grant Agreement no. 215193).

## **NANO-HOST**

**Overview.** This project is aimed at generating new fundamental knowledge and fostering new prospects and frontiers, training and transfer of knowledge in the field of highly efficient, highly selective, supported, recyclable catalysts. Targets of the research programme are strongly innovative methodologies for the preparation, recovery and reuse of single-site, multipurpose, nanostructured catalytic materials, and the engineering of reactors based on these catalysts, as this represents an essential part towards the elaboration of sustainable production processes of high-added value fine chemicals. The approach pursued will be the immobilization of homogeneous catalysts, and particularly transition metal complexes, onto preformed (in)soluble supports (heterogenised catalysts). Materials defined at the nanometric level obtained by surface organometallic chemistry will be included. The focus will be on their applications on specific, selected reactions. In this project, we plan to use advanced catalyst design to develop catalysts in which the support allows improvements in terms of activity, selectivity, catalyst lifetime and versatility, compared to their homogeneous counterparts. This will be an interdisciplinary, jointly executed research project encompassing complementary, synthetic (inorganic supports, ligands, organometallic compounds, functionalized polymers, dendrimers, nanoparticles), reactivity (homo- and heterogeneous catalysis), characterization (of materials and in situ), engineering (continuous / supercritical flow reactors) and modelling activities. The network aims at implementing a joint training programme directed to a high-level, high-competency multisectorial education of early stage and experienced Fellows.

Starting date: 01/10/2008

Duration 48 months

The maximum Community contribution to the project is about 3,385,000 €.

## **INITIAL TRAINING NETWORKS**

**Objective.** To improve young researchers' career prospects in both the public and private sectors. This will be achieved through a transnational networking mechanism, aimed at structuring the existing high-quality initial research training capacity. What is funded. The networks are built on joint research training programmes, responding to well identified training needs in defined scientific areas, with reference to interdisciplinary and newly emerging supradisciplinary fields. Support is provided for: • Recruitment of researchers who are within the first five years of their careers in research for initial training. Recruitment of Senior Visiting Scientists of outstanding

stature in international training and collaborative research. Networking activities, organisation of workshops and conferences, involving the participants own research staff and external researchers. Training is focused on scientific and technological knowledge through research on individual, personalised projects, complemented by substantial training modules addressing other relevant skills and competences. Researchers are normally required to undertake transnational mobility when taking up appointment.

**Participants.** Organisations members of a network selected by the Commission which contributes directly to the implementation of the joint research training programme of the network, by recruiting and employing and/or hosting eligible researchers and by providing specialised training modules.

**Network partners.** The Network includes seven participants whereas the work will be carried out by different teams:

Consiglio Nazionale delle Ricerche

Istituto di Chimica dei Composti OrganoMetallici - Firenze

Istituto di Scienze e Tecnologie Molecolari - Milano

Centre National de la Recherche Scientifique

Laboratoire de Chimie, Catalyse, Polymères et Procédés - Lyon

Institut Charles Gerhardt - Montpellier

Consejo Superior de Investigaciones Científicas

Instituto de Investigaciones Químicas - Sevilla

Instituto de Ciencia de Materiales de Aragón - Zaragoza

Katholieke Universiteit Leuven

Katholieke Universiteit Leuven - Leuven

The University Court of the University of St. Andrews

School of Chemistry - St. Andrews

BASF Nederland B.V.

Catalyst Research Center - De Meern

National Research School Combination Catalysis

Technische Universiteit Eindhoven - Eindhoven

Utrecht University - Utrecht

All participants are members of the FP6 Network of Excellence IDECAT

**Associated partners.**

Dowpharma - Chirotech Technology Limited

Bruker BioSpin S.r.l.

Hybrid Catalysis B.V.

Science and Technology Facilities Council - ISIS Pulsed

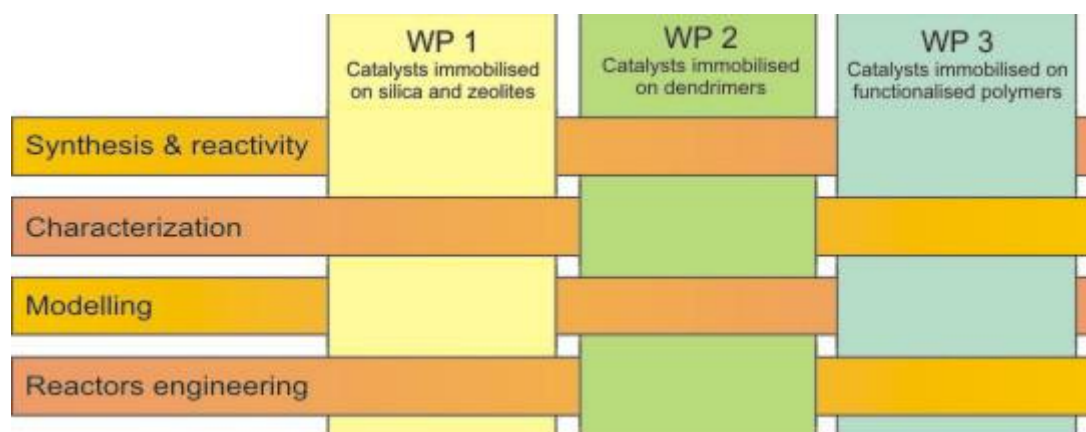
Neutron & Muon Source

**Research programme.** The research activities carried out by NANO-HOST are based on a jointly executed research programme. The scientific work is broken down into three Work Packages with identified tasks.

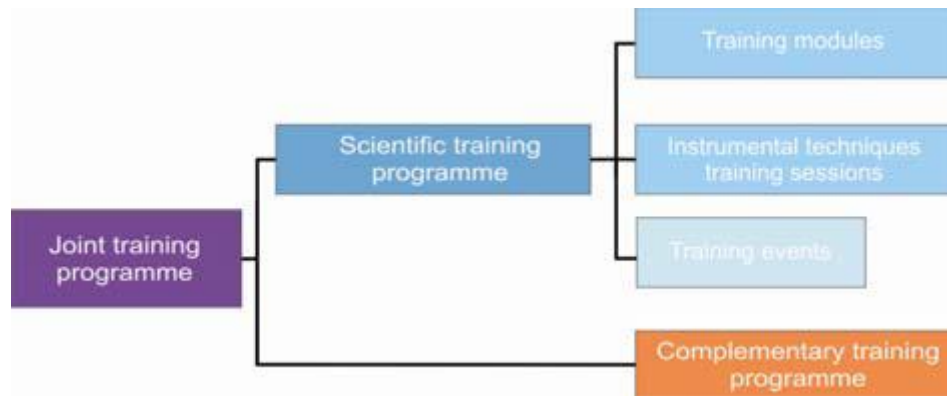
**WP1** “Catalysts immobilized on silica and zeolites” is centred on: a) the development of innovative strategies for the design and the mastered elaboration of micro- and mesoporous inorganic matrices with structured porosity and controlled surface properties, b) the immobilisation of homogeneous catalyst precursors on these matrices, c) the use and recycle of the heterogenized catalysts in selective reactions, d) development of (super critical) flow / monolithic reactors.

**WP2** “Catalysts immobilized on dendrimers” is centred on the design and the synthesis of new dendritic materials and nanoparticle hybrids, and the catalysts based on them, and their use in chemical transformations with enhanced selectivity.

**WP3** “Catalysts immobilized on functionalised polymers” is centred on the development of methodologies for covalent and non-covalent immobilization of metal complexes onto functionalized organic or hybrid polymers: latex polymers, ion-exchange resins, carbon nanotubes, metal-organic frameworks, metal oxide nanotubes, polymer ligands.



**Training programme.** The jointly executed training programme is based on a comprehensive set of scientific and complementary elements and in an appropriate number of training events. The programme includes multi-lateral collaborative research / training projects and those of the individual recruited researchers.



The scientific training programme will be fully integrated with the research activity of the Network and will include:

- training modules, corresponding to the research activities required to accomplish the goals of the project,
- a set of advanced instrumental techniques training sessions,
- an appropriate number of training events.

The elements of the scientific training programme will be provided by the recruiting institutions and by secondments. The recruiting institutions will afford the primary training. Secondments will include visits, short stays, stages, attendance to courses, etc. and they will be carried out at the collaborating institutions. The complementary training programme will include a set of skills coherent with the overall activities of the Network. The complementary activities will be offered by the recruiting institutions, by secondments and by the associated partners. The Network as a whole will provide training activities for a total minimum of 530 person-months of Early Stage (12) and Experienced Researchers (10) whose appointment will be financed by the contract.